

Abstract

Chaotic optical communication system (COC) is a novel communication scheme that utilizes optical chaotic waveform to transmit information at high bit rate. Its potential applications include secure communications and spread-spectrum communications. The semiconductor laser is well suited for COC systems since the internal laser oscillation is easily interfered with a field from optical injection or optical feedback. This thesis simulate the performance of different issues related to semiconductor laser-based COC systems.

The performance of a semiconductor laser subjected to a delay optical feedback is investigated using laser rate equations that describe the temporal variation of photon density, carrier density, and the phase of the lasing field. The simulation results show how semiconductor lasers are sensitive to external optical perturbations and how rich chaotic signal with large information entropy can be generated with controlled optical feedback.

The analysis is carried out further to assess synchronization between the transmitter laser and the receiver laser employed in a delayed optical feedback-based COC system. The synchronization behavior is modeled here as a result of the dynamics of two coupled subsystems, each is described by laser rate equations. The model is quite general and takes into account different parameters related to external feedback system and transmitter/receiver laser systems. The results yield to the conditions required to achieve synchronization and show how synchronization state is affected by various communication system parameters (k_f , k_{inj} , I_r , τ , τ_f and Δw). The simulation results are used as a guideline to transmit digital information in a secure fashion between the transmitter and the receiver. A

secret key is used in the transmitter in order to achieve cryptography-mode of operation where the target receiver can recover the information using the same key. The results indicate clearly that in order to achieve COC system, both transmitter and receiver lasers must have identical parameters and operate at the same lasing frequency at bias conditions. A frequency detuning as low as 10 GHz may affect the synchronization state between these lasers. The simulation results reported in this thesis are obtained by using MATLAB 7.0 environment.

References

- [1] N. Grote and H. Venghaus, "Fiber optic communication device", Springer-Verlag Berlin Heidelberg, 2001.
- [2] C. Decusatis, "Fiber optic data communication: Technological trends and advances" Academic Press, China, 2002.
- [3] R. Tricker, "Optoelectronics and fiber optic technology", Great Britain by Biddles Ltd., 2002.
- [4] K. Hirano, K. Amano, and A. Uchida, "Characteristics of fast physical random bit generation using chaotic semiconductor lasers", IEEE. J. Quantum Electron. , vol. 45, no. 11, pp. 1367-1379, 2009.
- [5] I. Hen and N. Merhav, "On the threshold effect in the estimation of chaotic sequences", IEEE Transactions on Information Theory, vol. 50, no. 11, pp. 2894-2904, 2004.
- [6] Y. Kouomou, "Nonlinear dynamics of semiconductor laser systems with feedback", PhD Thesis, University of the Balearic Islands, 2006.
- [7] J. Liu, H. Chen, and S. Tang, "Optical communication systems based on chaos in semiconductor lasers", IEEE Transactions on Circuits and Systems, vol. 48, no. 12, pp. 1475-1483, 2001.
- [8] D. Syvridis and A. Bogris, "Secure communications links based on chaotic optical carriers", Spie news, 2006.
- [9] S. Donati and C. R. Mirasso, "Introduction to the feature section on optical chaos and applications to cryptography", IEEE. J. Quantum Electron. , vol. 38, no. 9, pp. 1138-1140, 2002.

- [10] I. Fischer, Y. Liu, and P. Davis, "Synchronization of chaotic semiconductor laser dynamics on sub nanosecond time scales and its potential for chaos communication", *Physical Rev. A*, vol. 62, no. 011801, pp.1-4, 2000.
- [11] H. F. Chen and J. M. Liu, "Open-loop chaotic synchronization of injection-locked semiconductor lasers with gigahertz range modulation", *IEEE J. Quantum Electron.* vol. 36, no. 1, pp. 27-34, 2000.
- [12] A. Uchida, Y. Liu, I. Fischer, P. Davis, and T. Aida, "Chaotic antiphase dynamics and synchronization in multimode semiconductor lasers" *Physical Rev. A*, vol. 64, no. 023801, pp. 1-6, 2001.
- [13] S. Sivaprakasam, I. Pierce, P. Rees, P. S. Spencer, and K. A. Shore, "Inverse synchronization in semiconductor laser diodes", *Physical Rev. A*, vol. 64, pp. 013805, (1-8), 2001.
- [14] Y. Liu, H. F. Chen, J. M. Liu, P. Davis, and T. Aida, "Communication using synchronization of optical-feedback-induced chaos in semiconductor lasers", *IEEE Trans. on Circuits and Systems*, vol. 48, no. 12, pp. 1484-1490, 2001.
- [15] S. Wieczorek, B. Krauskopf, and D. Lenstra, "Sudden chaotic transitions in an optically injected semiconductor laser" *Optics Letters*, vol. 26, no. 11, pp. 816-818, 2001.
- [16] M. Peil, T. Heil, I. Fischer, and W. Elsässer, "Synchronization of chaotic semiconductor laser systems: a vectorial coupling-dependent scenario", *Physical Rev. Letters*, vol. 88, no. 17, pp. 1-4, 2002.
- [17] J.-M. Liu, H.-F. Chen, and S. Tang, "Synchronized chaotic optical communications at high bit rates", *IEEE J. Quantum Electron.*, vol. 38, no. 9, pp. 1184-1196, 2002.

- [18] Y. Liu, P. Davis, Y. Takiguchi, T. Aida, "Injection locking and synchronization of periodic and chaotic signals in semiconductor lasers" *IEEE J. Quantum Electron.* vol. 39, no. 2, pp. 269-278, 2003.
- [19] M. Bulinski, M. L. Pascua, I. R. Andreia, "Phase synchronization and coding chaos with semiconductor lasers" *Journal of Optoelectronics and Advanced Materials*, vol. 6, no. 1, pp. 77-86, 2004.
- [20] D. Kanakidis, A. Bogris, A. Argyris, and D. Syvridis, "Numerical investigation of fiber transmission of a chaotic encrypted message using dispersion compensation schemes" *J. of Lightwave Technology*, vol. 22, no. 10, pp. 2256-2263, 2004.
- [21] M.W. Lee, P. Rees, K.A. Shore, S. Ortin, L. Pesquera and A. Valle, "Dynamical characterization of laser diode subject to double optical feedback for chaotic optical communications", *IEE Proc. Optoelectron.*, vol. 152, no. 2, pp. 97-102, 2005.
- [22] Y. C. Kouomou, P. Colet, L. Larger, and N. Gastaud, "Mismatch-induced bit error rate in optical chaos communications using semiconductor lasers with electro optical feedback" *IEEE J. Quantum Electron.* , vol. 41, no. 2, pp. 156-163, 2005.
- [23] D. Kanakidis, A. Argyris, A. Bogris, and D. Syvridis, "Influence of the decoding process on the performance of chaos encrypted optical communication systems" *J. of Lightwave Technology*, vol. 24, no. 1, pp.335-341, 2006.
- [24] N. Shibasaki, A. Uchida, S. Yoshimori, and P. Davis, "Characteristics of chaos synchronization in semiconductor lasers subject to polarization - rotated optical feedback" *IEEE J. Quantum Electron.*, vol. 42, no.3, pp. 342-350, 2006.

- [25] J. F. Avila, R. Vicente, J. R. Leite, and C. R. Mirasso, "Synchronization properties of bidirectionally coupled semiconductor lasers under asymmetric operating conditions" *Physical Rev. E*, vol. 75, no. 066202, pp. 1-6, 2007.
- [26] A. Bogris, P. Rizomiliotis, K.E. Chlouverakis, A. Argyris, and D. Syvridis, "Feedback phase in optically generated chaos: a secret key for cryptographic applications" *IEEE J. Quantum Electron.* vol. 44, no. 2, pp. 119-124, 2008.
- [27] J.-Z. Zhang, A.-B. Wang, J.-F. Wang and Y.-C. Wang, "Wavelength division multiplexing of chaotic secure and fiber-optic communications" *Optics Express*, vol. 17, No. 8, pp. 6357-6367, 2009.
- [28] Y. Liu, Y. Takiguchi, P. Davis, T. Aida, S. Saito, and J. M. Liu, "Experimental observation of complete chaos synchronization in semiconductor lasers," *Appl. Phys. Lett.*, vol. 80, pp. 4306-4308, 2002.
- [29] A. N. Pisarchik and F. R. R.-Oliveras, "Optical chaotic communication using generalized and complete synchronization", *IEEE J. Quantum Electron.* vol. 46, no. 3, pp. 279-284, 2010.
- [30] G. P. Agrawal and N. K. Dutta, "Long wavelength semiconductor Lasers", Van Nostrand Reinhold Company Inc., 1986.
- [31] J. N. Blakely, "Experimental control of a fast chaotic time-delay optoelectronic device", PhD Thesis, Duke University, 2003.
- [32] M. C. Schu, "External cavity diode lasers, controlling laser output via optical feedback", B.Sc thesis, Williamsburg, Virginia, 2003.
- [33] S. M. Sze and K. K. Ng, "Physics of semiconductor devices" John Wiley and Sons, Inc., 2007.

- [34] J. Y. Law, "Static, dynamic, and noise characteristics of Vertical-cavity surface-emitting lasers" PhD Thesis, University of Rochester, New York, 1997.
- [35] T. Fordell, "Dynamics of free running, pump-modulated and coupled semiconductor and solid-state lasers" Academic Dissertation, Helsinki, 2007.
- [36] Y. Lien, "Intensity dynamics of slow-inversion lasers", Research Program, Nederland's Organization, 2002.
- [37] W. W. Chow, S. W. Koch, "Semiconductor laser fundamental", Springer-Verlag, Berlin Heidelberg, 1999.
- [38] S. Eriksson, "Nonlinear dynamics of optically injected semiconductor lasers" Academic Dissertation, Helsinki, 2002.
- [39] A. Argyris, D. Kanakidis, A. Bogris, and D. Syvridis, "Spectral synchronization in chaotic optical communication systems", IEEE J. Quantum Electron. vol. 41, no. 6, pp. 892-897, 2005.
- [40] J. S. Lawrence, "Diode lasers with optical-feedback, optical-injection, and phase-conjugate feedback", PhD Thesis, Macquarie University, 2000.
- [41] S. Tang and J. M. Liu, "Chaotic pulsing and quasi-periodic route to chaos in a semiconductor laser with delayed opto-electronic feedback" IEEE J. Quantum Electron., vol. 37, no. 3, pp. 329-336, 2001.
- [42] J. Ohtsubo, "Semiconductor lasers, stability, instability and chaos" Springer-Verlag, 2006.
- [43] D. Zhong, G. Xia, Z. Wu, "Synchronization and communication based on semiconductor lasers with phase conjugate feedback", J. of Optoelectronics and Advanced Materials, vol. 6, no. 4, pp. 1233-1241, 2004.

- [44] G. D. Wiggeren and R. Roy, "Optical communication with chaotic waveforms", *Physical Rev. Letters*, vol. 81, no. 16, pp. 3547-3550, 1998.
- [45] S. Bauer, "Nonlinear dynamics of semiconductor lasers with active optical feedback", PhD Thesis, Humboldt University, Berlin, 2005.
- [46] C. Masoller, "Anticipation in the synchronization of chaotic semiconductor lasers with optical feedback", *Physical Rev. Letters*, vol. 86, no. 13, pp. 2782-2785, 2001.
- [47] K. H. Jeong, K. H. Kim, S. H. Lee, M. H. Lee, B.-S. Yoo, and K. A. Shore, "Optical injection-induced polarization switching dynamics in 1.5- μm wavelength single-mode vertical-cavity surface-emitting lasers", *IEEE Photonics Technology Letters*, vol. 20, no. 10, pp. 779-781, 2008.
- [48] A. Murakami and J. Ohtsubo, "Synchronization of feedback-induced chaos in semiconductor lasers by optical injection", *Physical Rev. A*, vol. 65, no. 033826, pp. 1-7, 2002.
- [49] K. M. Cuomo and A. V. Oppenheim, "Circuit implementation of synchronized chaos with applications to communications", *Physical Rev. Letter*, vol. 71, no.1, pp. 65-68, 1993.
- [50] L. E. Larson, J.-M. Liu and .L S. Tsimring, "Digital communications using chaos and nonlinear dynamics" Springer Science and Business Media, LLC, America, 2006.
- [51] F. Dachselt and W. Schwarz, "Chaos and cryptography" *IEEE Transaction: Fundamental theory and applications*, vol. 48, no. 12, pp. 2001.
- [52] C. R. Mirasso, J. Mulet, and C. Masoller, "Chaos shift-keying encryption in chaotic external-cavity semiconductor lasers using a

- single-receiver scheme”, IEEE Photonic Technology Letters, vol. 14, no. 4, pp. 456-458, 2002.
- [53] S. kumar, “Analysis of nonlinear phase noise in coherent fiber-optic system based on phase shift keying”, J. Lightwave Technology, vol. 27, no. 21, pp. 4722-4733, 2009.
- [54] G. Li, "Recent advances in coherent optical communication", Advances in Optics and Photonics, pp. 279-307, 2009.
- [55] G. P. Agrawal, “Fiber-optic communication systems” John Wiley and Sons, Inc. 1997.
- [56] V. A.-Lodi, S. Merlo, M. Norgia and A. Scirè, “Characterization of a chaotic telecommunication laser for different fiber cavity lengths”, IEEE J. Quantum Electron. , vol. 38, no. 9, pp. 1171-1177, 2002.
- [57] V. Ahlers, U. Parlitz, and W. Lauterborn, “Hyperchaotic dynamics and synchronization of external-cavity semiconductor lasers”, Physical Rev. E, vol. 58, no. 6, pp. 7208-7213, 1998.

Certification

We certify that this thesis was prepared under our supervision at University of Technology – Laser and Optoelectronics Engineering Department in partial fulfillment of the requirements for the degree of Doctor of Philosophy in Laser Engineering.

Signature:

Prof. Dr. Mohammed S. Mehde

Supervisor

Date: / 5 / 2010

Signature:

Prof. Dr. Raad S. Fyath

Supervisor

Date: / 5 / 2010

In view of the available recommendation, I forward this thesis for debate by the Examining Committee.

Signature:

Assist. Prof. Dr. Mohammed Abud-Al-whab

Deputy Head Science and P. Grad. Studies

Date: / 5 / 2010

Certification

We certify that we have read this thesis entitled (Performance analysis of semiconductor laser based chaotic optical communication system) and examined the student (Shatha Mizhir Hasan) in its content and that in our opinion; it meet the standard of a thesis for the degree of doctor philosophy in Laser Engineering.

Signature:

Name: Dr. Raad M. S. Al-Haddad

Title: Professor. (Chairman)

Date: / 5 / 2010

Signature:

Name: Dr. Munqith S. Dawood

Title: Assist. Prof. (Member)

Date: / 5 / 2010

Signature:

Name: Dr. Mohammed A. Abdala

Title: Assist. Prof. (Member)

Date: / 5 / 2010

Signature:

Name: Dr. Mohammed S. Ahmed

Title: Assist. Prof. (Member)

Date: / 5 / 2010

Signature:

Name: Dr. Kadhim A. Hubeatir

Title: Assist. Prof. (Member)

Date: / 5 / 2010

Signature:

Name: Dr. Mohammed S. Mehde

Title: Professor. (Supervisor)

Date: / 5 / 2010

Signature:

Name: Dr. Raad S. Fyath

Title: Professor. (Supervisor)

Date: / 5 / 2010

Approved by University of Technology – Laser and optoelectronics Engineering Department.

Signature:

Name: Dr. Mohammed Hussian Ali

Title: Assist. Prof.

Head of Department

Date: / 5 / 2010

Chapter One

Introduction

1.1 General Introduction

Optical communication is any form of telecommunication that uses light as the transmission channel. An optical communication system consists of a transmitter, which encodes a message into an optical signal, a channel, which carries the signal to its destination, and a receiver, which reproduces the message from the received optical signal[1], see Fig.1.1. Optical fiber is the most common type of channel for optical communications; however, other types of optical waveguides are used within communications gear, and have even formed the channel of very short distance links in laboratory trials. The transmitters in optical fiber links are generally light-emitting diodes (LEDs) or laser diodes. Infrared light around 800, 1310 and 1550 nm, rather than visible light is used more commonly, because optical fibers transmit infrared wavelengths with less attenuation and dispersion [2].

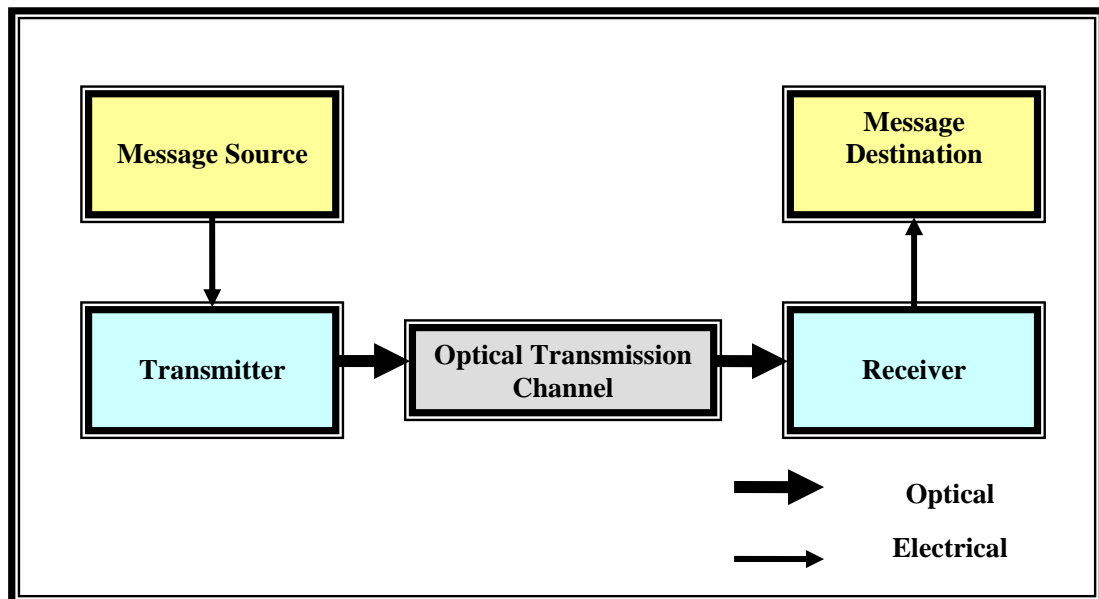


Fig. 1.1 Elements of any optical communication system.

The principal advantages of optical communications are [3]

- (i) Wider available transmission bandwidth due to higher carrier frequency.
- (ii) Ability to concentrate the power in extremely narrow beams.
- (iii) Significant reduction in component sizes because of the extremely small optical wavelengths.

To make transmitted information secure, optical communication system can use a short secret parameter (key) to encode the message directly. Cryptosystems are especially suitable for exchanging secure information over large complex networks. As computational power increases, heightening the potential of security attack on such systems, the key length may be increased and the extra computing power available ensures that the time delay for encrypting the data does not increase significantly. Improving the security of an encrypted message can be achieved by additional encoding at the physical hardware layer and, in particular, by using chaotic carriers generated by components in the system [4].

Chaotic systems are used in various applications due to their ability to generate highly complicated signals by a simple recursive procedure [5]. Chaotic sequences are attractive candidates for use in signal analysis, signal synthesis, practical engineering, and communications applications. Chaotic systems are used as models for a wide range of signal processing applications as well as for practical engineering systems like analog-to-digital converters and power converters. Chaotic systems have the potential to give rise to good joint source–channel codes due to their ability to separate orbits of nearby initial states while maintaining global boundness, thus conforming with energy and peak amplitude constraints. Chaotic signals are also used in spread spectrum applications, where the power of the transmitted signal is spread across a broad range of frequencies.

1.2 Optical Communication with Chaotic Signal

Chaos is a paradigmatic name used to describe deterministic dynamical systems whose behavior is complex, unpredictable and extremely sensitive to initial conditions. Chaos is theoretically and experimentally encountered in almost all types of lasers (solid-state, gas, semiconductor, etc...). Methods to lead lasers to chaos are numerous and based on two necessary conditions: nonlinearity and threefold dimensionality [6]. Hence, when the nonlinearity of the laser (system) is not strong enough, an external nonlinear element can be introduced. Along the same line, when the dimensionality of the laser system is not high enough, it can be increased by parameter modulation or by delayed feedback loops.

Ideal components to generate optical chaotic carriers are semiconductor lasers which can act as transmitters and receivers in optical communication systems. Semiconductor lasers are the most important light sources for optical communications because of their compact size, efficiency, high speed, and semiconductor laser has the ability to be electrically pumped and current modulated. Single-mode semiconductor lasers, such as the distributed-feedback lasers and the vertical-cavity surface emitting lasers, are particularly important for high-bit-rate optical communication systems. For these reasons, single-mode semiconductor lasers are used as transmitters and receivers for chaotic optical communications [7]. Figure 1.2 shows the operating principle of a chaos-based optical communication system. In this system, a data message encoded on a deterministically chaotic carrier is recovered by using a receiver incorporating a similar deterministically chaotic oscillator [8].

The transmitter consists of an optical oscillator forced by external feedback to operate in the chaotic regime, producing an optical carrier with a broad (GHz-wide) spectrum. Information is encoded on this chaotic carrier using different techniques. Assuming a high complexity in

signal carrier and low message amplitude, it is practically impossible to extract this encoded information using techniques like linear filtering, frequency-domain analysis or phase-space reconstruction. At the receiver side, a second chaotic oscillator is used similar to that of the transmitter. This similarity refers to structural, emission, and intrinsic parameters of the semiconductor laser, to the feedback loop characteristics, and to the operating parameters.

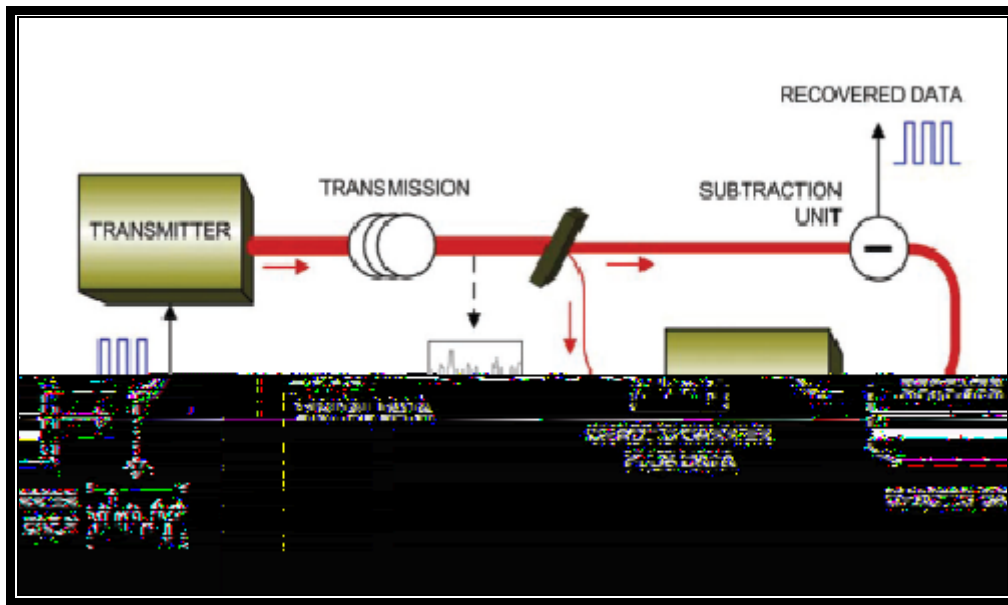


Fig.1.2 Chaos based-optical communications [8].

Generally speaking, chaotic optical communication (COC) is a novel communication scheme that utilizes optical chaotic waveform to transmit messages at a high bit rate. Its potential applications include secure communications and spread-spectrum communications. In a chaotic optical communication system, a nonlinear dynamical system is used to generate the optical chaotic waveform for message transmission. Messages are encoded through chaos encryption where the messages are mixed with the chaotic waveform. Message recovery is achieved by comparing the received signal with a reproduced chaotic waveform which synchronizes with the chaotic waveform from the transmitter.

The generation of optical chaos in semiconductor laser systems may be achieved by optical injection, optical feedback and optoelectronic

feedback [9]. Optical feedback is a popular technique and can be achieved by using a mirror that reflects some of the laser output back into the laser cavity. The distance from the laser to the mirror (the external-cavity length), the feedback strength, and the feedback phase all affect the dynamics of the chaos produced in the laser.

Communications using chaotic waveforms as "carriers" of information promise possible advantages over traditional communications strategies [8].

- (i) Efficient use of the designated bandwidth of a communication system, leading to expanded information bearing capacity or an increased number of channels for the system.
- (ii) Ability of a chaotic communication system to utilize, rather than avoid, the inherent nonlinearity of communication devices.
- (iii) A chaotic communication system allows large-signal modulation for message encoding and eliminates complicated measures to maintain linearity.

Therefore, a chaotic communication system can potentially function over a larger dynamical range, operates at a higher power level, and consist of fewer and simpler components than a conventional communication system.

1.3 Literature Survey

Fischer et al. ([10], 2000) presented experimental evidence for the synchronization of two semiconductor lasers exhibiting chaotic emission on subnanosecond time scales. The transmitter system consists of a semiconductor laser with weak to moderate coherent optical feedback and therefore exhibits chaotic oscillations. The receiver system is realized by a solitary semiconductor laser in which a fraction of the transmitter signal is coherently injected. They have found that for a considerably large parameter range, synchronized receiver output can be achieved. The physical mechanism behind chaotic state has been discussed which demonstrates that the receiver acts as a chaos pass filter, which reproduces the chaotic fluctuations of the transmitter laser, but suppresses additionally encoded signals. Signal extraction at frequencies of up to 1 GHz has been achieved. A simple and robust optical chaos synchronization system has been provided which is promising for the realization of communication by sending signals with chaotic carriers.

Chen et al. ([11], 2000) generated a chaotic carrier waveform from different chaotic state in transient rather than from a fixed chaotic state in static. A message signal is attached no matter which modulation scheme is applied. The setup performs remote synchronization with good signal recovery without the need to use any auxiliary optical or electronic filters to filter out the synchronization error. Good quality of synchronization has been found over a wide range of amplitude and bandwidth, up to an order of 100 GHz, for the message signal.

Uchida et al. ([12], 2001) presented experimental evidence that shows antiphase dynamics occurs in the high frequency chaotic state of a multimode semiconductor laser with optical feedback. An external mirror has been set in front of the laser to provide optical feedback which results in chaotic fluctuation of the laser output. The round-trip time of the light in the external cavity is 3.8 ns, corresponding to a frequency of 0.265

GHz. The results indicate that the antiphase dynamics can be produced in a second laser which is synchronized to the first by optical injection.

Sivaprakasam et al. ([13], 2001) used an optical coupling to affect synchronization between two diode lasers in a master-slave configuration. The effect of frequency detuning between the master and slave lasers on the character of the observed synchronization has been studied. Experimental conditions are found under which the synchronization plot (formed by plotting the output power of the slave laser against that of the master at each instant in time) makes a transition from a positive gradient to a negative gradient.

Liu et al. ([14], 2001) proposed an optical communication system based on the synchronization of optical feedback induced chaos in two semiconductor lasers. Synchronization of chaos is performed by a direct optical-injection scheme that consists of a transmitter laser with an external optical feedback and a receiver laser with optical injection from the transmitter laser. Both numerical and experimental results on synchronization of giga-hertz chaotic signals have been presented. Direct encoding of 2.5Gb/s messages on the chaotic waveform has been numerically demonstrated.

Wieczorek et al. ([15], 2001) studied sudden changes in the chaotic output of an optically injected semiconductor laser. Bifurcations that cause abrupt changes between different chaotic outputs, or even sudden jumps between chaotic and periodic output are identified. These sudden chaotic transitions involve attractors that exist for large regions in parameter space. They have used modern tools from bifurcation theory that is facilitated experimental exploration of these transitions. Two points concerning the sudden transitions are mentioned briefly. First, one can obtain switching between two different chaotic signals (chaos shift keying) for reliable and safe transmission of information by changing parameter values near an interior crisis. Second, using chaotic signals

close to a boundary crisis may be dangerous, in that a small parameter variation may lead to loss of the chaotic attractor and to periodic laser output instead.

Peil et al. ([16], 2002) demonstrated the influence of vectorial coupling on the synchronization behavior of complex systems.

They have studied two semiconductor lasers subject to delay optical feedback which are unidirectionally coherently coupled via their optical fields. The experimental and numerical results demonstrated a characteristic synchronization scenario in dependence on the relative feedback phase leading cyclically from chaos synchronization to almost uncorrelated states, and back to chaos synchronization.

Liu et al. ([17], 2002) studied system performance numerically at a bit rate of 10Gb/s for the application of three encryption schemes, namely chaos shift keying, chaos masking, and additive chaos modulation, to three chaotic semiconductor laser systems, namely the optical injection system, the optical feedback system, and the optoelectronic feedback system. By causing synchronization error in the forms of synchronization deviation and desynchronization bursts, the channel noise and the laser noise both have significant effects on the system performance at high bit rates.

Liu et al. ([18], 2003) investigated experimentally the synchronous response of a semiconductor laser to the injection of a periodic or chaotic oscillating optical signal that is generated by a similar semiconductor laser with optical feedback. They have shown two different types of synchronous response, appearing in separate regimes of laser frequency detuning and injection strength. The two distinguished by the time lag of the slave-laser response with respect to the injection signal from the output of the master laser.

Bulinski et al. ([19], 2004) presented numerical simulations of synchronized chaotic semiconductor lasers that are unidirectional coupled

by their electric fields. They analyzed the variation of the phase synchronization error between master and slave in a chaos masking and modulation data transmission scheme. A good decoding of the message is provided by those systems where the chaotic orbits of the master and the slave are as close as possible. The chaos masking system achieved theoretically data transfer rates up to 10Gb/s.

Kanakidis et al. ([20], 2004) presented a detailed numerical investigation of the transmission properties of all-optical chaotic communication systems for two data-encoding techniques and for various dispersion compensation maps. A semiconductor laser subjected to optical feedback generates the chaotic carrier, and the data is encoded on it by chaotic modulation (CM) or chaotic-shift-keying (CSK) methods.

Lee et al. ([21], 2005) characterized a chaotic semiconductor laser subjected to double optical feedback in terms of the statistical analysis, power spectrum analysis and forecast error analysis of the chaotic dynamics. Varying the relative lengths of the two external cavities, the dynamics have been observed and compared to that of a single cavity. The results show that in the case of integer multiple external-cavity lengths, the round-trip time delays can be deduced from the forecast error analysis.

Kouomou et al. ([22], 2005) analyzed the influence of parameter mismatch between emitter and receiver systems on the bit error rate of an optical chaos communication scheme. Intensity hyperchaos is generated in the system by semiconductor lasers with electrooptical feedback. Analytical predictions for the dependence of the bit error rate with the amplitude of the various mismatches and the statistical properties of the hyperchaotic carrier have been found.

Kanakidis et al. ([23], 2006) investigated two different decoding methods of all optical chaotic communication system when chaotic modulation encoding format is employed. The transmitter consists of an

external cavity semiconductor laser generating a chaotic carrier which is modulated using an external modulator. The receiver is either a solitary semiconductor laser diode identical to that of the transmitter or a laser diode coupled to an external cavity, forming open- or a closed-loop configuration, respectively.

Shibasaki et al. ([24], 2006) investigated numerically the detailed characteristics of chaos synchronization in semiconductor lasers subjected to polarization-rotated optical feedback. The emission of the dominant TE mode of a drive laser is rotated by 90° and fed back to the laser with time delay. The polarization-rotated TE mode has been also injected with time delay into the TM mode of a second laser. Two types of synchronization with different time-lags have been found, as in the case for synchronization in semiconductor lasers with nonrotated optical feedback.

Fredy et al. ([25], 2007) studied both experimentally and numerically, a system of two coupled semiconductor lasers in an asymmetric configuration. A laser subjected to optical feedback has been bidirectionally coupled to a free running laser. While maintaining the coupling strength, the feedback rate has been changed and transition from highly correlated low-frequency fluctuations to episodic synchronization between dropouts and jump-ups has been observed.

Bogris et al. ([26], 2008) considered the feedback phase in a chaotic system consisting of a semiconductor laser subjected to delayed optical feedback for the first time as a secret key for secure chaotic communications not exclusively based on hardware uniqueness. Extensive numerical simulations illustrate that the feedback phase is of extreme importance as far as synchronization is concerned.

Zhang et al. ([27], 2009) numerically analyzed a wavelength division multiplexing transmission of COC and conventional fiber-optic communication. For an 80-km-long two-channel communication system,

a 1Gb/s secure message in COC channel and 10Gb/s digital signal in channel have been simultaneously achieved with 100GHz channel spacing. The numerical simulations demonstrate that the COC can realize no-crosstalk transmission of 80km when the peak power of channel is less than 8dBm. The results show that the crosstalk between the chaotic system and conventional does not depend on channel spacing when the channel spacing exceeds 100GHz.

It is clear from this survey that optical feedback can lead to a rich variety of chaos in semiconductor lasers. However, there are many challenges appear in this system compared with other chaos schemes. Among these challenges is how to characterize semiconductor laser subjected to optical feedback when it is internally modulated. These try to solve some of these problems by investigating the main parameters affecting the chaos of semiconductor laser in the presence of feedback. The results are to be used later as a guideline to design COC system incorporating internal modulated semiconductor laser.

1.4 Aim of this Work

The aim of this work is to investigate the synchronization between transmitter and receiver semiconductor lasers employed in chaotic optical communication systems. The analysis will focus on a delayed optical feedback-based system since it offers a rich variety of chaotic dynamics. The aim will be achieved through the following steps

- (i) Modeling the chaotic dynamics of a semiconductor laser subject to optical feedback.
- (ii) Addressing synchronization states between transmitter laser operating in chaotic regime and the receiver laser.
- (iii) Achieving secure communication over optical chaotic transmission links.

- (iv) Assessing the effect of various external and internal laser system parameters on chaotic behavior and synchronization states.

1.5 Thesis Layout

The layout of this thesis will be in the following manner:

Chapter 1 presents an introduction for an optical communication system and explains briefly the chaos in semiconductor laser. The advantages of using chaos in the security of optical communication system are stated.

Chapter 2 states briefly the main concepts behind semiconductor laser diode and its types, the laser classes, and the semiconductor laser rate equations. The chaos generation techniques are presented to explain system synchronization.

Chapter 3 explains the optical feedback technique which is used to achieve chaos in this work. The chaos data transmission and the chaos modulation types are presented.

Chapter 4 contains the results and discussions of the work which is based on the optical feedback technique. The results include the free running operation of solitary semiconductor laser, generation of chaos signal, and data transmission with chaos security. This chapter also discusses the effects of external-cavity, external mirror reflectivity, optical feedback, optical injection, time delay, flight time from transmitter to receiver, transmitter and receiver bias current, and frequency detuning on achieve system synchronization.

Chapter 5 summarizes the main conclusions drawn from this study and gives suggestions for future work.

Chapter Two

Semiconductor Laser and Chaos Generation

2.1 Introduction

The semiconductor laser is well suited for a chaotic device, since the internal laser oscillation is easily interfered with a field from external light injection or optical feedback [28]. Semiconductor lasers are also sensitive to external perturbations and high dimensional chaotic signals with large information entropy are generated by means of delayed feedback. These perturbations may cause pulsations of the laser output and induce complex dynamics. This makes the semiconductor laser systems to be of great relevance from the nonlinear dynamics point of view: the ease of control and their common availability constitutes them as a perfect tool to study different bifurcation scenarios and routes to chaos [29].

In this chapter the generation of chaos in semiconductor laser and the techniques of this generation are discussed.

2.2 Semiconductor Laser

The semiconductor laser is a key component of optical telecommunications systems. Reasons for its suitability include its compact size (relative to other lasers) and the fact that its power can be directly modulated through variation of the injection current.

Most types of lasers involve three basic elements: a pumping mechanism, a gain medium, and a resonator. The pumping mechanism adds energy to the gain medium, maintaining it in an excited state (i.e., a population inversion). Photons propagating through the excited medium

stimulate coherent emission of more photons. The resonator ensures that each photon passes several times through the gain medium, and is thereby amplified many times before escaping. Light leaves the resonator in the form of an intense, coherent beam. All three of these elements are present in a diode laser [31]. The laser diode is essentially a semiconductor p-n junction fabricated as a homojunction or heterojunction structure. Light is emitted when electrons and holes recombine in the depletion region of the junction which constitutes the gain medium. The pumping mechanism is an injected current that produces electron-hole pairs. Two cleaved facets of the semiconductor crystal form a Fabry-Perot resonator. A schematic drawing of a homojunction diode laser is shown in Fig. 2.1a where both p-and n- type regions are of the same material.

Modern laser diodes differ from simple p-n junctions because additional layers of n-type or p-type are added (forming a heterojunction) to confine the injected current to the active region. The various layers each have a different index of refraction and conveniently constitute a dielectric waveguide that confines the optical field to the gain region. The entire sandwich of semiconductor layers is referred to as a heterostructure. One type of GaAlAs heterostructure is shown in Fig. 2.1b. If the width of the active layer is comparable to the DeBroglie wavelength of the electrons (~ 10 nm), carrier motion normal to the active layer is confined to a quantum well. So called quantum well lasers tend to have high gain at lower current densities. The dynamical behavior of a semiconductor laser can be modeled by rate equations, a set of first-order differential equations that describe the evolution of the optical field and carrier density [31].

Laser diode is unlike other types of lasers, the light emitted by a diode laser greatly diverges in an oval shape pattern with the highest spread of light at an angle of about 25 degrees [32]. Such a wide beam is practically

useless to an experimentalist. Therefore, it is necessary to collimate the output of the laser diode, that is, bend the diverging light through a lens so that all the output goes in one direction. One can achieve this result using a single lens as long as the laser is placed exactly at the focal point of the lens chosen.

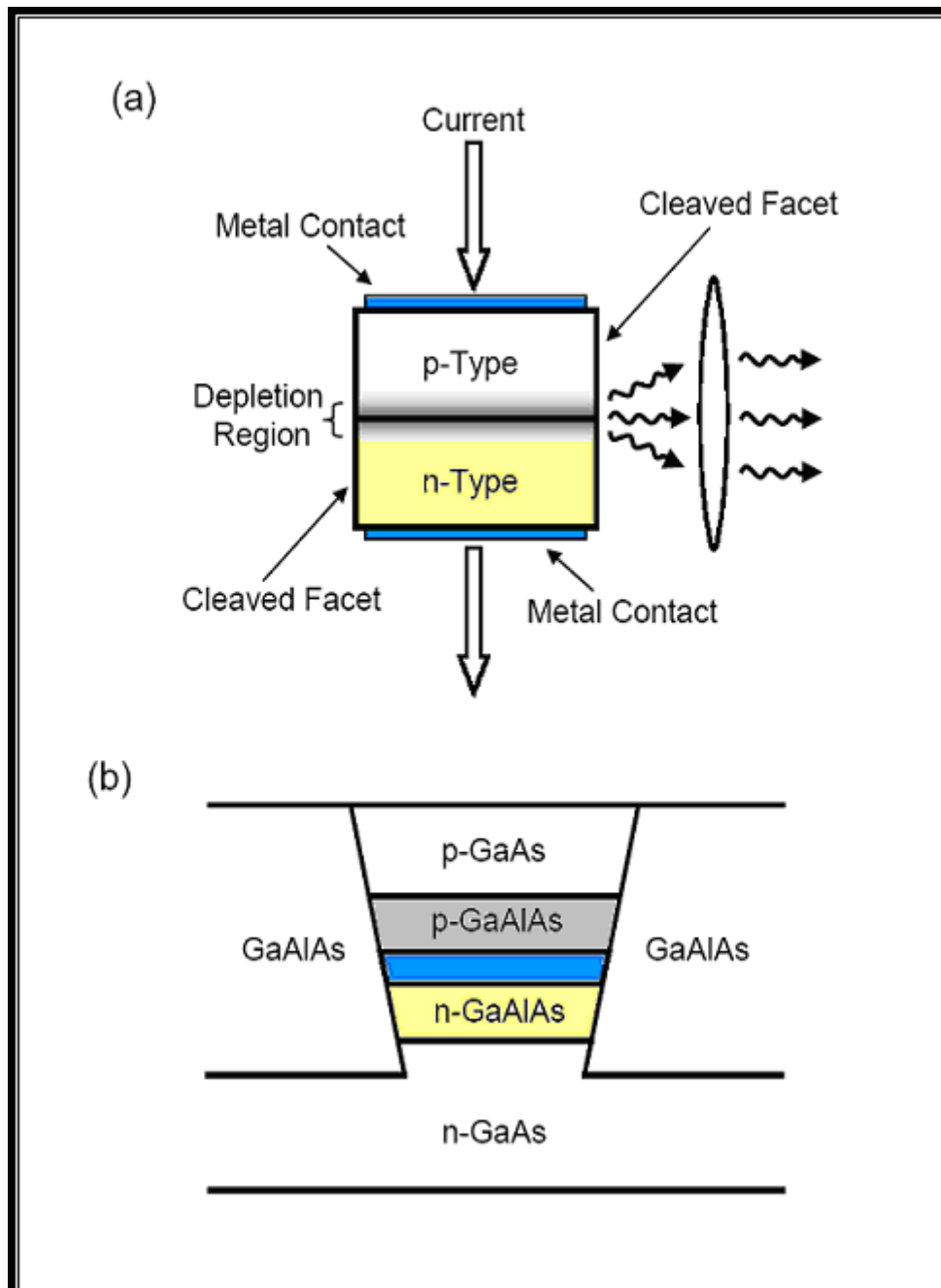


Fig. 2.1 (a) Simplified schematic of a semiconductor laser. (b) Schematic of a typical buried heterostructure laser [33].

The focal point of a lens is also the point through which all light parallel to its normal axis will converge. Hence, if the laser diode placed at the focal point of collimating lens all light from the laser diode that passes through the lens will exit parallel to the normal axis and all light that enters the face of the lens at normal incidence will be focused the laser diode. This property of optics allows sending optical feedback back into the laser.

2.3 Types of Diode Lasers

Traditional diode lasers provide a horizontal resonator structure where the double heterostructure serves to guide the light vertically in the active zone [33]. According to the different refractive indices of the different layers, the light is guided in the active zone. The lateral limitation of the light is achieved either by index guiding or by gain guiding.

Index-guided lasers provide an additional built-in refractive index profile perpendicular to the direction of light propagation. With gain-guided lasers, the guiding in the narrow stripe is achieved by lateral tightening and concentration of the stimulating electrical field. A principal structure of laser diode is shown in Fig. 2.2.

Gain-guided lasers are easier to produce, are offered at a lower price, and have a higher reliability. Index-guided lasers provide a better beam quality and require a lower threshold current. Due to its better characteristics, the index-guided laser has clearly overtaken the gain-guided laser in the telecommunications market. This applies especially to the Distributed Feedback (DFB) laser. With this kind of laser, the reflections are not affected by the plane mirrors of the crystal but by a corrugation of the

semiconductor substrate. These undulated elevations have the effect of a mirror with a high reflection power as shown in Fig. 2.3.

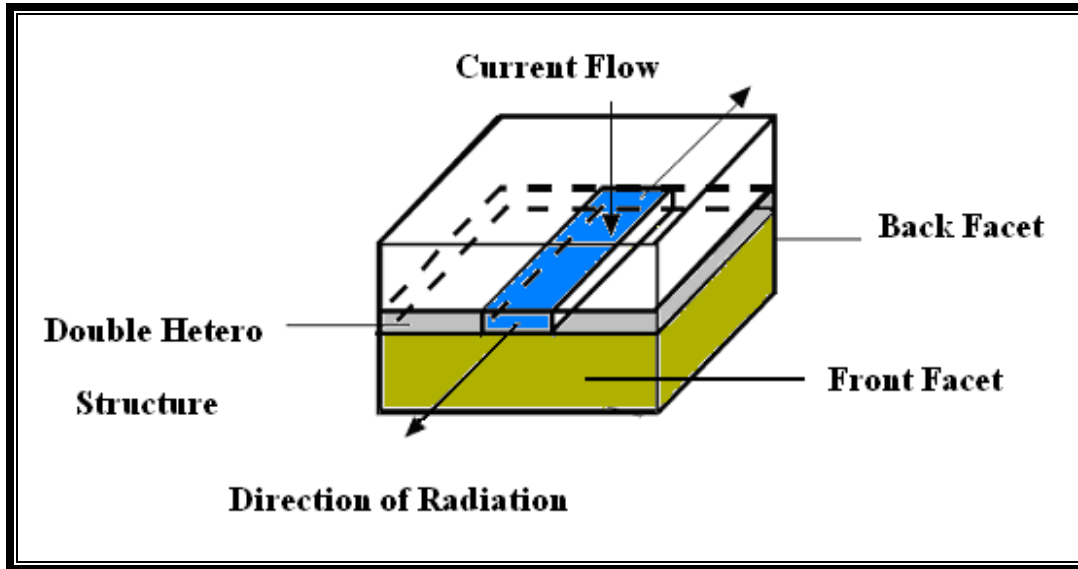


Fig. 2.2 Principal structure of a laser diode guided in the active region [33].

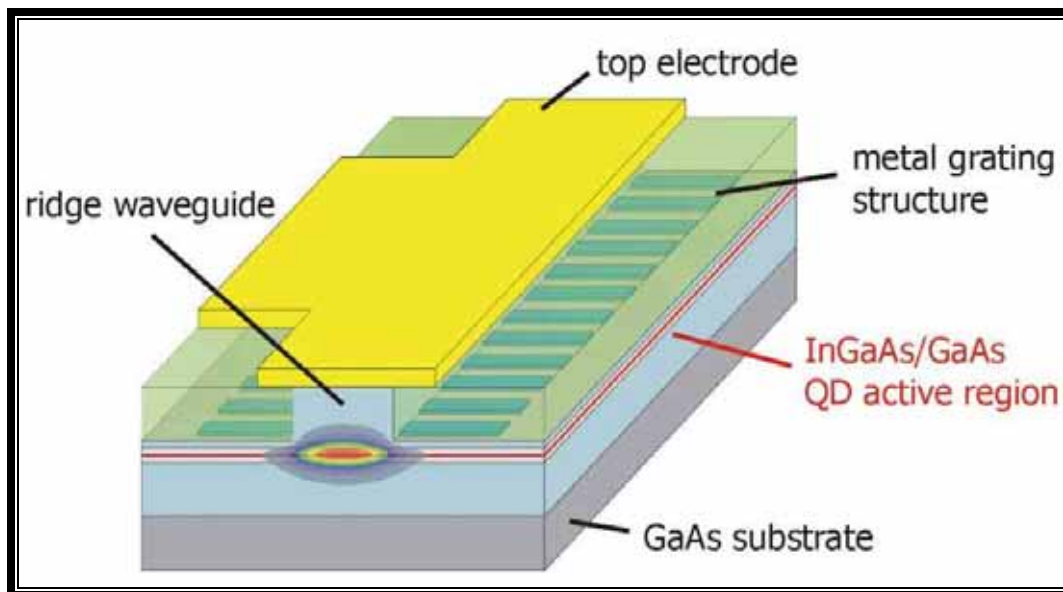


Fig. 2.3 Schematic structure of a DFB laser [34].

DFB lasers are very selective. Contrary to the Fabry-Perot resonator, this principle is called a Bragg reflector. Only one mode of the spectrum

fulfills the resonance condition and is amplified. Thus, it is possible to realize very narrow-band lasers that result in small signal distortion by chromatic dispersion of a fiber, using the laser as a carrier for data. In connection with single-mode fibers, DFB lasers are, therefore, especially suited to realize large bandwidths and long transmission distances [33].

Another important type of laser is the vertical cavity surface emitting laser (VCSEL) [33,34] as shown in Fig. 2.4. This type disposes of a resonator that is in a right angle to the active layer. The laser emits at the surface. The resonator consists of multi-layer mirrors above and below the active zone. Since in VCSELs the photons only pass a relatively short distance in the active zone, these mirrors must have a considerably higher reflection than those of horizontal- emitting laser diodes. VCSELs typically emit with relatively large symmetric apertures, thus the beam is round and shows little divergence. Due to their structure, surface emitting laser diodes have only one beam window, compared to common diodes. This is a disadvantage as a second beam is necessary for many applications for controlling purposes; e.g., to stabilize the output power.

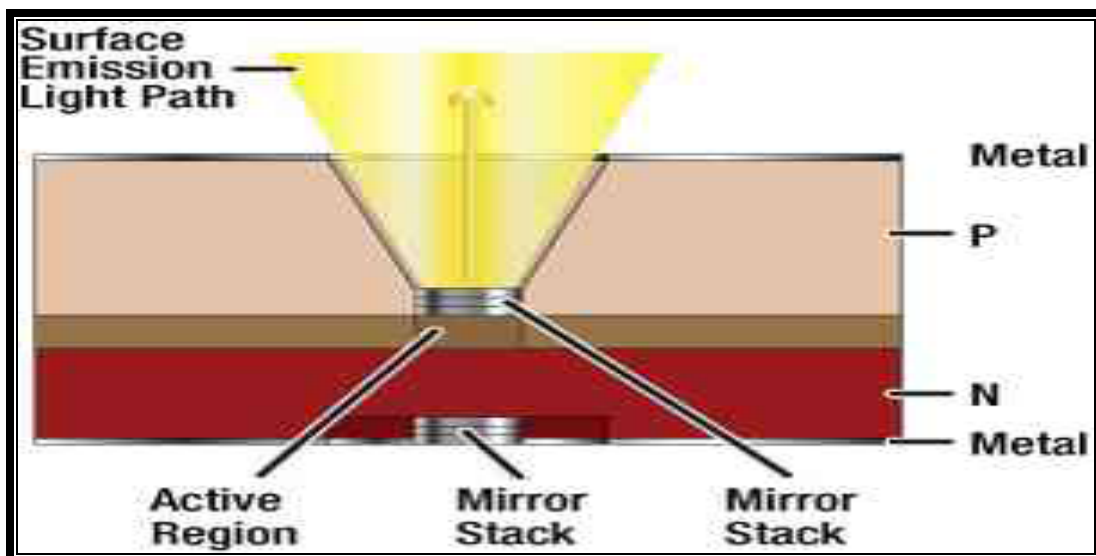


Fig. 2.4 Vertical cavity surface emitting laser (VCSEL) [34].

Many other types of lasers with increasingly complicated structures have been developed to improve certain parameters. One type is the setup of laser bars (arrays). Here several single lasers are arranged next to each other (laser bars) or stacked onto each other (laser stacks). With laser bars and laser stacks, very high optical powers can be achieved. This is the reason why these devices are highly interesting for applications in material treatment (e.g., rapid prototyping).

Further applications for these components are, for example, point-to-point communication in space, laser printing, laser beam writing, and also the optical pumping of solid-state lasers such as Nd-YAG. However, the higher optical power can only be used if it is coupled into a medium with sufficiently large dimensions (diameter and numeric aperture). When coupled into a single-mode fiber with a very small numerical aperture, even with additional collimating lenses, it is not possible to get more power into the fiber than with only a single laser. This is due to general physical laws that do not allow an increase in beam density.

2.4 Laser Classes

It is convenient to classify lasers not by their construction, but by their degrees of freedom. Single-mode lasers can be described by three autonomous first-order differential equations – one for the slowly varying complex amplitude of the electromagnetic (EM) field, one for the slowly varying complex material polarization, and one for the population inversion. The relative magnitudes of the damping rates of these three quantities play a fundamental role in the type of behavior displayed by lasers [35].

In class-A lasers, e.g., dye lasers, the population and the material polarization relax much faster than the EM field. Before the EM field has

time to change, the population and the material polarization will have decayed to their steady state values and can, therefore, be adiabatically eliminated, i.e., replaced by their steady-state values. This adiabatic elimination reduces the dimensionality of the system of equations to just one. Hence, only fixed-point (steady-state) solutions can exist.

In class-B lasers, e.g., semiconductor and Nd:YVO₄ solid-state lasers, only the material polarizations can be adiabatically eliminated. The system of equations is thus two dimensional. The phase of the EM field decouples and what is left is a system of equations with only two degrees of freedom the slowly varying amplitude of the electric field and the population inversion. In a two-dimensional autonomous system only constant or periodic solutions exist.

In class-C lasers, all the variables relax on similar time scales and none of them can be adiabatically eliminated. In a nonlinear system with at least three degrees of freedom very complex dynamics is allowed, including quasiperiodicity and chaos.

To be more clear, the defining characteristics of a laser class are usually the relative sizes of the following decay rates: the decay of the upper lasing level γ_1 , the decay of the atomic polarization γ_{\perp} , and the cavity decay rate Γ_c [36]. In both class A and class B lasers, γ_{\perp} is much faster than the other cavity parameters like the cavity decay rate, and the atomic polarization can therefore be adiabatically eliminated. This is the good cavity approximation. In class-A lasers also the inversion can be adiabatically eliminated so that the dynamics can be formulated in terms of the photon number only. Class- B lasers, on the other hand, have photon and inversion numbers that couple to give rise to relaxation oscillations. In addition to class- A and class-B lasers, more exotic lasers such as the class-C laser exist. In this type of laser, all three parameters γ_1 , γ_{\perp} and Γ_c are

approximately equally large, allowing for very complex or even chaotic behavior.

Semiconductor lasers are classified into stable class-B lasers that are described by the rate equations of the field and the population inversion (the carrier density), but they show chaotic behavior for additional perturbations such as optical feedback, or external optical injection [37].

2.5 Chaos Generation Techniques

The generation techniques of optical chaos in semiconductor laser achieved by optical injection, optoelectronic feedback, and optical feedback.

2.5.1 Laser Diode with Optical Injection

The process of optical injection is illustrated in Fig. 2.5. A single-frequency signal from a master source, generally a tunable laser, is injected into the active region of the slave laser diode. The master laser is optically isolated from the slave laser (typically by a polarization dependent optical isolator) [39,40].

Similar to optical feedback, such optical injection has a variety of effects on the operating characteristics of the slave laser. It can induce various dynamic instabilities and chaotic behavior, locks the two lasers together in phase and frequency (injection locking), excite the relaxation oscillation frequency of the slave laser, or produce phase conjugation through four-wave-mixing.

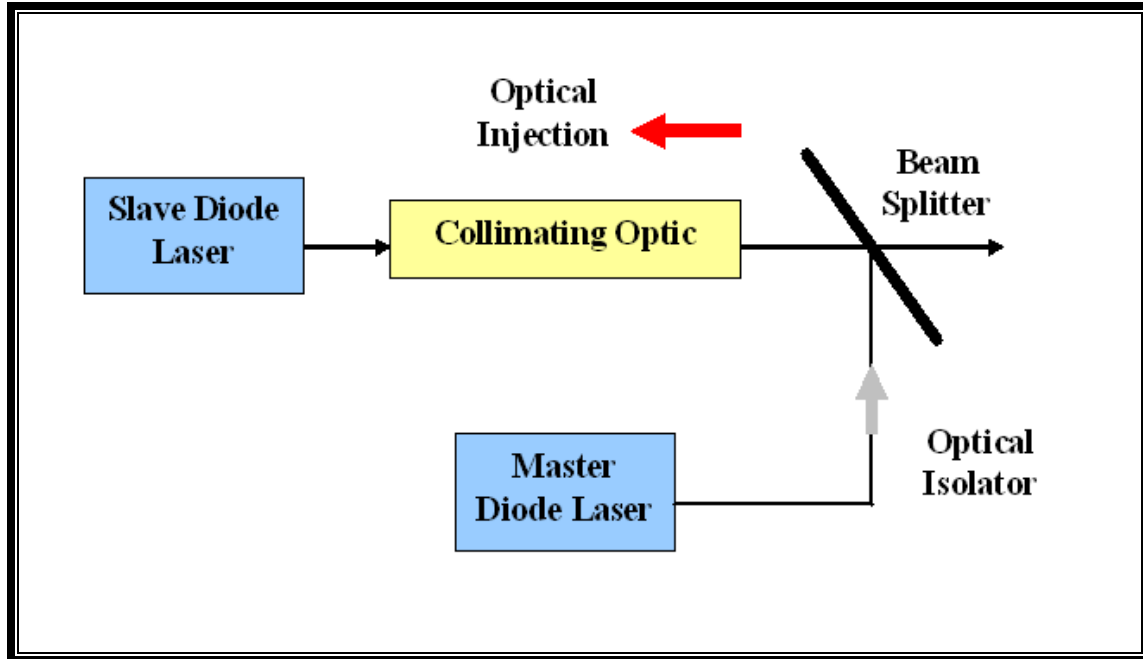


Fig. 2.5 Schematic diagram of laser diode with optical injection from another laser source [40].

2.5.2 Laser Diode with Optoelectronic Feedback

Semiconductor laser with delayed optoelectronic feedback is schematically shown in Fig. 2.6. In this configuration, a combination of photo detector and amplifier is used to convert the optical output of the laser into an electrical signal that is fed back to the laser by adding it to the injection current [7]. Because the photo detector responds only to the intensity of the laser output, the phase of the laser field is not part of the dynamics of this system.

In optoelectronic feedback, chaotic pulses may be generating by positive or negative feedback. Positive optoelectronic feedback is different from negative optoelectronic feedback in the mechanism that drives the nonlinear dynamics of a semiconductor laser. In the case of negative

optoelectronic feedback, the feedback current is deducted from the bias current.

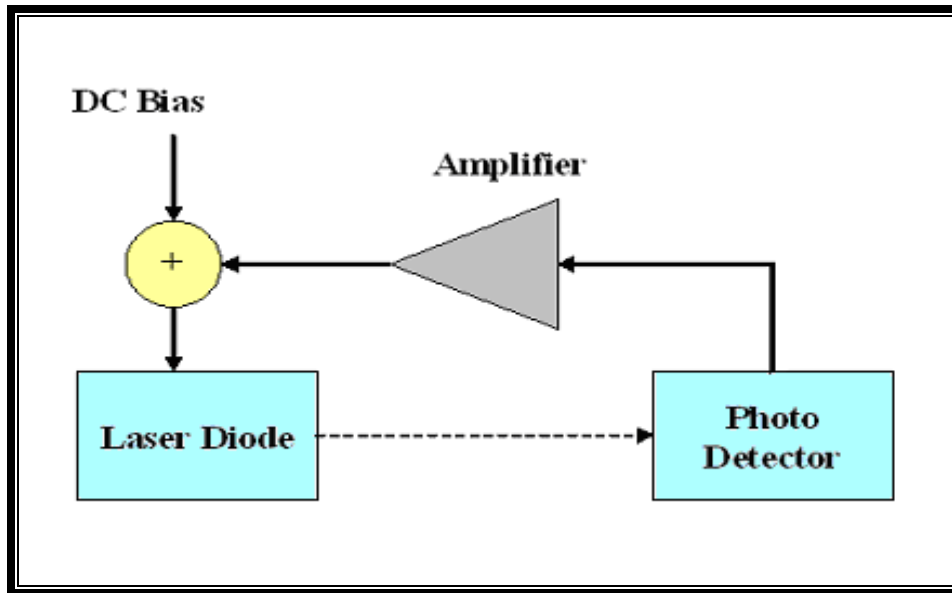


Fig. 2.6 Schematic diagram of laser diode with delayed optoelectronic feedback [7].

This negative feedback current sharpens and extracts the first spike of the relaxation oscillation in the laser. In the case of positive optoelectronic feedback, however, the feedback current is added to the bias current. This positive feedback current tends to drive the laser into pulsing because of the mechanism of gain switching [41]. Positive optoelectronic feedback has long been used to generate periodic short laser pulses. The repetition rate of the pulses is found to be an integral multiple of the inverse of the feedback-loop delay time that is closest to the relaxation resonance frequency of the laser.

2.5.3 Laser Diode with Optical Feedback

A semiconductor laser with optical feedback is an excellent model for generating chaos in its output power and the system has proven to be very useful in practical applications. In semiconductor lasers, self-optical-

feedback effects are frequently used for the control of oscillation frequency, selection of mode, and suppression of side modes. Indeed, the linewidth of laser oscillations can be stabilized by a strong optical feedback and chirping of oscillation frequency can be compensated by optical feedback [42]. Optical feedback is introduced into a diode laser by returning some portion of the optical output back into the device. This is shown schematically in Fig. 2.7. The introduction of such feedback has been found to have dramatic and varied effects on the operating characteristics of the solitary diode laser [40]. Feedback can be disadvantageous, as it may cause unwanted instabilities in the laser output, or advantageous, as under certain conditions it can improve various features of the solitary laser, such as increasing the side mode suppression and narrowing the linewidth.

There exist two types of all-optical feedback. One is the conventional mirror optical feedback (CMOF), where the laser output is coupled into the laser internal cavity by the CMOF and the laser phase changes with the delayed feedback time. Therefore, the dynamic behaviors of laser depend on the precision positioning of the conventional mirror. The other is the phase-conjugate optical feedback (PCOF), which is considerably different from the CMOF. Compared with the CMOF, the PCOF can compensate the feedback phase shift. Furthermore, semiconductor laser subject to PCOF can display richer chaotic dynamics or higher dimension chaos, and the dynamics do not depend on an accurately positioning of the phase-conjugate mirror (PCM). [43].

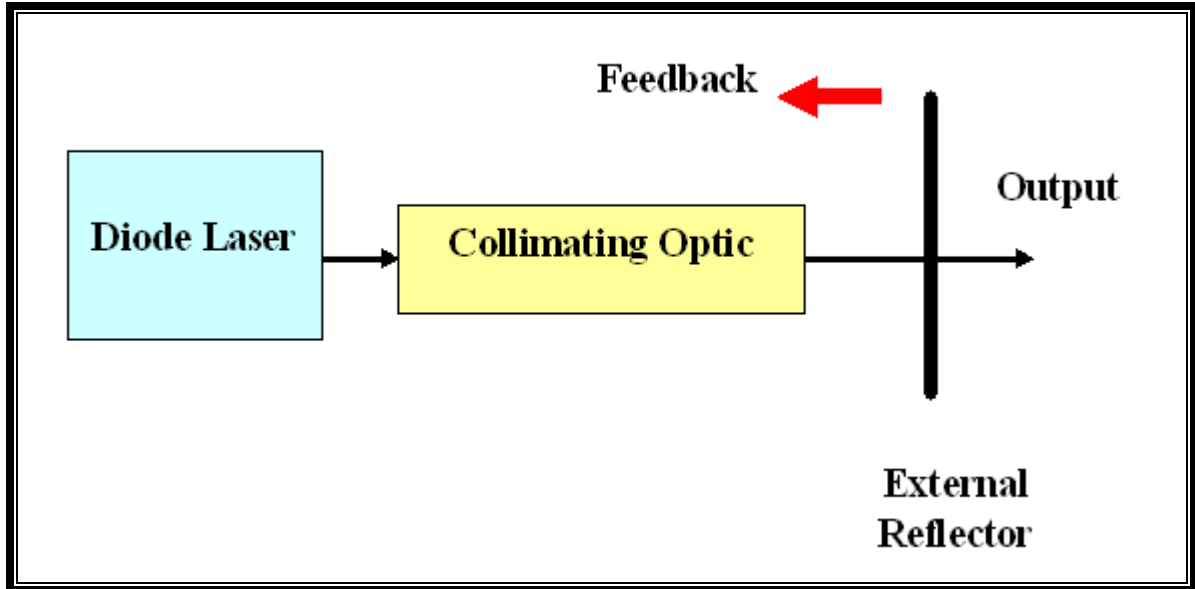


Fig. 2.7 Schematic diagram of laser diode with optical feedback [40].

2.6 Advantages of Chaotic Optical Feedback

Most of the chaotic laser systems based on semiconductor lasers employ optical feedback or optical injection [43], where optical feedback includes all-optical feedback and optoelectronic feedback. Semiconductor laser with delayed optical feedback can produce hyper-chaos dynamics [44], which makes message more secret. Because chaos carrier bandwidth generated by optoelectronic feedback lasers is limited by photodetector bandwidth bottleneck, the optical cryptosystem based on all-optical feedback has greater potential application.

Optical communication systems have number of advantages in using chaotic signals generated in a semiconductor laser with external optical feedback [14, 25]

- (i) An optical feedback induced chaotic state can have a very high dimension due to the delay induced dynamics.

- (ii) The optical feedback induced chaos can achieve a high bandwidth ranging from a few giga-hertz to tens of giga-hertz.
- (iii) The optical feedback scheme is very simple and can be easily implemented in module.

2.7 Optical Feedback Regimes

A semiconductor laser with optical feedback shows various interesting dynamic behaviors depending on the system parameters. The instabilities of the laser here are categorized into five regimes, depending on the feedback fraction [45, 39]

Regime I: Very small feedback (the feedback fraction of the amplitude is less than 0.01%) and small effects. The linewidth of the laser oscillation becomes broad or narrow, depending on the feedback fraction.

Regime II: Small, but not negligible effects (less than 0.1% and the case for $C_f > 1$, where C_f is a parameter that gives a measure of instability). Generation of the external modes gives rise to mode hopping among internal and external modes.

$$C_f = \frac{k_f}{\tau_{in}} \sqrt{1 + \alpha^2} \quad (2-1)$$

Where

k_f = Feedback fraction coefficient

τ_{in} = Round-trip time of light in the internal laser cavity

α = Linewidth-enhancement factor that plays an important role in semiconductor lasers.

In this regime, generation of the external modes gives rise to mode hopping among internal and external modes.

Regime III: This is a narrow region around 0.1% feedback. The mode-hopping noise is suppressed and the laser may oscillate with a narrow linewidth.

Regime IV: Moderate feedback (around 1%). The relaxation oscillation becomes undamped and the laser linewidth is broadened greatly. The laser shows chaotic behavior and sometimes evolves into unstable oscillations in a coherence collapse state. The noise level is enhanced greatly under this condition.

Regime V: Strong feedback regime (higher than 10% feedback). The internal and external cavities behave like a single cavity and the laser oscillates in a single mode. The linewidth of the laser is narrowed greatly.

2.8 System Synchronization and Chaotic Data

Transmission

A system of semiconductor lasers with optical feedback modeled by delay-differential equations have two types of chaos synchronization:

(i) Complete Chaos Synchronization in which the two systems, transmitter and receiver systems, are mathematically described by an equivalent set of delay-differential equations and the two systems exhibit entirely almost the same chaotic outputs when a small portion of a transmitter signal is sent to the receiver [46]. In complete chaos synchronization, the receiver system outputs the signal in advance of receiving the transmitter signal; therefore the scheme is sometimes called anticipating chaos synchronization. The frequency detuning between the transmitter and receiver lasers must be almost zero and the other parameters must also be nearly identical. Complete chaos synchronization in semiconductor laser systems is realized when the optical injection fraction is small (typically less than a few percent of the chaotic intensity variations) .

(ii) Generalized Chaos Synchronization which is based on phenomena of injection-locking characteristics and signal amplification in nonlinear systems [47,48]. In this case, the receiver system responds immediately after receiving a signal from the transmitter since the allowance of parameter mismatches for chaos synchronization in the nonlinear systems is not severe compared with the case of complete chaos synchronization.

Early work carried out on communication systems using chaos to hide a message employed electric circuits [49]. The work demonstrated experimentally that if two chaotic electric circuits are synchronized, a

message may be transmitted and recovered in two ways. Firstly, the message is used to modulate a transmitter coefficient thus causing a synchronization error at the receiver. Using the synchronization error, the modulation can be detected. Secondly, a noise like masking signal (the generated chaos) is added to the message at the transmitter and at the receiver the chaotic masking is removed. In chaotic communication system, a chaos generator is used to generate a chaotic waveform, which has the characteristics of a noise like time series and a broadband spectrum. The message to be transmitted is encoded in the time domain on the chaotic waveform through a certain chaotic encryption scheme. An identical chaos generator at the receiver end regenerates the chaotic waveform. Message decoding is then accomplished by comparing the received signal with this reproduced chaotic waveform. This basic concept is illustrated in Fig. 2.9 [50].

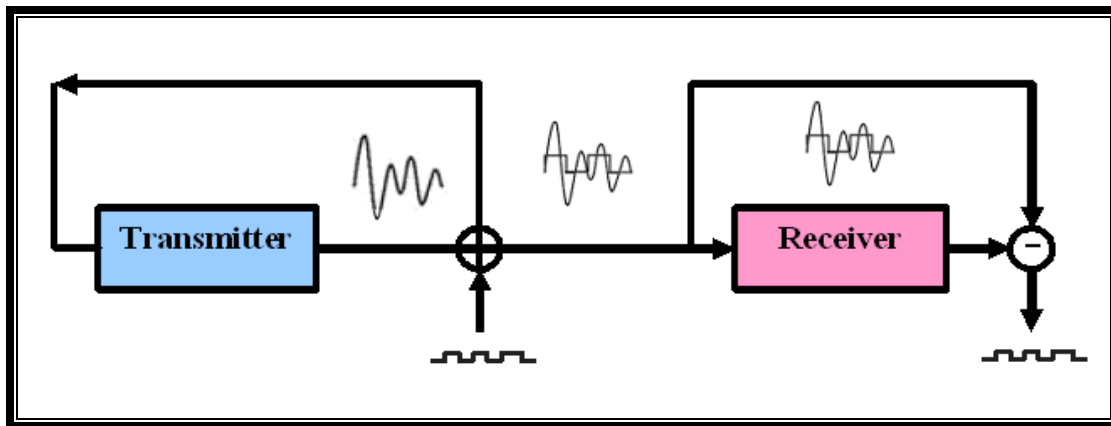


Fig. 2.9 Basic concept of synchronized chaotic communication with unidirectional coupled transmitter and receiver [50].

In laser systems, for encoding and decoding of messages, three types of synchronization schemes have been proposed [23, 41, 51]

- 1- Chaos MODulation (CMO)
- 2- Chaos MAsking (CMA)
- 3- Chaos Shift Keying (CSK)

In the CMO scheme, the chaos is modulated by the message as shown in Fig. 2.10. In the CMA scheme, the message is simply added to the chaotic signal. The CSK scheme uses two separate states corresponding to a bit sequence. The message can be decoded depending on the synchronization quality of the transmitter to the receiver.

In CMA, the transmitter and receiver lasers are driven into chaos by application of external-cavity feedback [50]. Coupling between the transmitter and receiver lasers was adjusted such that the lasers synchronized.

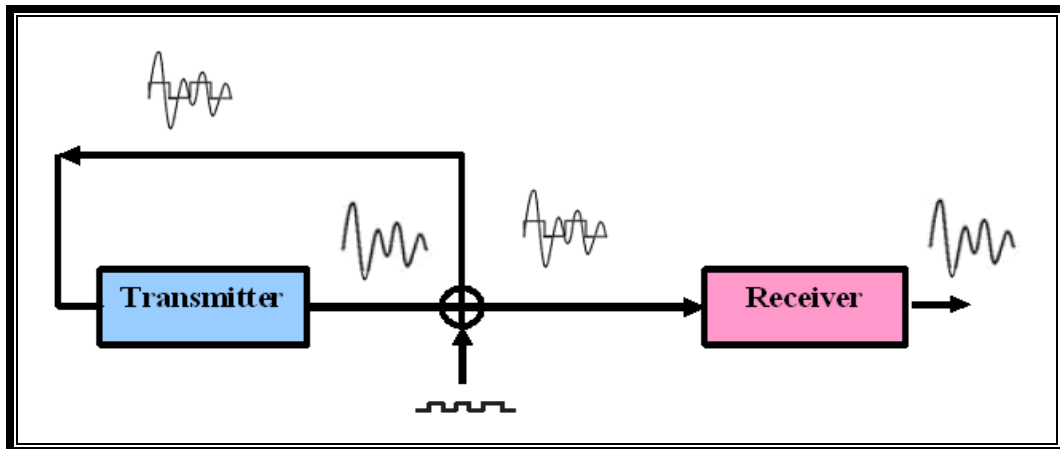


Fig. 2.10 Schematic diagram of CMO technique [51].

A square wave message was added to the chaotic transmitter by direct amplitude modulation and message recovery was achieved by subtraction of the receiver output from the receiver input as shown in Fig. 2.11. In this case the receiver laser synchronizes to the chaotic output of the message. Therefore, the input to the receiver laser contains both the chaos and the message, whilst the output from the receiver laser contains the chaos and a much reduced amplitude message.

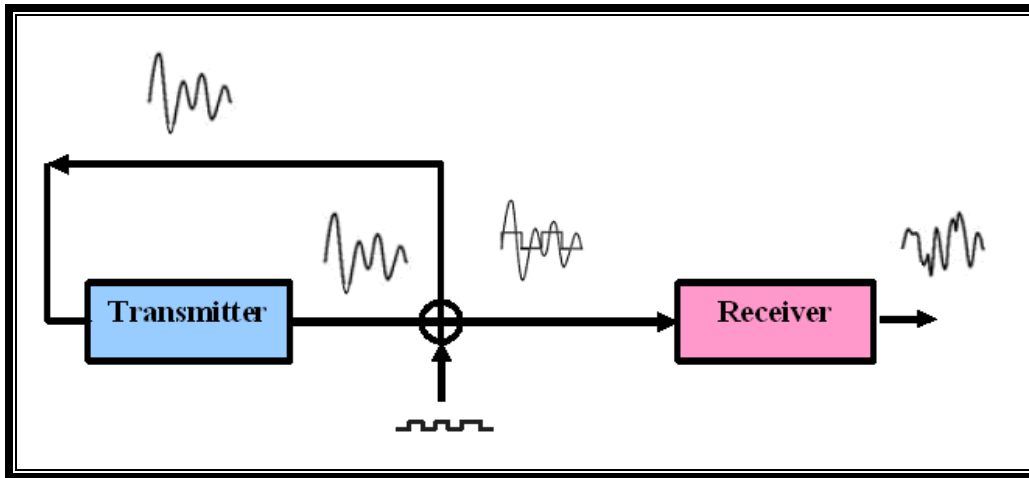


Fig. 2.11 Schematic diagram of CMA technique [50].

By subtracting the output of the receiver laser from the input to the receiver laser the message may be recovered. However, the quality of message recovery depends on the synchronization quality between the transmitter and receiver.

In CSK, two chaotic states according to binary message sequences are generated in time as the two values for a certain system parameter and they are transmitted to the receiver system [52]. For example, the bias injection current is selected as a parameter and two chaotic states corresponding to two different bias injection currents are used. In the receiver system, two chaotic systems are prepared and each system responds and synchronizes with the corresponding chaotic state of the transmitter. Then the message is decoded by the comparison of the signals from the outputs in the two systems. Fig. 2.12 shows a schematic diagram of CSK.

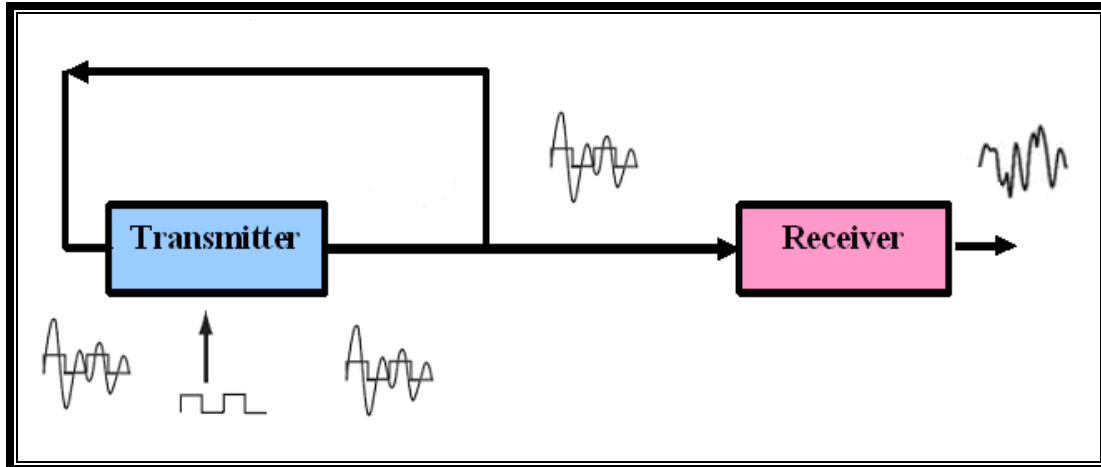


Fig. 2.12 Schematic diagram of CSK technique [52].

2.9 Principles of Modulation

In general, a semiconductor laser generates a continuous photonic beam. However, as in its simplest mode of operation a semiconductor laser produces a continuous wave (CW) or beam of light, this beam carries no information other than frequency or wavelength. However, when the beam is modulated, then it could carry data at a currently commercially available data rate of up to 40Gb/s and research continues to seek higher modulation rates [53].

Modulation is the action of temporally altering one or more of the parameters of the photonic signal. In optical communications, such parameters are phase, frequency, polarization, and amplitude. When the phase is modulated, the method is called phase shift keying (PSK); when the frequency is modulated, it is called frequency shift keying (FSK); when the state of polarization is modulated, it is called state-of polarization shift keying (SoPSK); and when the amplitude is modulated, it is called amplitude shift keying (ASK). The latter case includes the intensity modulation with direct detection (IM/DD) and the on-off keying (OOK) modulation methods. The On-Off Keying (OOK) modulation is an

amplitude-modulation (AM) method. The modulating signal closely resembles a square pulse that acts as a shutter on the laser beam, hence its name [53,54]. The OOK method generates a stream of pulses that are then transmitted over the fiber. Fig. 2.13 illustrates a binary pulse train, the spectrum of the square modulating signal, and the spectrum of the modulated signal. When the logic “one” is lighted for the full period T , this OOK is termed nonreturn-to-zero (NRZ), and when for a fraction of the period (such as $\frac{1}{3}$ or $\frac{1}{2}$), it is termed return-to-zero (RZ). As a consequence, NRZ modulation utilizes the full period as compared with RZ, which is a fraction of it. Thus, the energy within a NRZ bit is much more than the energy in a RZ bit, if everything else remains the same. This implies that either the NRZ signal can propagate to longer distances than the RZ or the NRZ power level can be lowered, for the same distance.

OOK modulation can be used in both coherent and direct detection. However, coherent detection requires phase stability. As a consequence, the laser source cannot be directly modulated, as this may shift the signal phase and add chirp. To reduce this, the signal amplitude is modulated externally using a titanium-diffused LiNbO₃ waveguide in a Mach–Zehnder configuration or a semiconductor directional coupler based on electro-absorption multiquantum well (MQW) properties and structures. On the other hand, direct detection does not require stable phase; however, direct modulation may alter the spectral content of the source, which raises other issues.

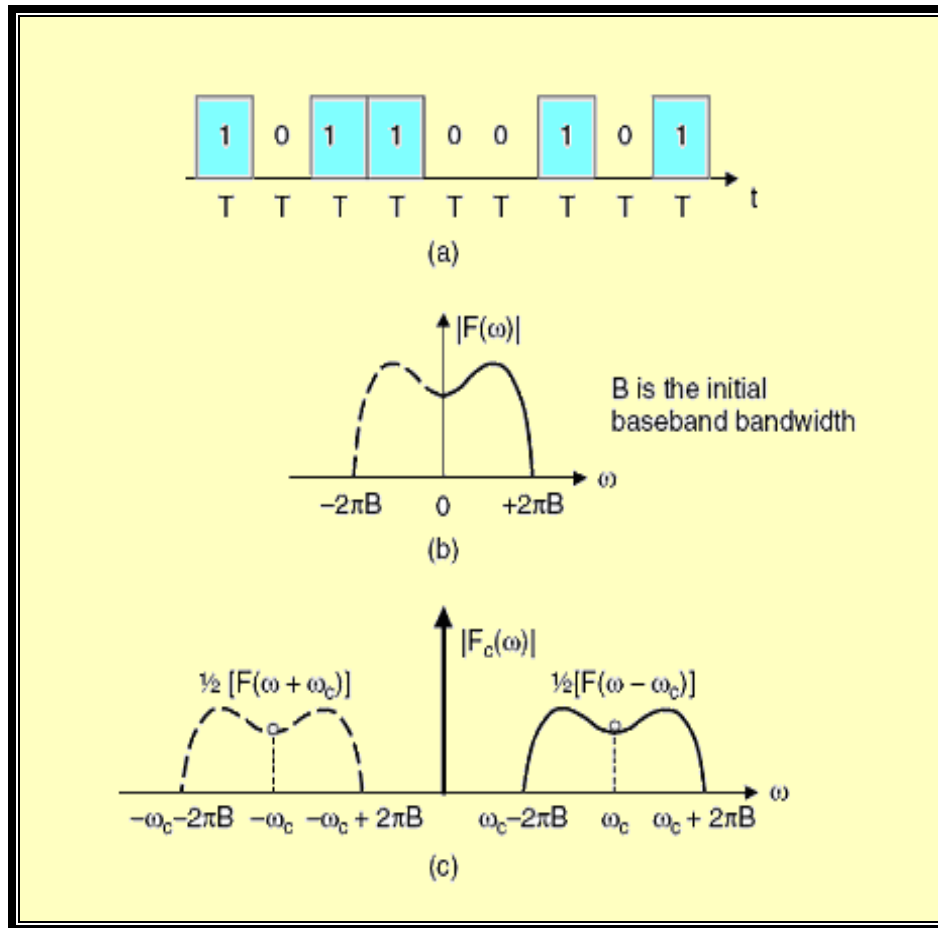


Fig. 2.13 Schematic diagram of OOK modulation
 (a) A binary OOK pulse train (b) the spectrum of the square modulating pulse
 (c) the spectrum of the modulated signal [53].

In optical communications, the modulation method plays a key role in the

- (i) Optical power coupled into the fiber
- (ii) Bit-rate limits
- (iii) Transportable amount of information per channel
- (iv) Dispersion limits
- (v) Fiber-span limit
- (vi) Linear and nonlinear contributing effects
- (vii) Overall signal-to-noise ratio and bit error rate
- (viii) Reliability of signal detection and receiver penalty

Chapter Three

Modeling of Chaotic Data Transmission

3.1 Introduction

In this chapter, the optical feedback technique is applied to the semiconductor laser in order to generate chaos signals. The techniques of chaos coding and decoding messages in optical communication system are presented.

3.2 Semiconductor Laser Rate Equations

The operating characteristics of semiconductor laser are well described by a set of rate equations that govern the interaction of photons and electrons inside the active region. For a single-mode laser, these rate equations are [30, 55]

$$\frac{dP}{dt} = GP + \frac{\Gamma}{V} R_{sp} - \frac{P}{\tau_p} \quad (3.1)$$

$$\frac{dN}{dt} = \frac{I}{qV} - \frac{N}{\tau_c} - \frac{1}{\Gamma} GP \quad (3.2)$$

$$\frac{d\phi}{dt} = \frac{1}{2} \alpha \left[G_N (N - N_{th}) - \frac{1}{\tau_p} \right] \quad (3.3)$$

where

P = Photon density in the active region

G = Net rate of stimulated emission

Γ = Confinement factor

V = Active region volume

R_{sp} = Rate of spontaneous emission coupled into the lasing mode

τ_p = Photon life time

N = Carrier density

I = Injected current

q = Electron charge

τ_c = Carrier life time

ϕ = Phase of the electric field

α = Linewidth enhancement factor

N_{th} = Carrier density at threshold

$$G_N = \frac{\partial G}{\partial N}$$

The net rate of stimulated emission can be expressed as

$$G = \Gamma v_g g \tag{3.4}$$

where

v_g = Group velocity

g = Material gain at the mode frequency

$$g = a(N - N_o)(1 - \epsilon P) \tag{3.5}$$

where N_o is the carrier density at transparency, where a is the differential gain coefficient, and ϵ is a parameter characterizes the strength of the material gain nonlinearity. Therefore,

$$G = G_N (N - N_o)(1 - \varepsilon p) \quad (3.6)$$

or

$$G = \Gamma \nu_g g(N - N_o) \text{ at threshold} \quad (3.7)$$

The parameter $G_N = \frac{\partial G}{\partial N}$ is then given by

$$G_N = \Gamma \nu_g a(1 - \varepsilon P) \quad (3.8)$$

The rate of spontaneous emission coupled to the lasing mode is related to G by [30]

$$R_{sp} = n_{sp} G \quad (3.9)$$

where n_{sp} is the spontaneous emission factor.

Further, τ_p is related to cavity loss α_{cav} by

$$\frac{1}{\tau_p} = \nu_g \alpha_{cav} \quad (3.10)$$

If R1 and R2 are the reflectivities of the laser facets, L is the external cavity length, then τ_p can be expressed as

$$\tau_p = \frac{1}{\nu_g \alpha_{cav}} = \frac{1}{\nu_g (\alpha_{int} + \alpha_m)} \quad (3.11)$$

where α_{cav} is the total cavity loss, α_{int} is the internal loss and α_m is the mirror loss.

$$\alpha_m = \frac{1}{2L} \ln \left(\frac{1}{R_1 R_2} \right) \quad (3.12)$$

The carrier life time τ_c can be expressed as

$$\frac{1}{\tau_c} = A_{nr} + BN + C_c N^2 \quad (3.13)$$

where

A_{nr} = Nonradiative recombination rate

B = Radiative recombination coefficient

C_c = Auger recombination coefficient

3.3 Threshold Solutions

The threshold solution takes a particularly simple form if spontaneous emission is neglected by setting $R_{sp}=0$. Below threshold, $G\tau_p < 1$, $P=0$, and

$N = \tau_c \frac{I}{q}$. The threshold is reached at a current for which $G\tau_p = 1$ or

$G = \frac{1}{\tau_p}$. The carrier population is then clamped to the threshold value

$$N_{th} = N_o + \frac{I}{G_N \tau_p} \quad (3.14)$$

The threshold current is given by

$$I_{th} = \frac{qVN_{th}}{\tau_c} \quad (3.15)$$

$$I_{th} = \frac{qV}{\tau_c} \left(N_o + \frac{I}{G_N \tau_p} \right) \quad (3.16)$$

3.4 Steady-State Solutions

The steady state solution is obtained by setting all time derivatives to zero $\frac{dP}{dt} = \frac{dN}{dt} = 0$

From eqns. 3.1 and 3.2

$$P = -\frac{\Gamma}{V} \frac{R_{sp}}{G - \frac{1}{\tau_p}} \quad (3.17)$$

$$I = qV \left(\frac{N}{\tau_c} + \frac{GP}{\Gamma} \right) \quad (3.18)$$

When the laser operates above threshold $I > I_{th}$, the photon number increase linearly with I therefore

$$I = I_{th} + \frac{qV}{\Gamma} GP \quad (3.19)$$

$$P = \frac{\Gamma \tau_p}{qV} (I - I_{th}) \quad (3.20)$$

The emitted power from each facet P_{out} is given by

$$P_{out} = \frac{V}{\Gamma} P \eta_{int} \nu_g \alpha_m h \nu \quad (3.21)$$

where

η_{int} = Internal quantum efficiency

$h \nu$ = Photon energy

When $R_1=R_2$ then

$$P_{out} = \frac{V}{2\Gamma} P \eta_{int} \nu_g \alpha_m h \nu \quad (3.22)$$

Substituting eqns. (3.20) and (3.11) into eqn. (3.22) yields

$$P_{out} = \frac{h \nu}{2q} \eta_d (I - I_{th}) \quad (3.23)$$

where η_d is the differential quantum efficiency

$$\eta_d = \frac{\eta_{int} \alpha_m}{\alpha_m + \alpha_{int}} \quad (3.24)$$

The output power emitted from each facet can also expressed as [38]

$$P_{out} = \frac{1}{2} \hbar \omega_o v_g \alpha_m V E^2 \quad (3.25)$$

where

$$E^2 = \frac{P}{\Gamma}$$

ω_o = Angular frequency

3.5 Semiconductor Laser Rate Equations with Optical Feedback

Consider a single-mode semiconductor laser subjects to optical feedback through an external mirror as shown in Fig. 3.1. In this case the phase of the feedback electric field of the optical signal plays a key role in determining the dynamic of the laser diode (LD). Therefore, complex electric field with amplitude $|E|$ and phase ϕ is used rather than photon density in the laser rate equations.

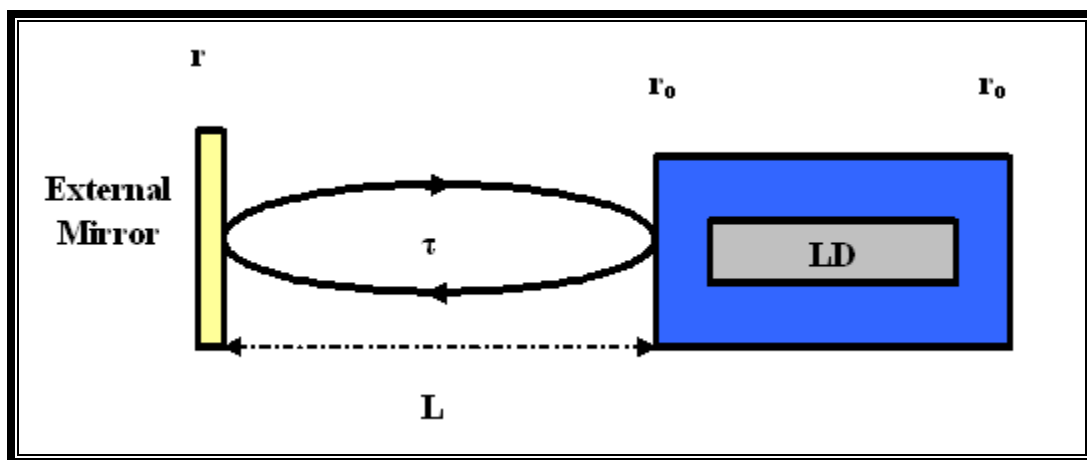


Fig. 3.1. Schematic diagram of the semiconductor laser with external optical feedback.

By means of electric field, the laser rate equations become [30]

$$\frac{dE(t)}{dt} = \frac{1}{2} G_N (N(t) - N_{th}) E(t) \quad (3.26)$$

$$\frac{d\phi(t)}{dt} = \frac{1}{2} \alpha G_N (N(t) - N_{th}) \quad (3.27)$$

$$\frac{dN(t)}{dt} = \frac{I}{qV} - \frac{N(t)}{\tau_c} - G_N (N(t) - N_o) |E(t)|^2 \quad (3.28)$$

where $E(t)$ is the complex electric field.

To generate chaotic pulses in the laser diode, the terms shown below are added to the right hand side of eqns. 3.26 and 3.27, respectively.

$$\begin{aligned} & \frac{k_f}{\tau_{in}} E(t - \tau) \cos \theta(t) \\ & - \frac{k_f}{\tau_{in}} \frac{E(t - \tau)}{E(t)} \sin \theta(t) \end{aligned}$$

where

k_f = Feedback coefficient

$$\theta(t) = \omega_o \tau + \phi(t) - \phi(t - \tau) \quad (3.29)$$

$$\tau = \frac{2L}{c} \text{ Round trip time in the external laser cavity}$$

L =Length of the external cavity

c =Speed of light in vacuum

ω_o =Laser frequency at solitary oscillation

These terms represents the optical feedback effect on the laser diode [56,57].

Therefore, eqns. (3.1) and (3.2) become:

$$\frac{dE(t)}{dt} = \frac{1}{2} G_N (N(t) - N_{th}) E(t) + \frac{k_f}{\tau_{in}} E(t - \tau) \cos \theta(t) \quad (3.30)$$

$$\frac{d\phi(t)}{dt} = \frac{1}{2} \alpha G_N (N(t) - N_{th}) - \frac{k_f}{\tau_{in}} \frac{E(t - \tau)}{E(t)} \sin \theta(t) \quad (3.31)$$

$$\frac{dN(t)}{dt} = \frac{I}{qV} - \frac{N(t)}{\tau_c} - G_N (N(t) - N_o) |E(t)|^2 \quad (3.32)$$

The feedback coefficient k_f is computed from:

$$k_f = (1 - r_o^2) \frac{r}{r_o} \quad (3.33)$$

where

r_o = Amplitude reflectivities for the front and back facet (the amplitude reflectivities of the front and back facet are assumed to be the same).

r = Amplitude reflectivity of the external mirror

3.6 Communication System Model

The model under consideration is shown in Fig. 3.2. Two semiconductor lasers having almost the same device characteristics as light sources. The transmitter laser system has an optical feedback loop, whereas the receiver system is a solitary laser and it is a stable system by itself and has no optical feedback loop (this type of system is an open-loop system).

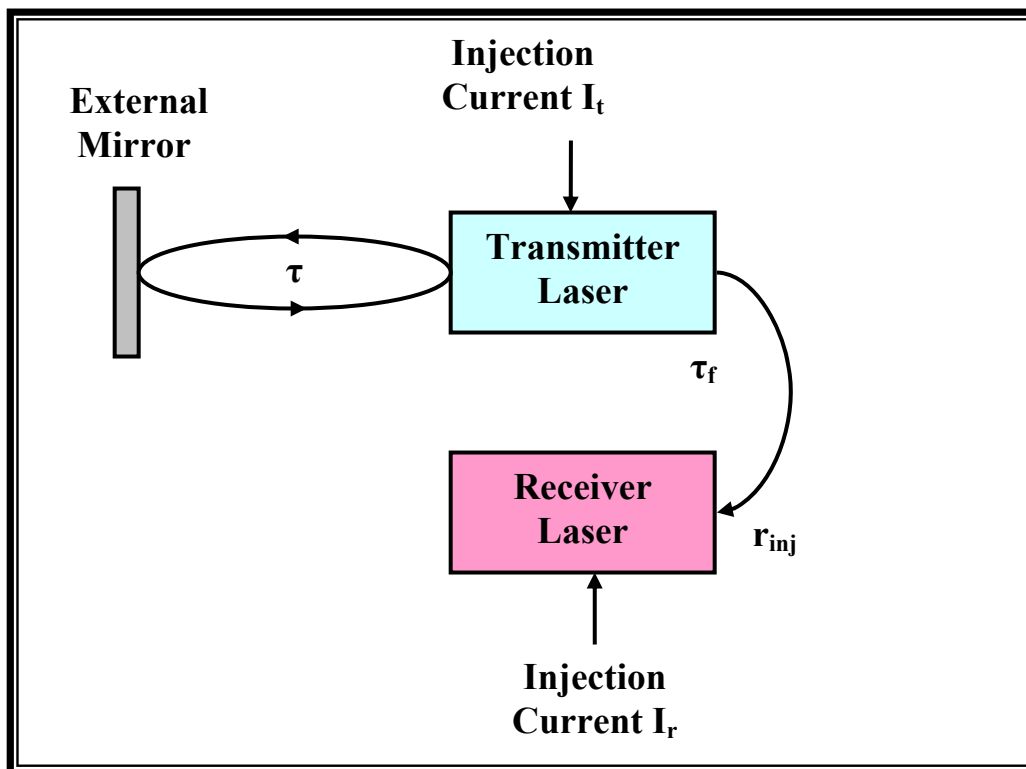


Fig. 3.2 Schematic diagram of a chaos optical feedback communication system.

The transmitter laser exhibits chaotic oscillations depending on the feedback parameters. With chaotic signal injection from the transmitter to the receiver, the receiver laser synchronizes with the transmitter laser under appropriate conditions.

The system is described by the following set of rate equations.

(i) For the transmitter side

$$\frac{dE_t(t)}{dt} = \frac{I}{2} G_{N,t} (N_t(t) - N_{th,t}) E_t(t) + \frac{k_f}{\tau_{in}} E_t(t - \tau) \cos \theta(t) \quad (3.34)$$

$$\frac{d\phi_t(t)}{dt} = \frac{I}{2} \alpha_t G_{N,t} (N_t(t) - N_{th,t}) - \frac{k_f}{\tau_{in}} \frac{E_t(t - \tau)}{E_t(t)} \sin \theta(t) \quad (3.35)$$

$$\frac{dN_t(t)}{dt} = \frac{I}{qV} - \frac{N_t(t)}{\tau_c} - G_{N,t} (N_t(t) - N_{o,t}) |E_t(t)|^2 \quad (3.36)$$

(ii) For the receiver side

$$\frac{dE_r(t)}{dt} = \frac{I}{2} G_{N,r} (N_r(t) - N_{th,r}) E_r(t) + \frac{k_{inj}}{\tau_{in}} E_r(t - \tau_f) \cos \zeta(t) \quad (3.37)$$

$$\frac{d\phi_r(t)}{dt} = \frac{I}{2} \alpha_r G_{N,r} (N_r(t) - N_{th,r}) - \frac{k_{inj}}{\tau_{in}} \frac{E_r(t - \tau_f)}{E_r(t)} \sin \zeta(t) \quad (3.38)$$

$$\frac{dN_r(t)}{dt} = \frac{I}{qV} - \frac{N_r(t)}{\tau_c} - G_{N,r} (N_r(t) - N_{o,r}) |E_r(t)|^2 \quad (3.39)$$

The subscripts t and r refer to transmitter and receiver, respectively. Further

k_{inj} = Injection coefficient or fraction from the transmitter to the receiver

τ_f = Transmission time of light from the transmitter to the receiver

$$k_{inj} = (1 - r_o^2) \frac{r_{inj}}{r_o} \quad (3.40)$$

where

r_{inj} = Injection rate

$$\zeta(t) = \omega_{o,t} \tau_f + \phi_r(t) - \phi(t - \tau_f) - \Delta\omega t \quad (3.41)$$

where

$\Delta\omega$ = Angular frequency detuning between the two lasers

$$\Delta\omega = \omega_{o,t} - \omega_{o,r}$$

$\omega_{o,t}$ = Transmitter laser frequency at solitary oscillation

$\omega_{o,r}$ = Receiver laser frequency at solitary oscillation

To achieve complete chaos synchronization in the system, the conditions below must be achieved [7]

$$k_f = k_{inj}$$

$$\Delta\omega = 0$$

The effects of k_f , k_{inj} , τ , $\Delta\omega$ and receiver current on the system characteristics are obtained.

3.7 Message Encoding and Decoding

The schematic diagram of communication systems using chaos as carrier to transmit messages is shown in Fig. 3.3. The encryption method considered in this work is CMA. In Fig. 3.3, $x(t)$ represents the chaotic carrier which is generated in the transmitter side (transmitter output), $m(t)$ is a pseudorandom bit sequence which represents the input message which is transmitted to the receiver, $k(t)$ is a secret key, $y(t)$ represents the output of the receiver, and $n(t)$ represents the production of subtraction of the receiver output from the receiver input.

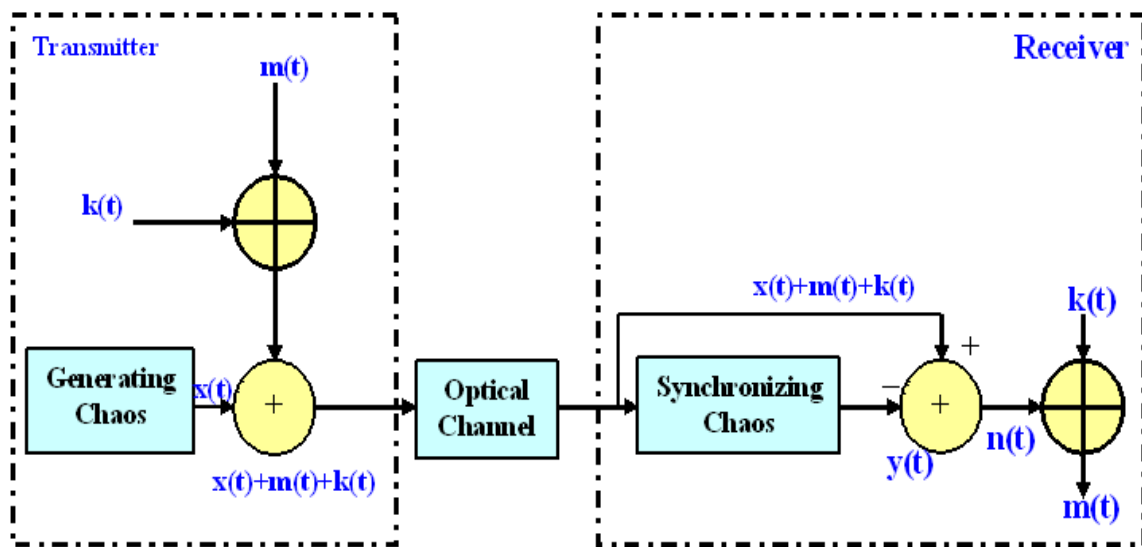


Fig.3.3 Schematic diagram of encoding-decoding system.

A secret key is used with message $m(t)$ to increase the security of the system. That means that the receiver which has this key can only receive the transmitted message correctly. Fig. 3.4 shows an example of

the binary message data used in the simulation while a sequence key is shown in Fig. 3.5.

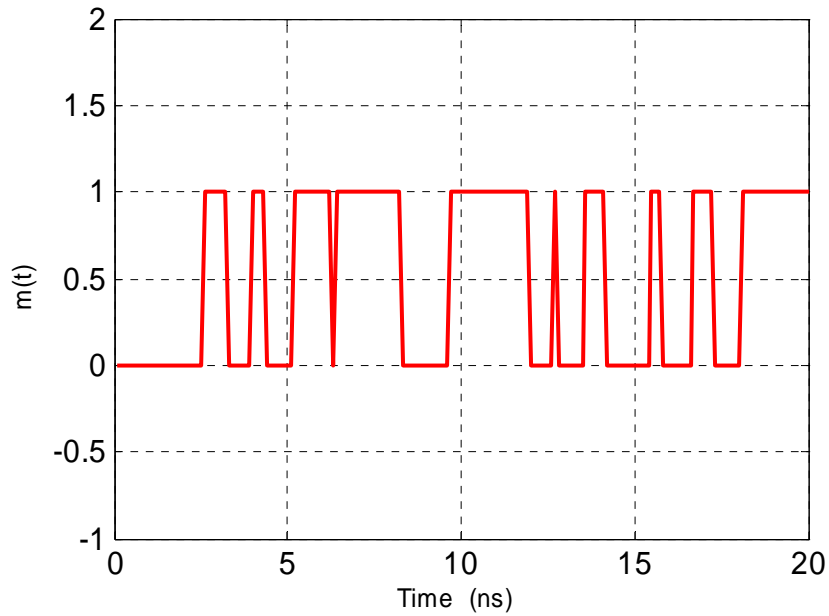


Fig. 3.4 Transmit message m(t).

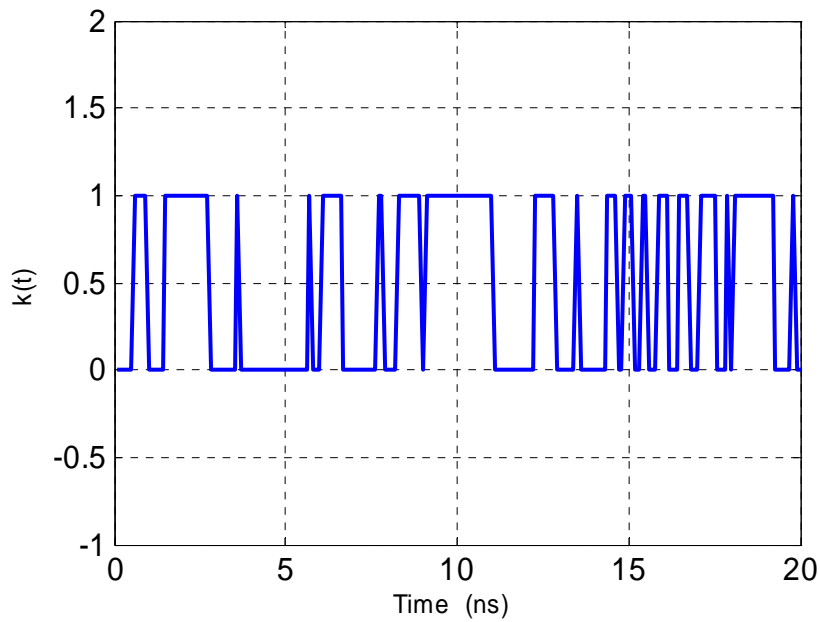


Fig. 3.5 Secret key k(t).

Chapter Four

Results and Discussion

4.1 Introduction

In this chapter, the results of semiconductor laser operating without optical feedback and in the presence of optical feedback in order to generate chaos signal are presented and discussed. The rate equations are solved to find out the carrier density $N(t)$, electric field $E(t)$, and field phase $\phi(t)$. The results are used to examine the synchronization between the transmitter and receiver lasers in optical communication system. Also a message transmitted and received in security fashion is achieved by this system.

Results are obtained using MATLAB program version 7.0 to access the influence of various structure and system parameters on the characteristics of chaotic optical feedback system.

The parameters values used in the computations are listed in Table 4.1 and they are related to a semiconductor laser operating at wavelength of 1550nm.

4.2 Free Running Operation

In this section, eqns. (3.1)-(3.3) are numerically calculated by employing fourth-order Runge-kutta algorithm with matlab program. Figure 4.1 illustrates the flowchart used for these calculations. When the semiconductor laser operates at free running (without any feedback i.e. $k_f = 0$) and by using the parameters values listed in Table 4.1, the characteristics are as shown in Figs. 4.2a-d. The injection current I is taken as $I = 1.4I_{th}$ where I_{th} is calculated by eqn. 3.15. The active region volume is calculated as

$$V = dlw$$

Where

d = Active region thickness

l = Active region length

w = Active region width

The output power is calculated from eqn. 3.25.

Table 4.1 Parameters values of 1550nm semiconductor laser used in the simulation [7].

Symbol	Parameter	Value
λ	Laser wavelength	1550nm
α	Linewidth enhancement factor	3
I_{th}	Threshold current	20.5 mA
$I_{t,r}$	Transmitter-receive injection current	$1.4 * I_{th}$
G_N	Gain coefficient	$8.4 * 10^{-13} \text{ m}^3 \text{ s}^{-1}$
N_{th}	Threshold carrier density	$2.018 * 10^{24} \text{ m}^{-3}$
N_o	Carrier density a transparency	$1.400 * 10^{24} \text{ m}^{-3}$
l	Active region length	300 μm
d	Active region thickness	0.2 μm
w	Active region width	2 μm
μ_g	Group refractive index	4
μ	Effective mode index	3.4
V	Active region volume	$1.2 * 10^{-16} \text{ m}^3$
τ_p	Photon life time	1.97ps
τ_c	Carrier life time	2.04 ns
τ_{in}	Round trip time in laser cavity	8ps
$f_{o,r,t}$	Transmitter-Receive frequency at free running	384.615THz
τ	Round trip time of light in the external cavity	1ns
r_o	Amplitude reflectivities for the front & back facet	0.556

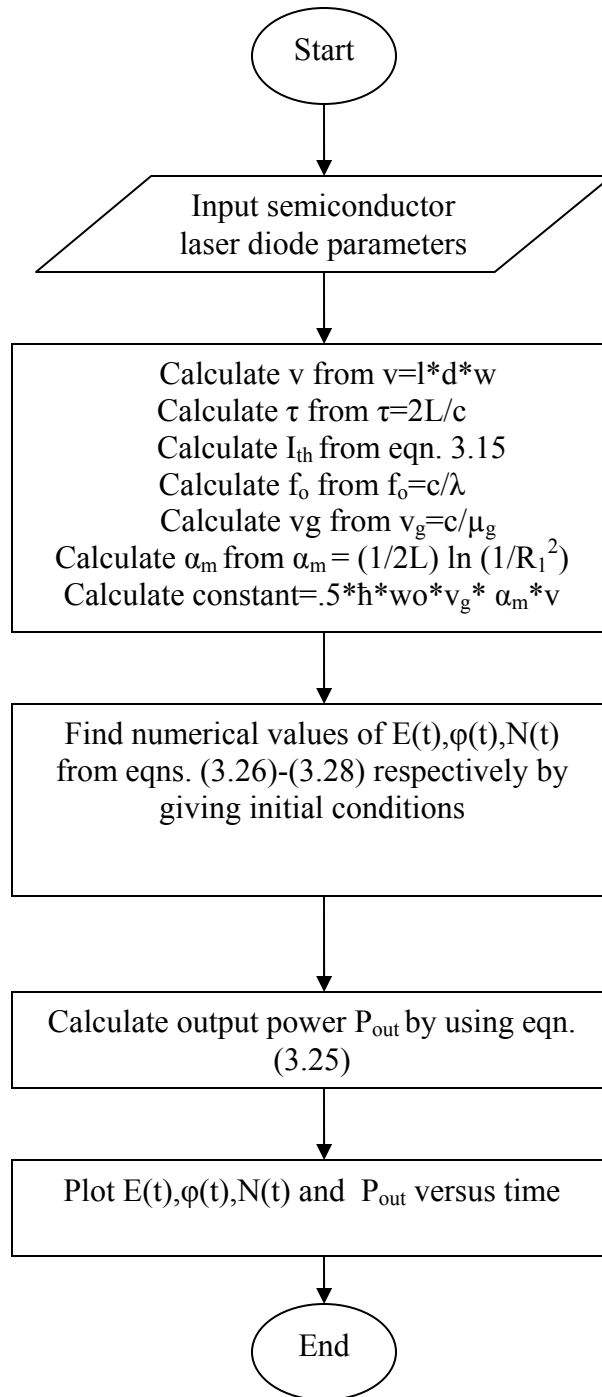
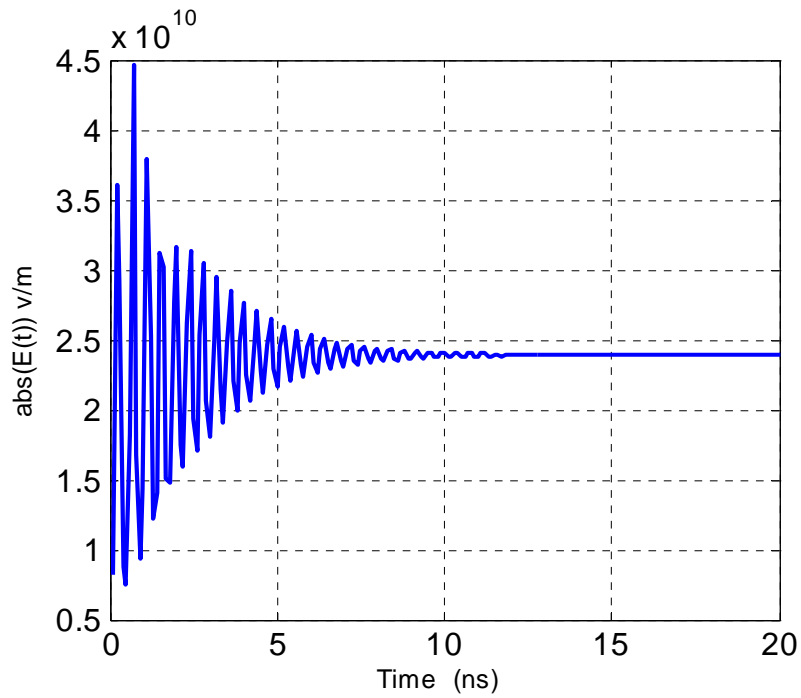
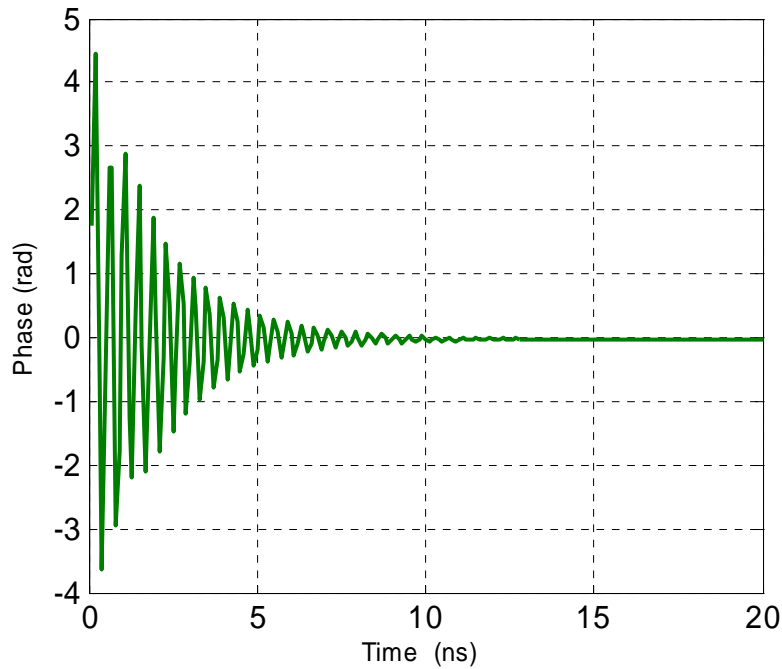


Fig. 4.1 Flowchart of the free running operation program.



(a)

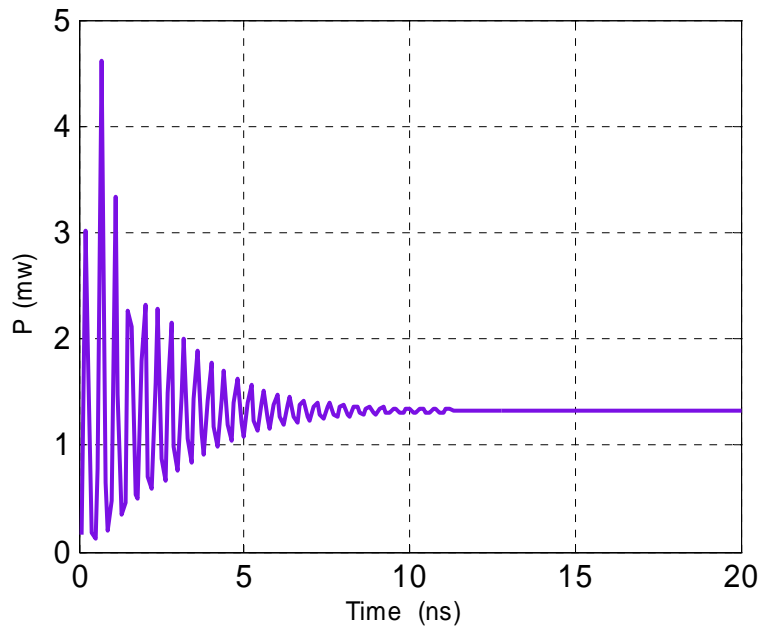


(b)

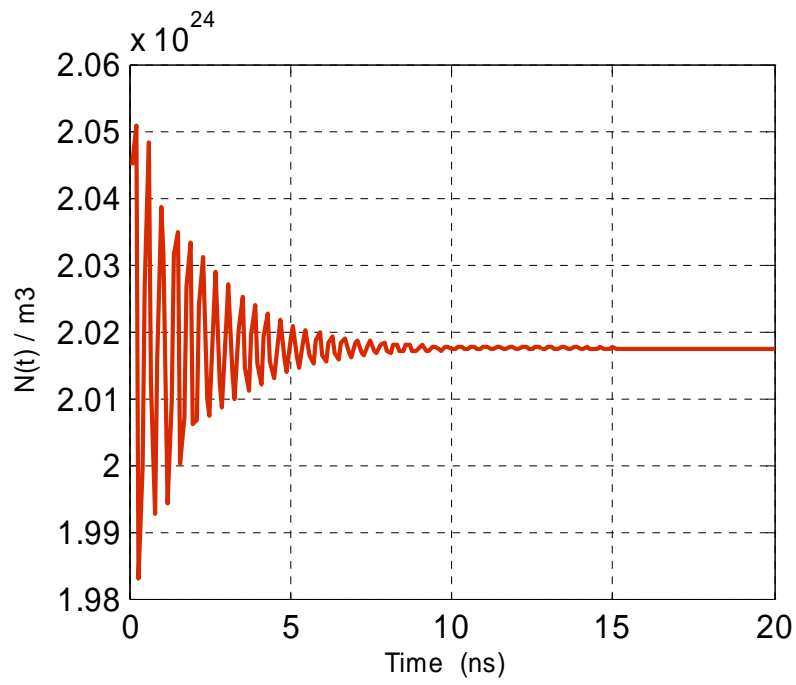
Fig.4.2. Characteristics of semiconductor laser at free running operation

(a) Electric field (b) Phase of electric field (c) Output power.

(d) Carrier density.



(c)



(d)

Fig. 4.2. (Continued).

Figs. 4.2a-d represent the operating characteristics for the solitary laser. The dynamics of the output power representation display characteristics of relaxation oscillations. The frequency of the relaxation oscillation generally depends on the amount of pumping which is applied to the laser via the injection current I . The relaxation oscillations are damped after a few ns and the laser approaches its stable steady state operating conditions.

4.3 Chaos Generation

When semiconductor lasers are subject to optical feedback their output dynamics often become chaotic. The external mirror and external cavity length play an important role in the chaotic dynamics of semiconductor lasers. Chaotic dynamics occur even for a small change of the external mirror position, compatible with the optical wavelength (λ). For a small change, the laser output shows periodic undulations (period of $\lambda/2$) and exhibits a chaotic bifurcation within the period. Actually, there is also hysteresis either for an increase or decrease of the external cavity length.

In this section, a continuous bifurcation from steady state to periodic states then quasiperiodic states and finally chaos are observed as the external reflectivity r is increase from 1% to 2 % and external cavity length L is varied from 15cm to 30cm. Simulation results are first reported when frequency detuning $\Delta\omega = 0$. The effect of $\Delta\omega$ will be reported later. Figure 4.3 illustrates the flowchart used to achieve the simulation results in this section.

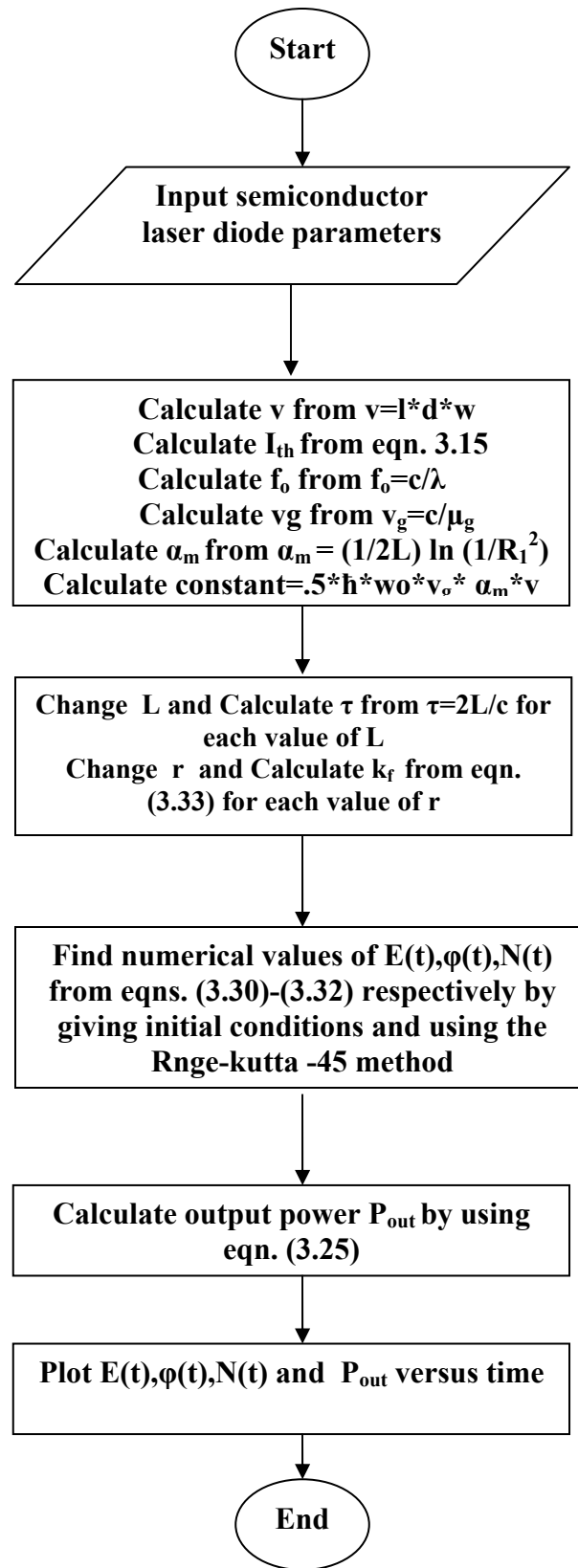
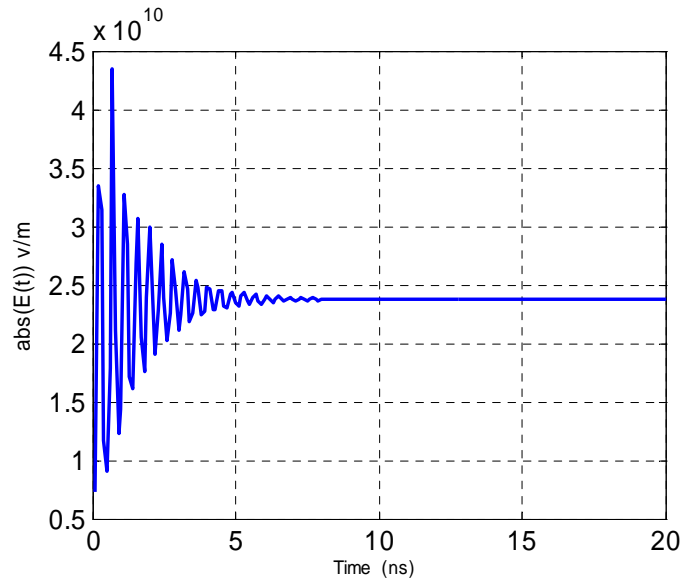


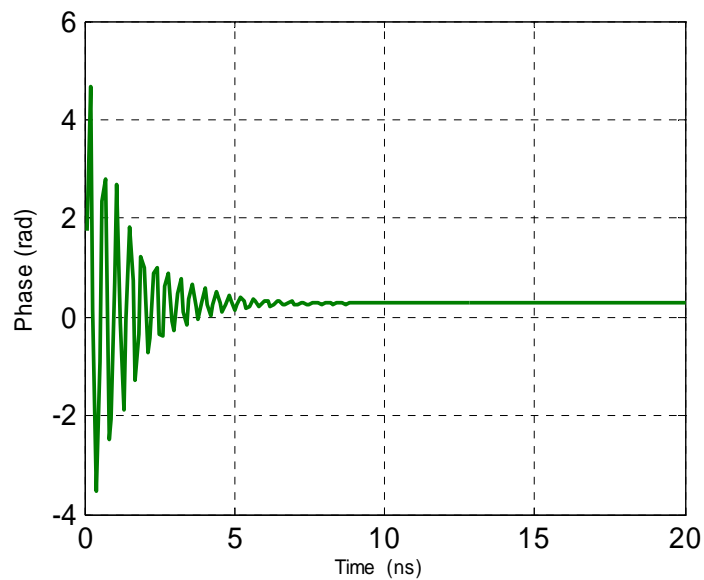
Fig. 4.3 Flow chart of the generation chaotic signal program.

4.3.1 Effect of External Cavity Length

When $L=15$ cm and $r = 1\%$, $|E(t)|$, $\phi(t)$, output power, $N(t)$, and the attractor according to the eqns. (3.30-3.32) are shown in Figs. 4.4a-e.



(a)

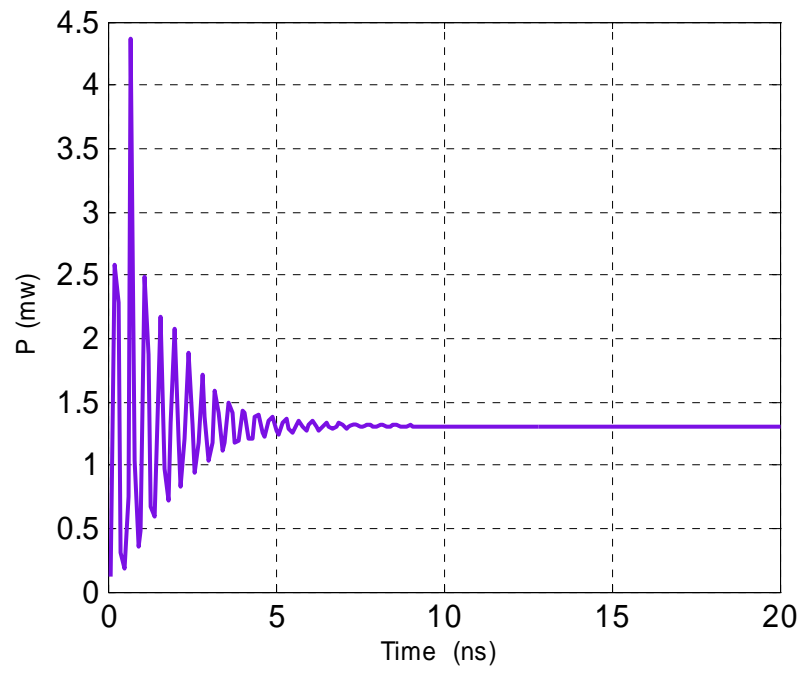


(b)

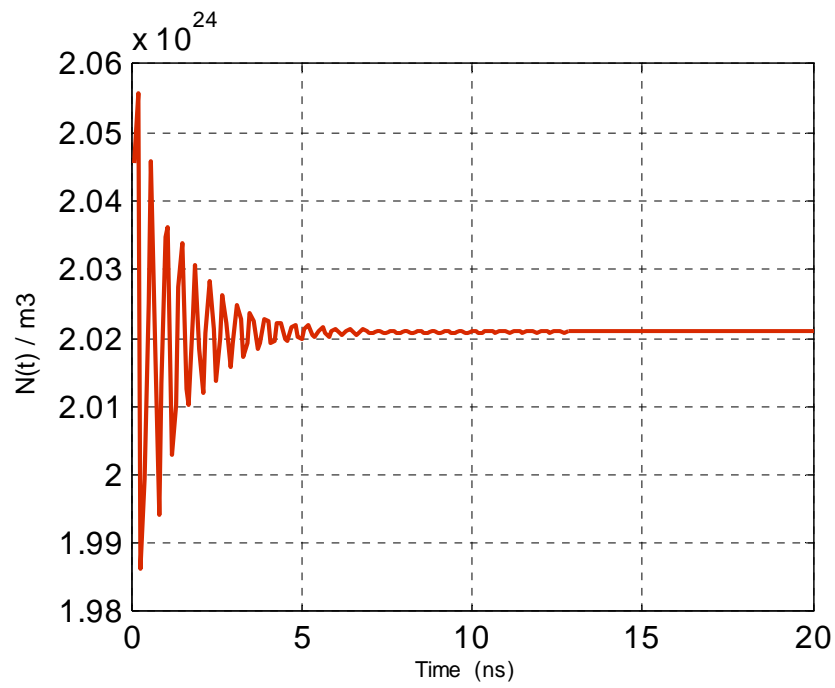
Fig.4.4. Characteristics of semiconductor laser with optical feedback when

$r = 1\%$ and $L=15$ cm

- (a) Electric field (b) Phase of electric field (c) Output power (d) Carrier density
(e) Attractor.

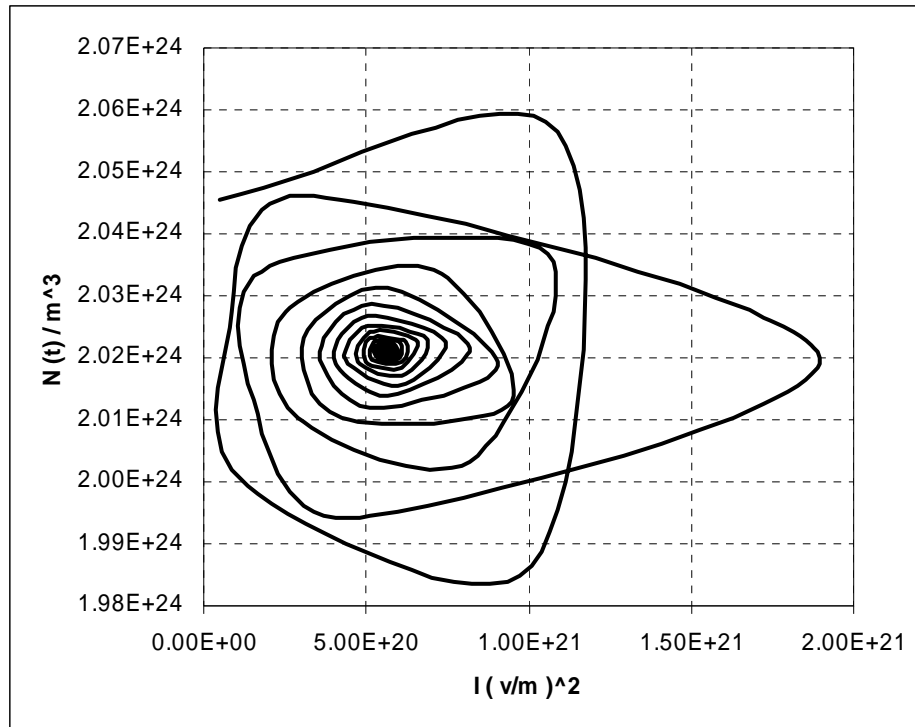


(c)



(d)

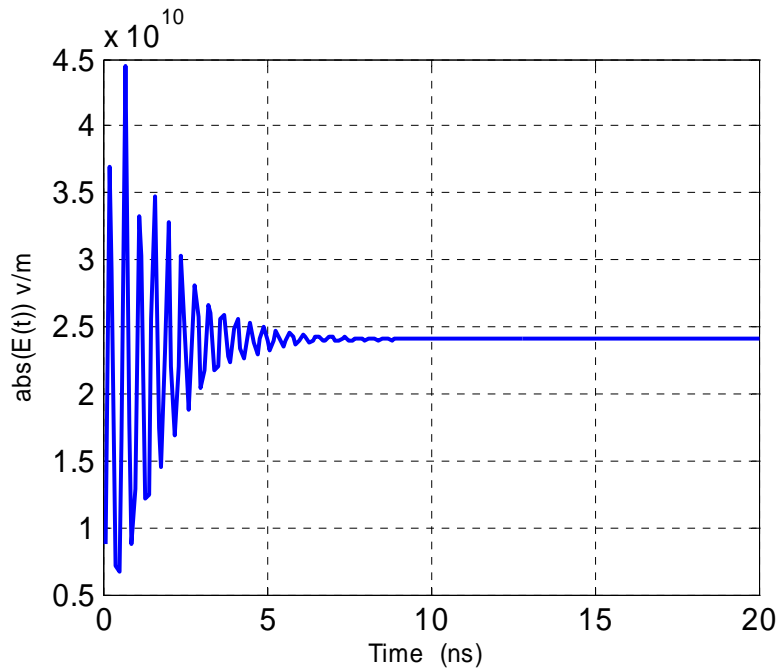
Fig. 4.4 (continued).



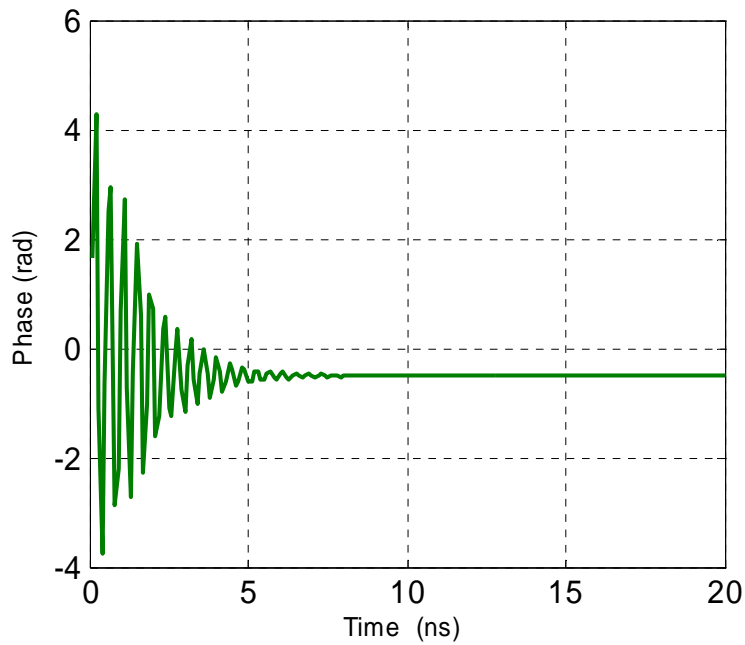
(e)

Fig. 4.4 (continued).

When L increases to 18 cm while r is fixed at 1%, the parameters $|E(t)|$, $\phi(t)$, output power, $N(t)$, and the attractor are as shown in Figs. 4.5a-e.



(a)



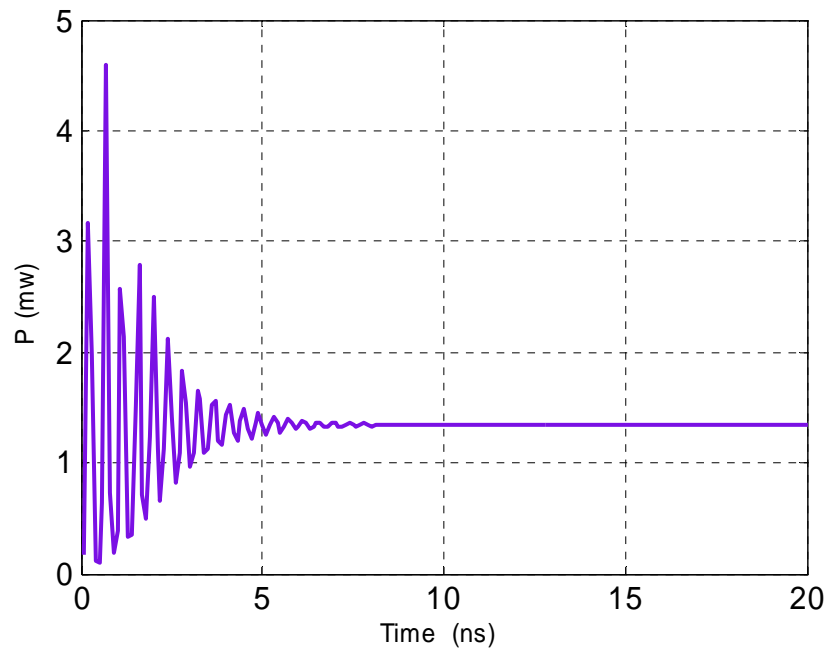
(b)

Fig.4.5. Characteristics of semiconductor laser with optical feedback when

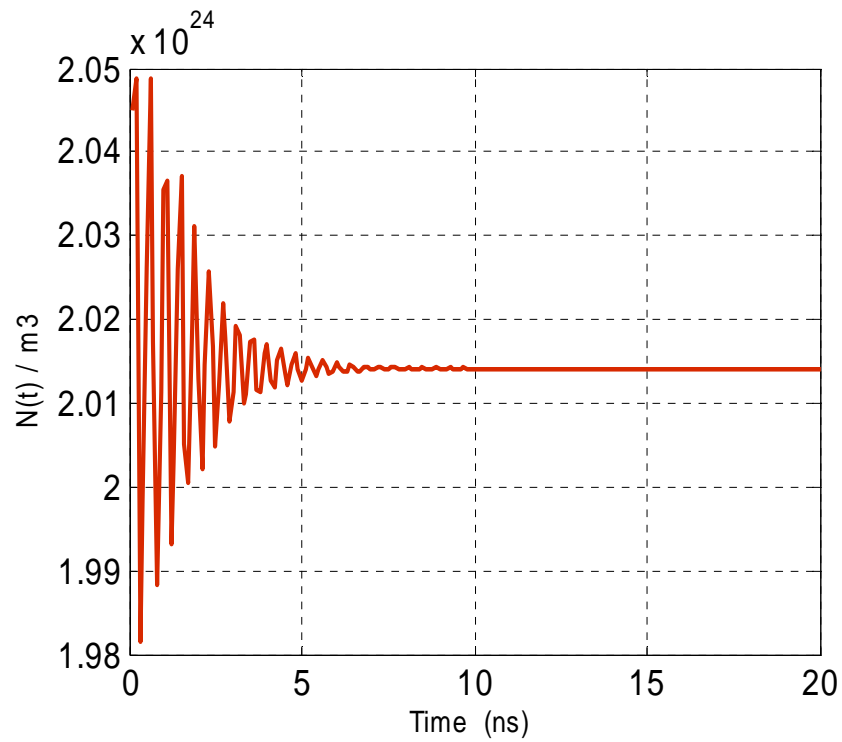
$$r=1\% \text{ and } L=18\text{cm}$$

(a) Electric field (b) Phase of electric field (c) Output power (d) Carrier density

(e) Attractor.

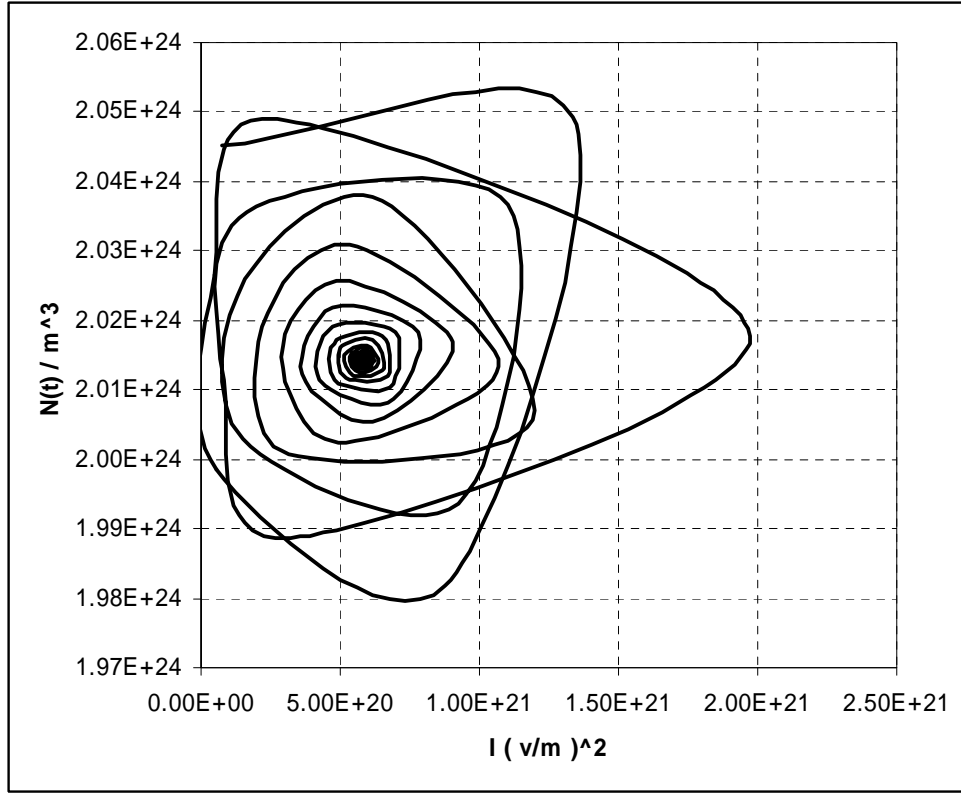


(c)



(d)

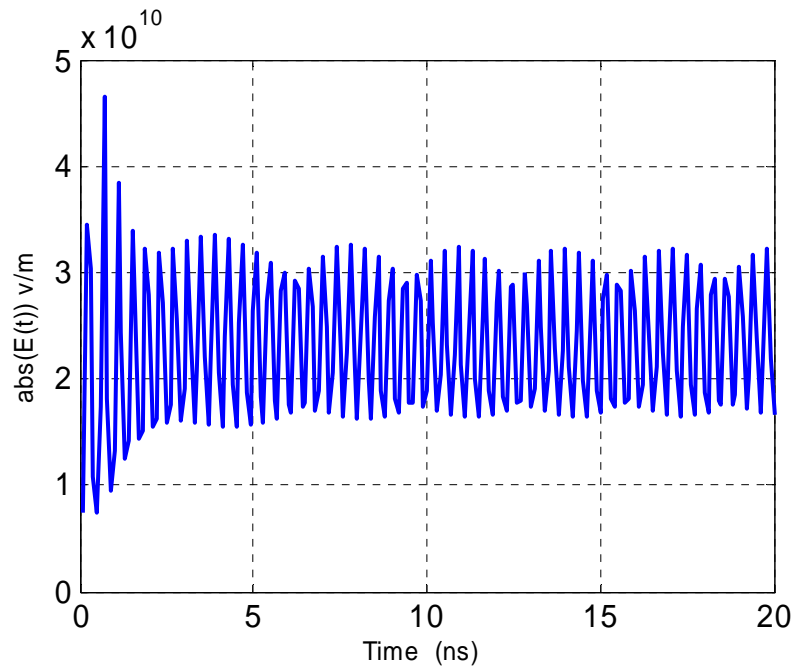
Fig. 4.5 (continued).



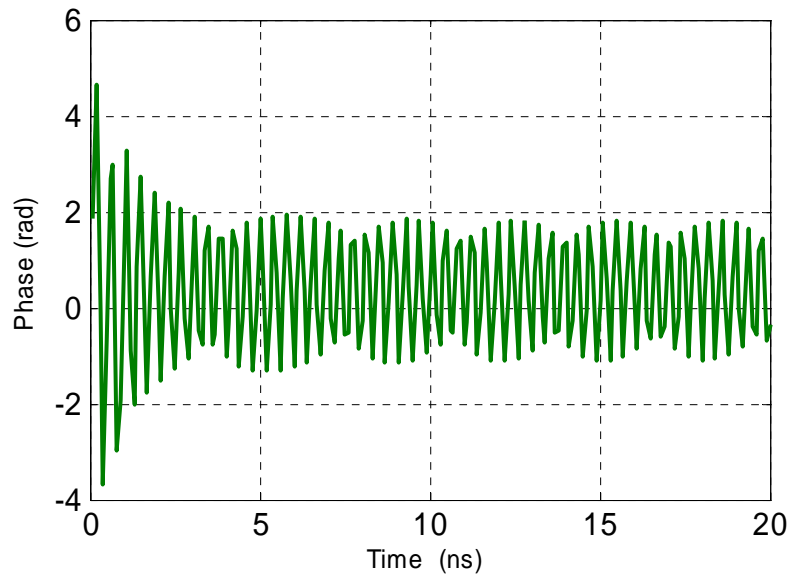
(e)

Fig.4.5 (continued).

The calculations are repeated for $L=20$ cm and the results are shown in Figs. 4.6a-e.



(a)

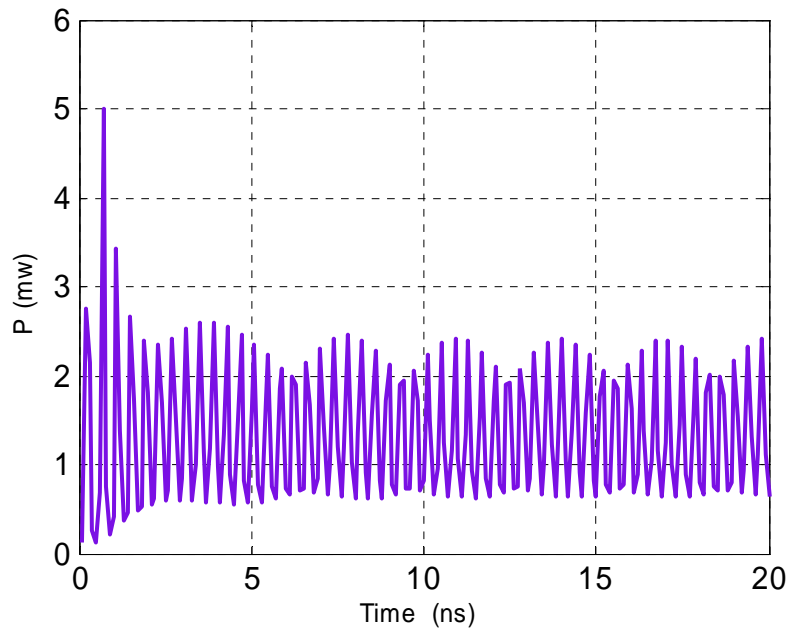


(b)

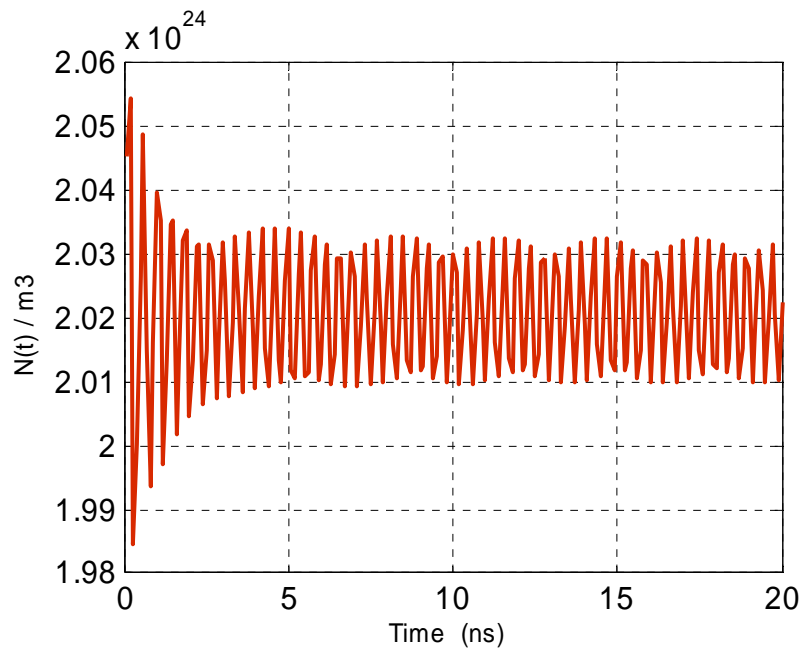
Fig.4.6. Characteristics of semiconductor laser with optical feedback when

$$r = 1\% \text{ and } L = 20\text{cm}$$

- (a) Electric field (b) Phase of electric field (c) Output power (d) Carrier density
 (e) Attractor.

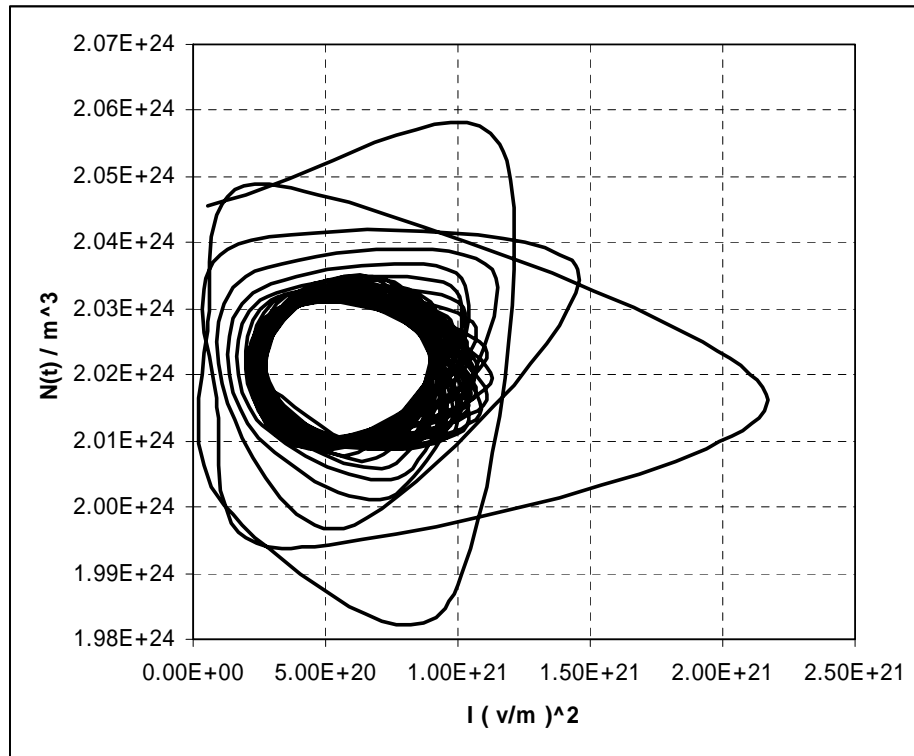


(c)



(d)

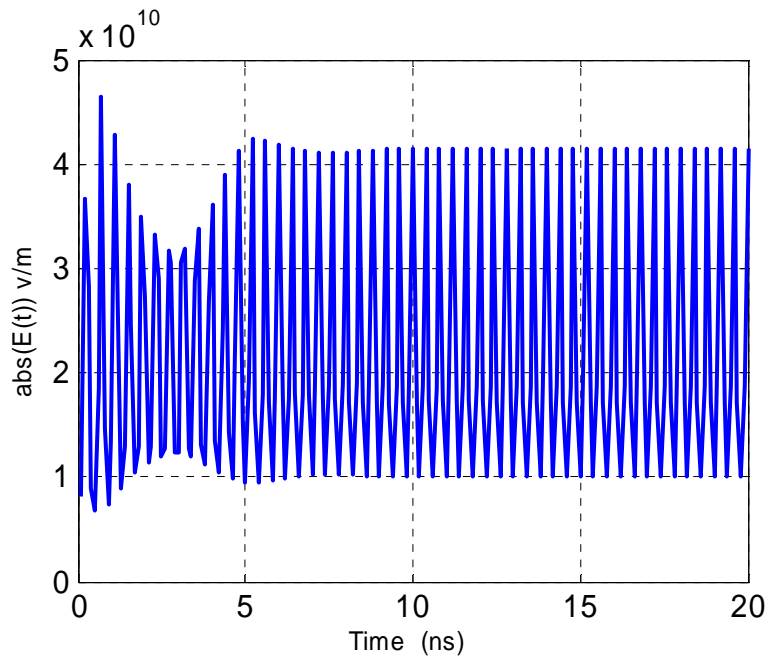
Fig. 4.6 (continued).



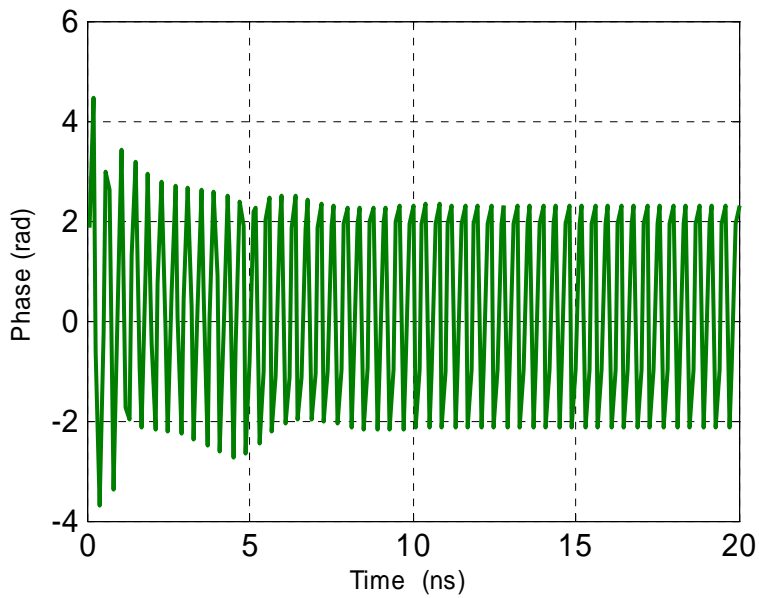
(e)

Fig. 4.6 (continued).

Another case when L increases to 25 cm with the same value of r is used. The characteristics of semiconductor laser are shown in Figs. 4.7a-e.



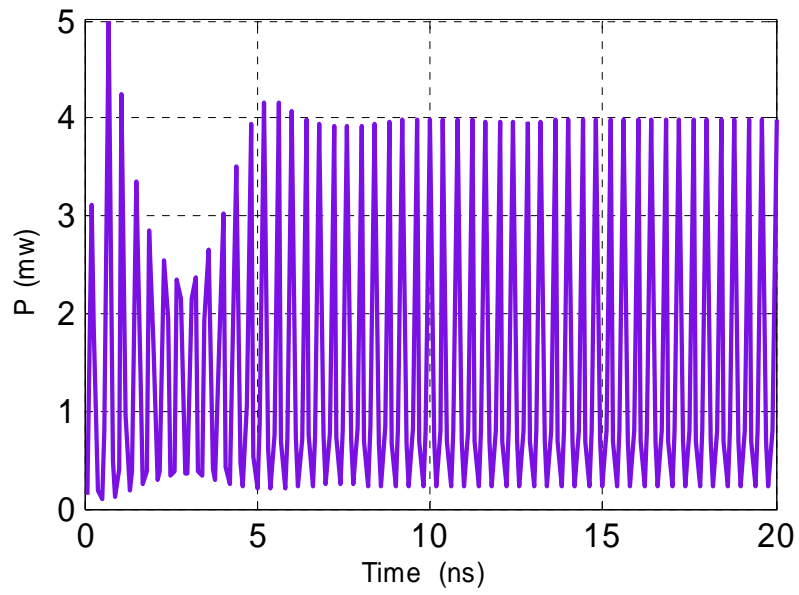
(a)



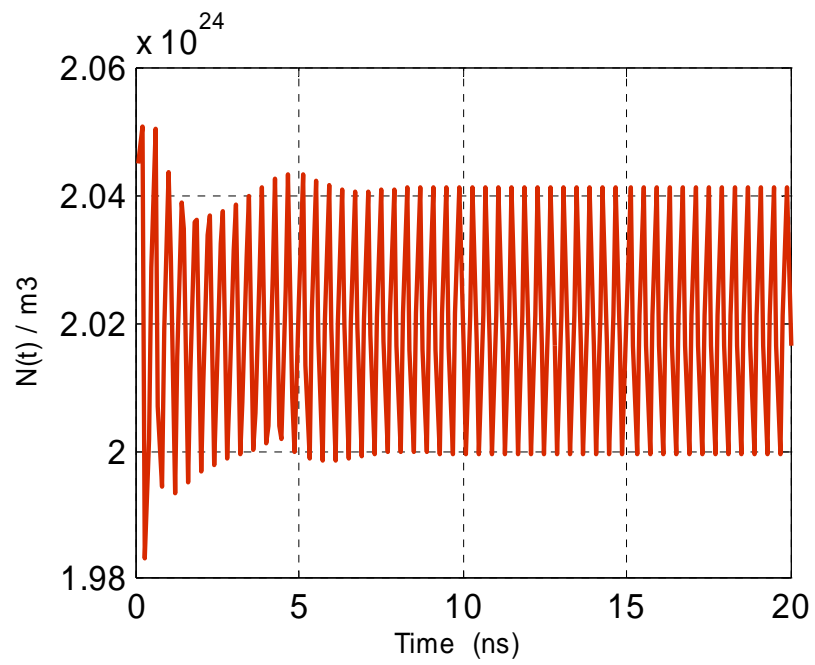
(b)

Fig.4.7. Characteristics of semiconductor laser with optical feedback when $r=1\%$ and $L=25\text{cm}$

- (a) Electric field (b) Phase of electric field (c) Output power (d) Carrier density
(e) Attractor.

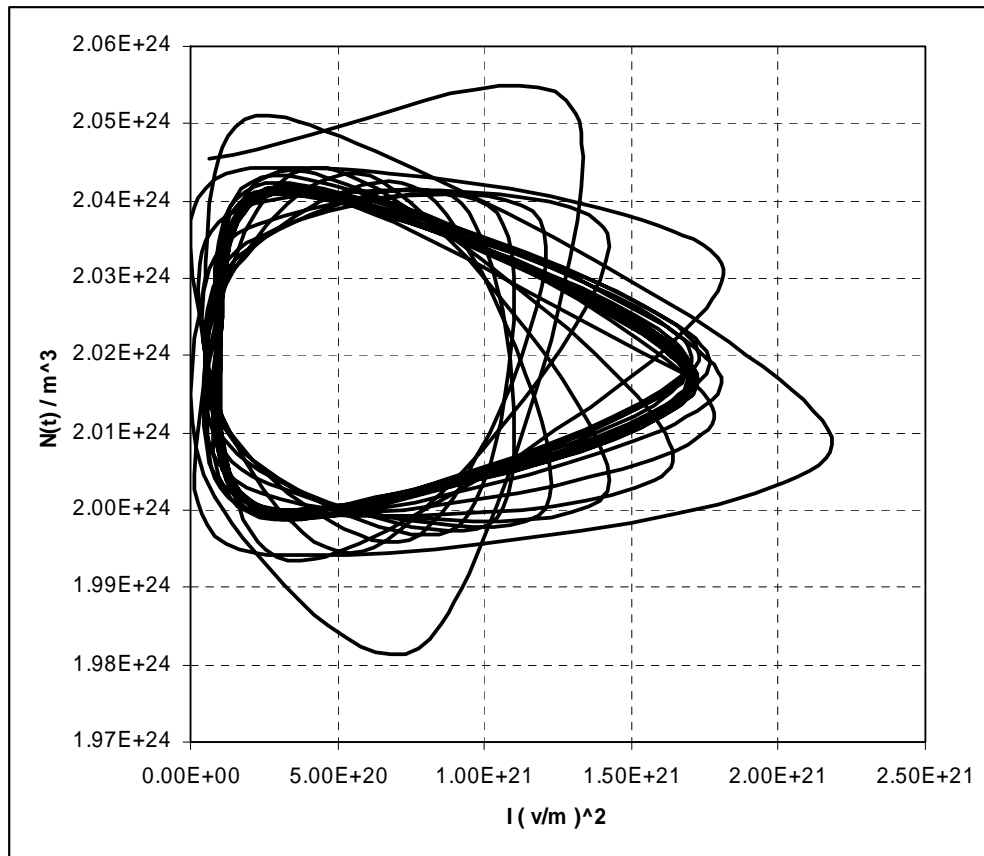


(c)



(d)

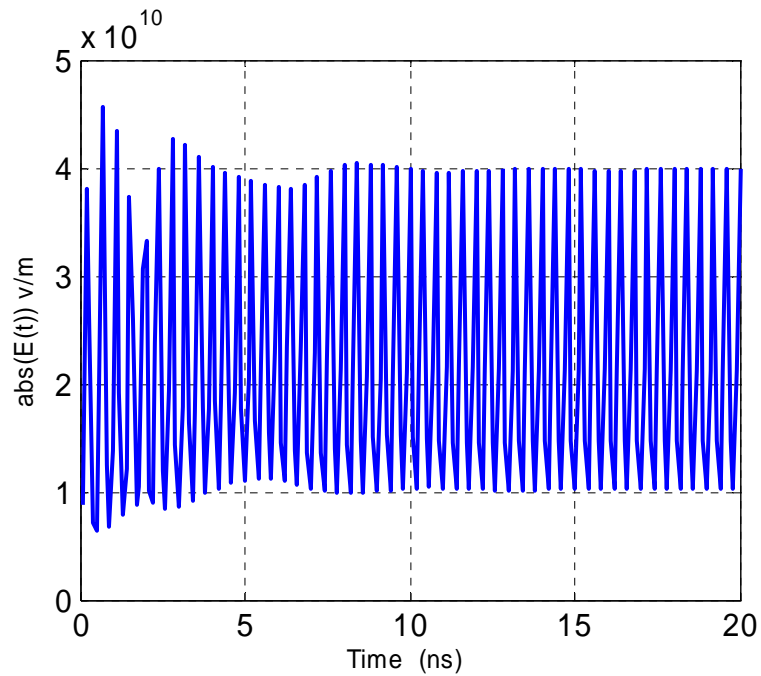
Fig. 4.7 (continued).



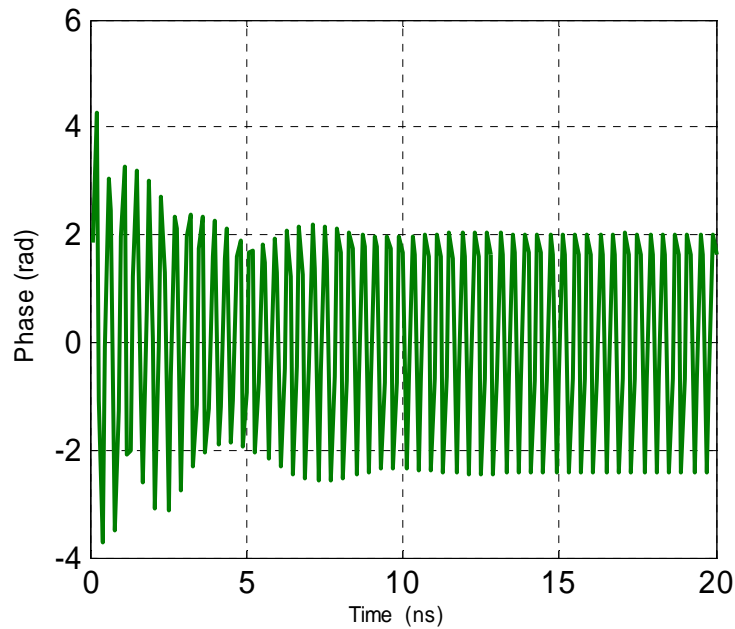
(e)

Fig. 4.7 (continued).

Finally when $L=30$ cm, the parameters $|E(t)|$, $\phi(t)$, output power, $N(t)$, and the attractor are as shown in Figs. 4.8a-e.



(a)



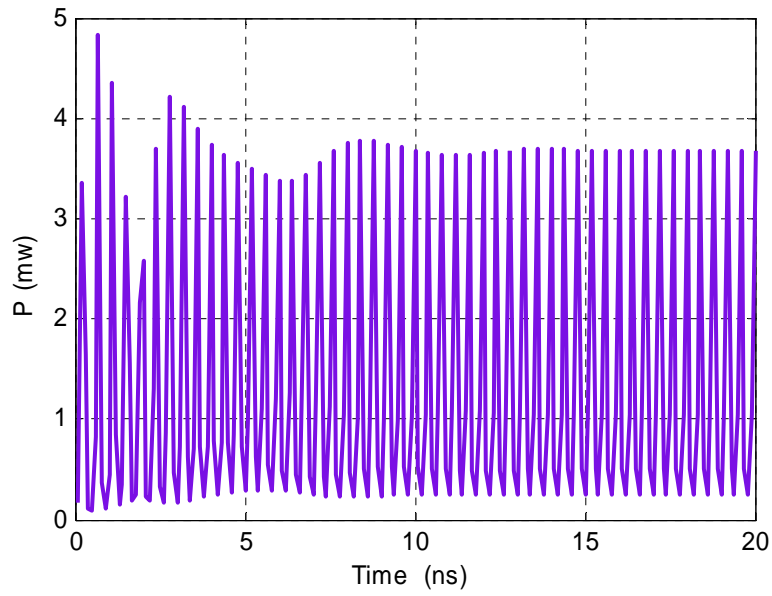
(b)

Fig.4.8. Characteristics of semiconductor laser with optical feedback when

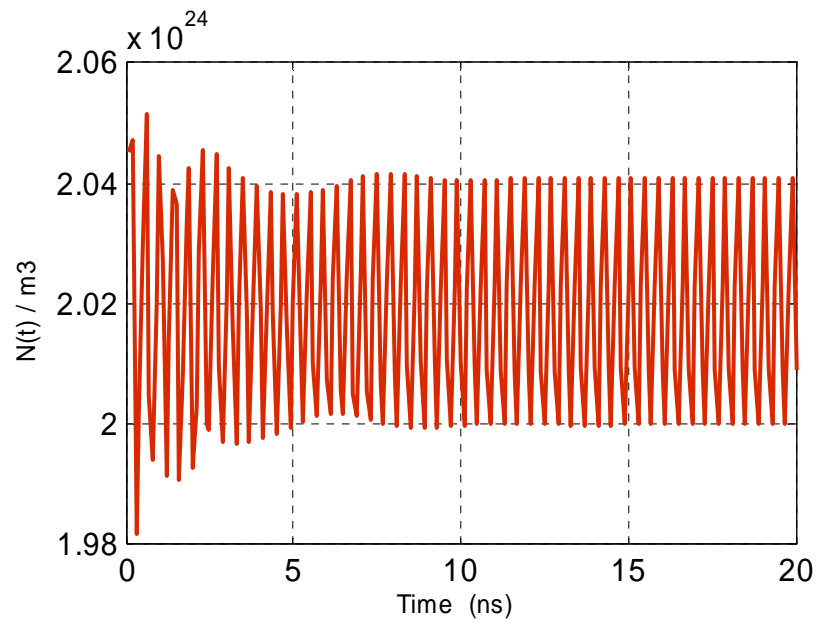
$$r=1\% \text{ and } L=30\text{cm}$$

(a) Electric field (b) Phase of electric field (c) Output power (d) Carrier density

(e) Attractor.

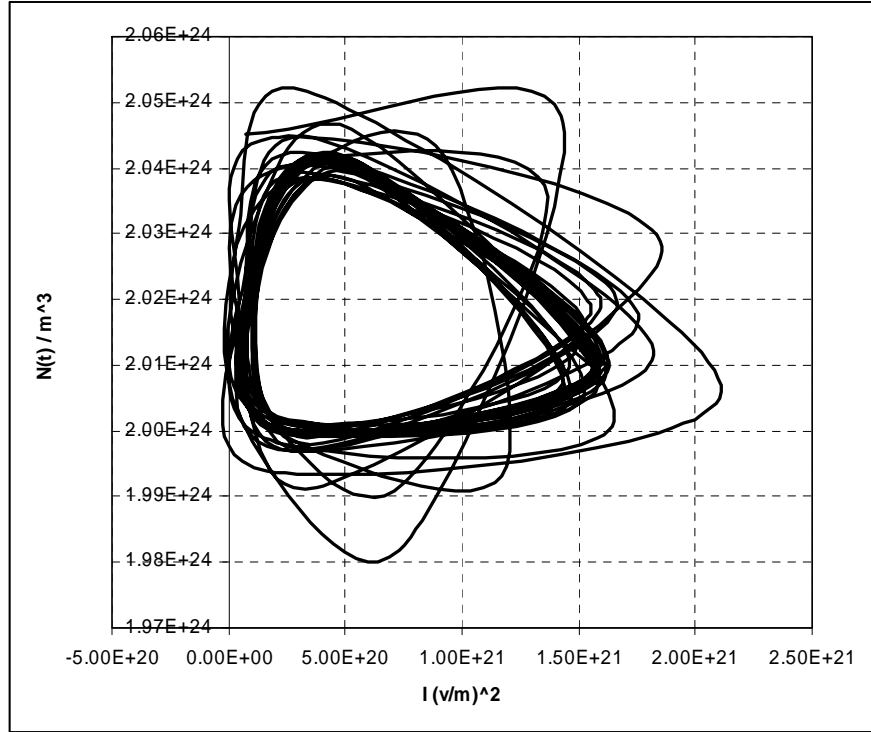


(c)



(d)

Fig. 4.8 (continued).



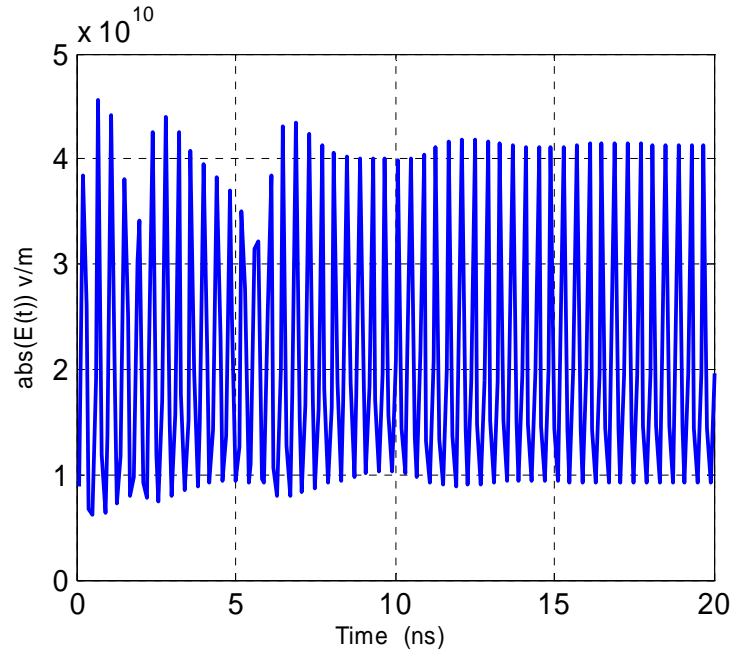
(e)

Fig. 4.8 (continued).

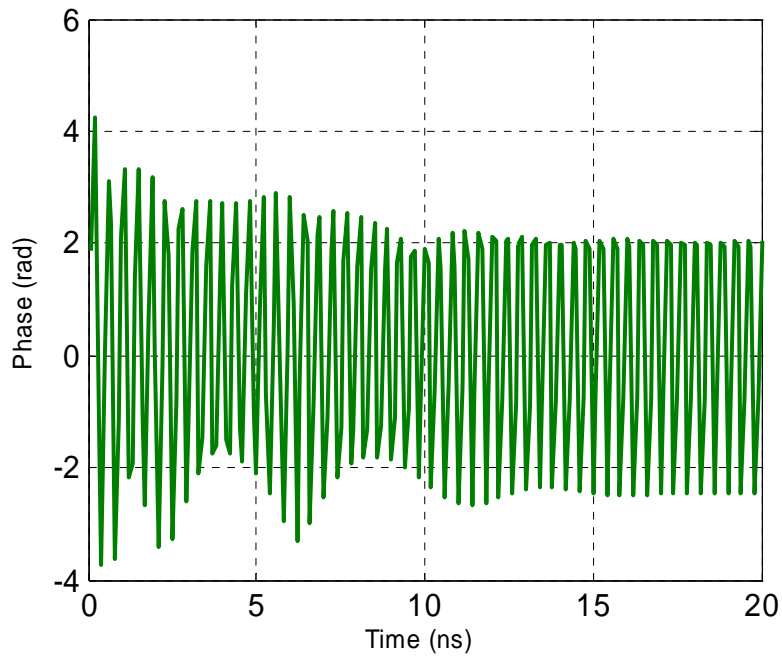
From Figs. 4.4-4.8 it is observed that the system evolves into chaos by varying the external cavity length only. The external cavity length is varied from 15cm to 30cm, this corresponds to the change of delay time (τ) from 1ns to 2ns where $\tau = 2L/c$ as shown in chapter two. The results are periodic solutions, subharmonic solutions, and chaos. Such phenomenon is one of the generic properties of the delay differential system; the output evolves into stability with the increase of the delay time.

4.3.2 Effect of External Mirror Reflectivity

In this section, the effects of external mirror reflectivity are observed. When $L=30$ cm and $r = 1.2\%$, the parameters $|E(t)|$, $\phi(t)$, output power, $N(t)$, and the attractor are as shown in Figs. 4.9a-e.



(a)

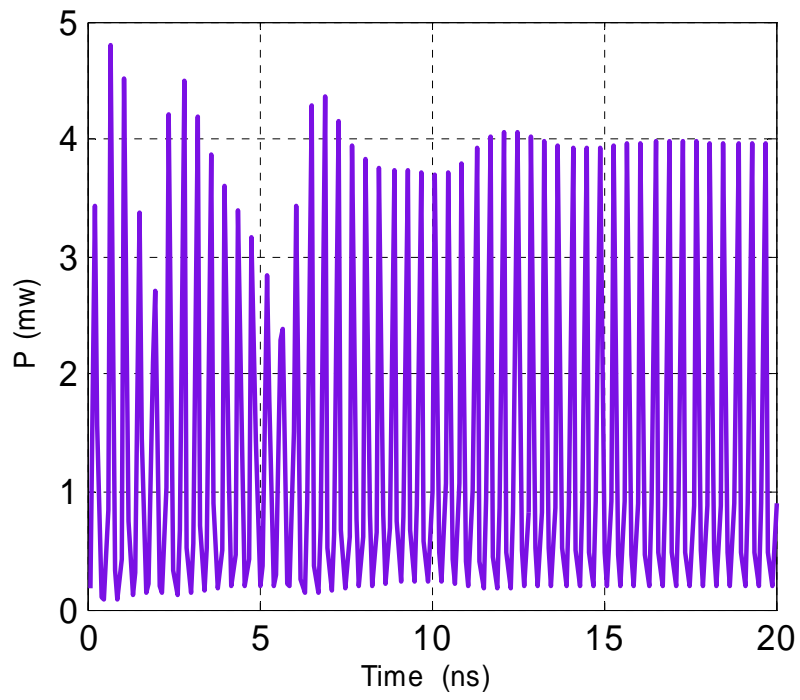


(b)

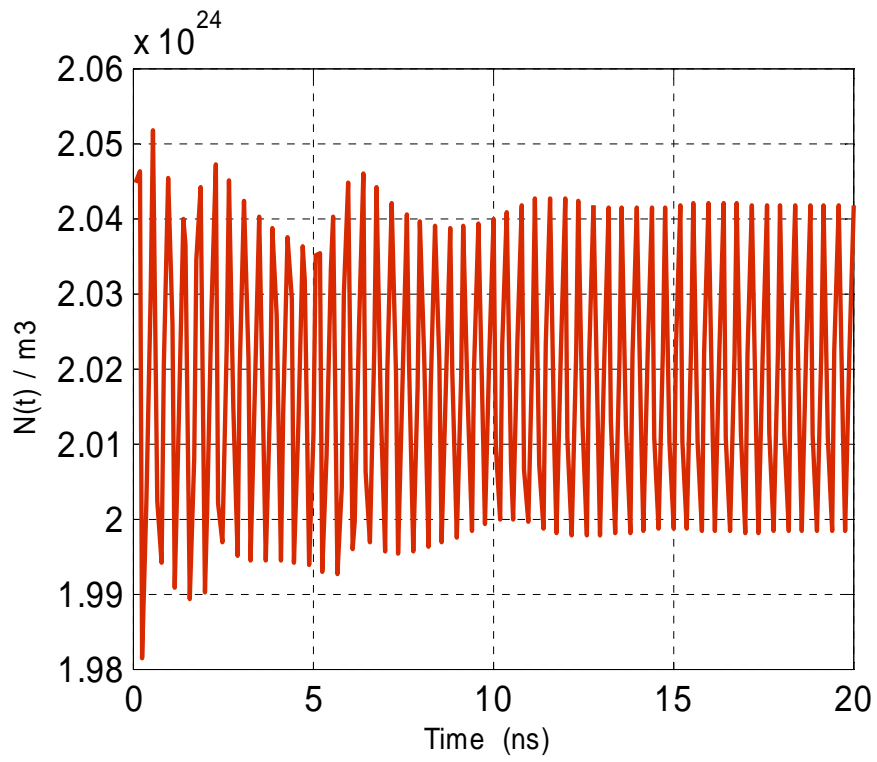
Fig.4.9. Characteristics of semiconductor laser with optical feedback when

$$L=30\text{cm and } r=1.2\%$$

- (a) Electric field (b) Phase of electric field (c) Output power (d) Carrier density
(e) Attractor.

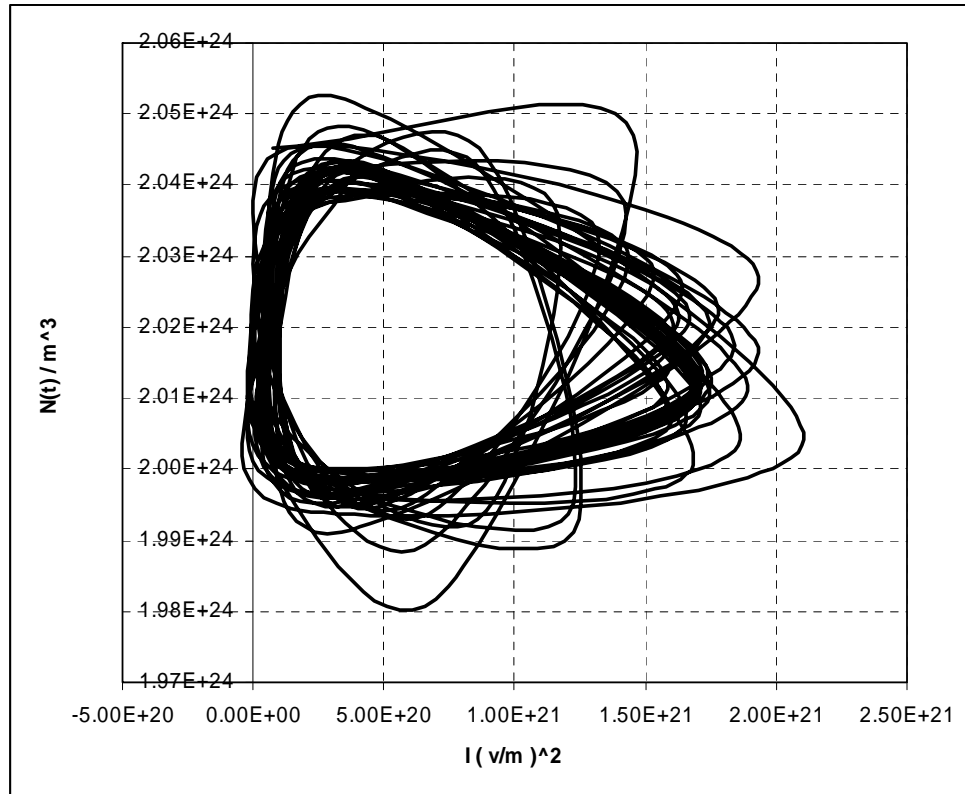


(c)



(d)

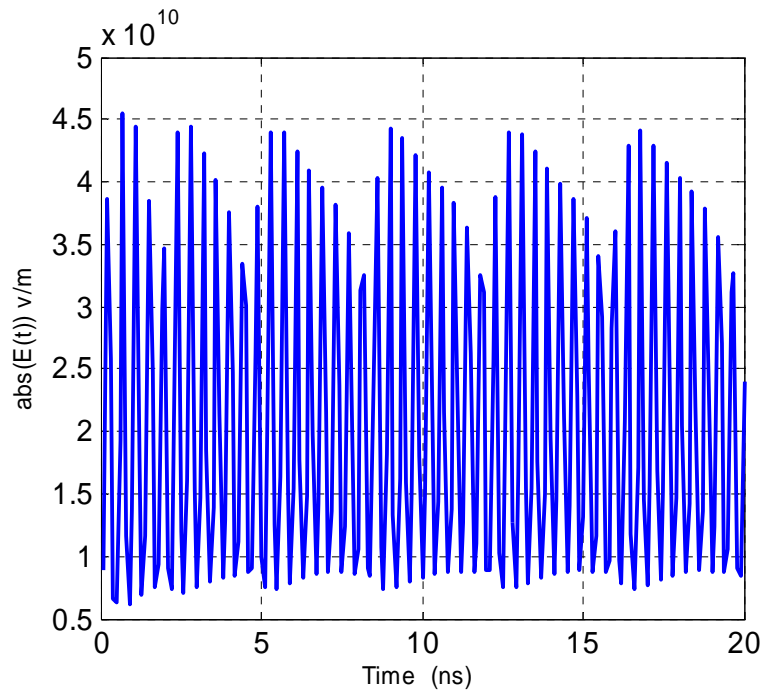
Fig. 4.9 (continued).



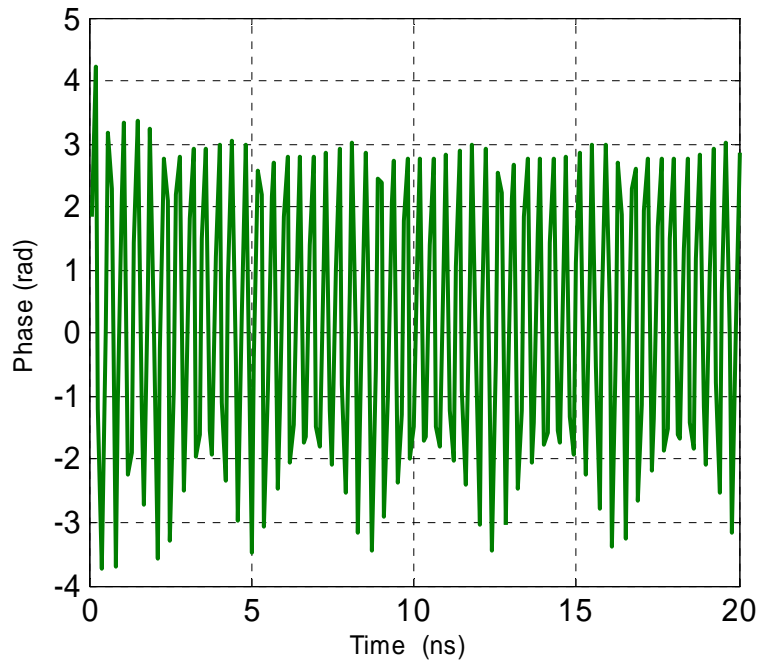
(e)

Fig. 4.9 (continued).

When L is fixed at 30 cm and $r = 1.3\%$, the parameters $|E(t)|$, $\phi(t)$, output power, $N(t)$, and the attractor are as shown in Figs. 4.10a-e.



(a)



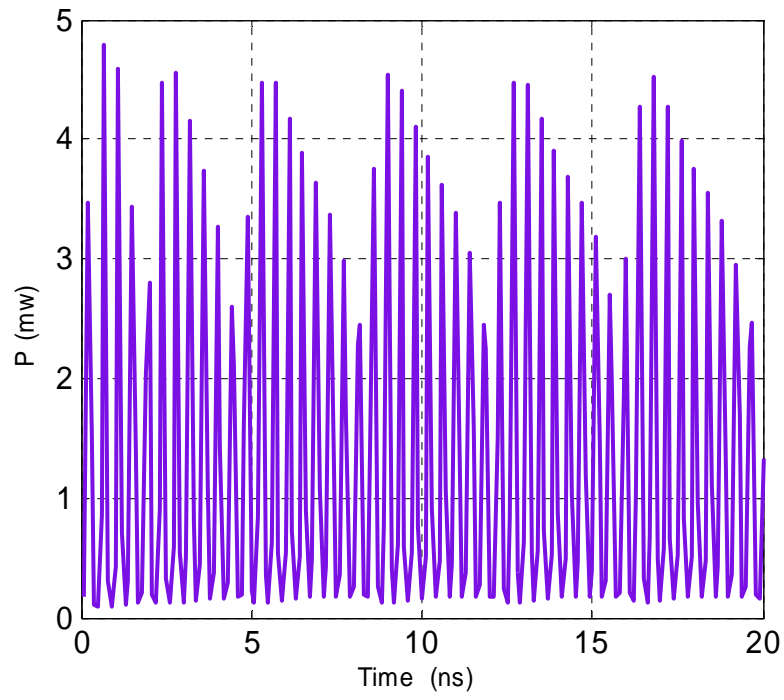
(b)

Fig.4.10. Characteristics of semiconductor laser with optical feedback when

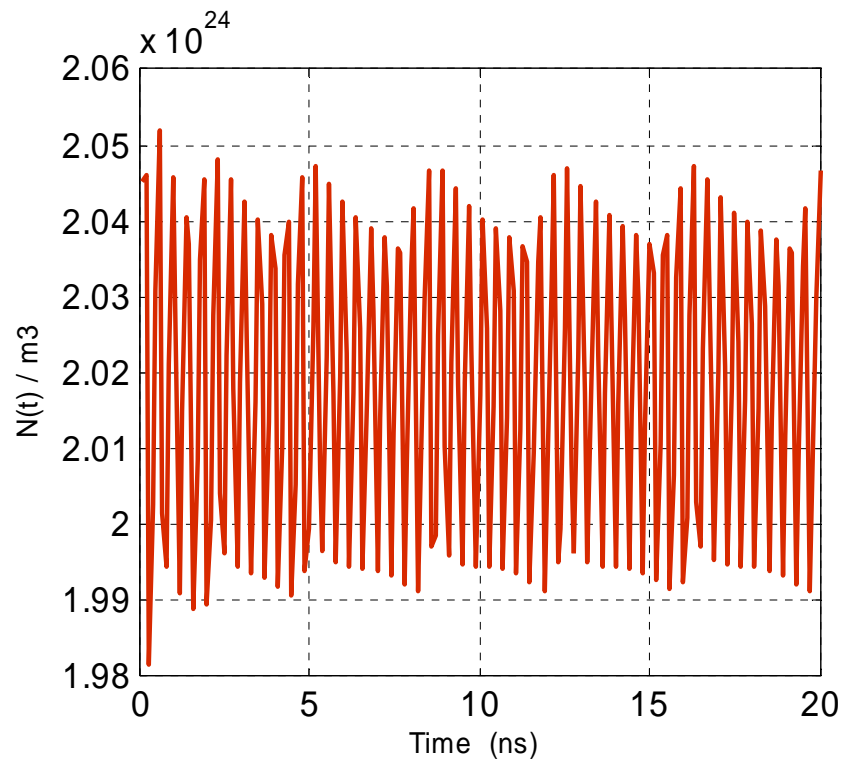
$$L=30\text{cm and } r=1.3\%$$

(a) Electric field (b) Phase of electric field (c) Output power (d) Carrier density

(e) Attractor.

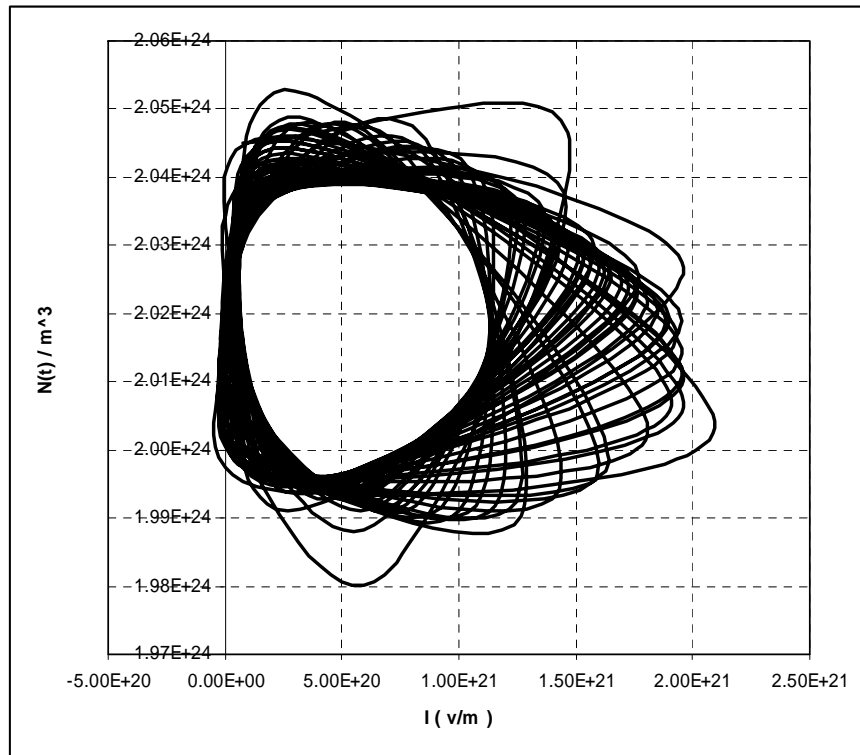


(c)



(d)

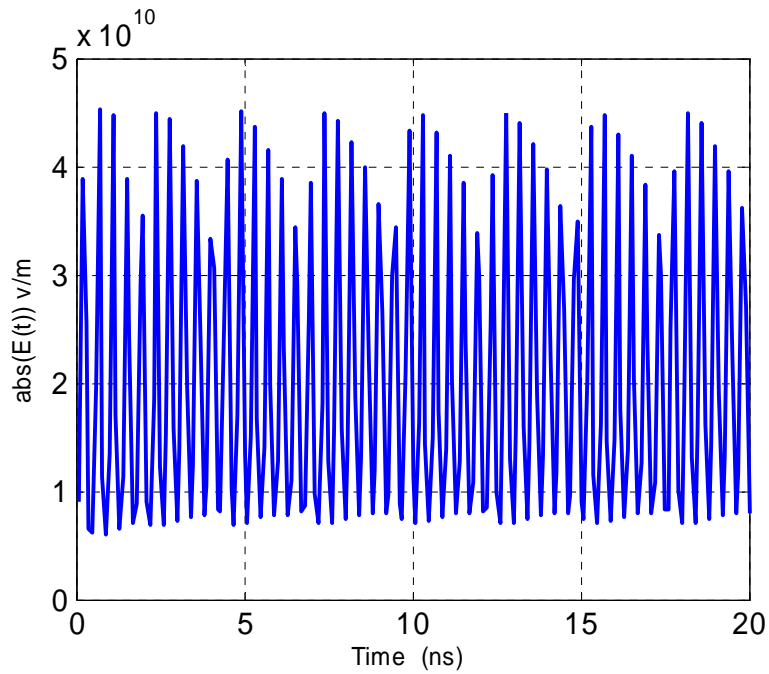
Fig. 4.10 (continued).



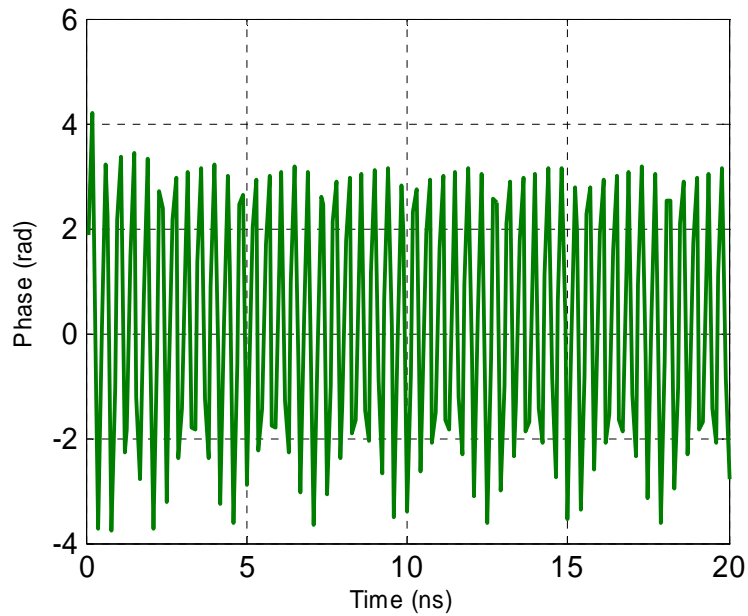
(e)

Fig. 4.10 (continued).

When $L = 30$ cm and $r = 1.4\%$, the parameters $|E(t)|$, $\phi(t)$, output power, $N(t)$, and the attractor are as shown in Figs. 4.11a-e.



(a)



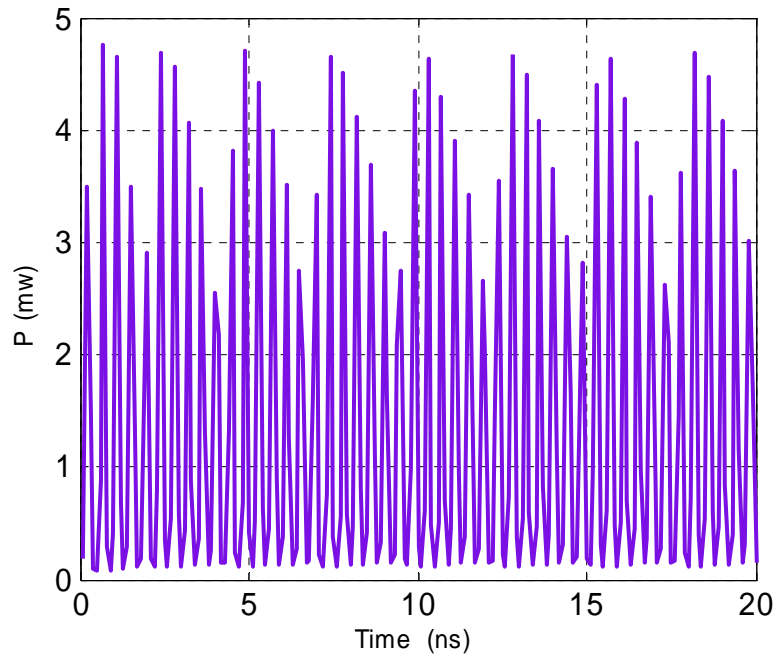
(b)

Fig.4.11. Characteristics of semiconductor laser with optical feedback when

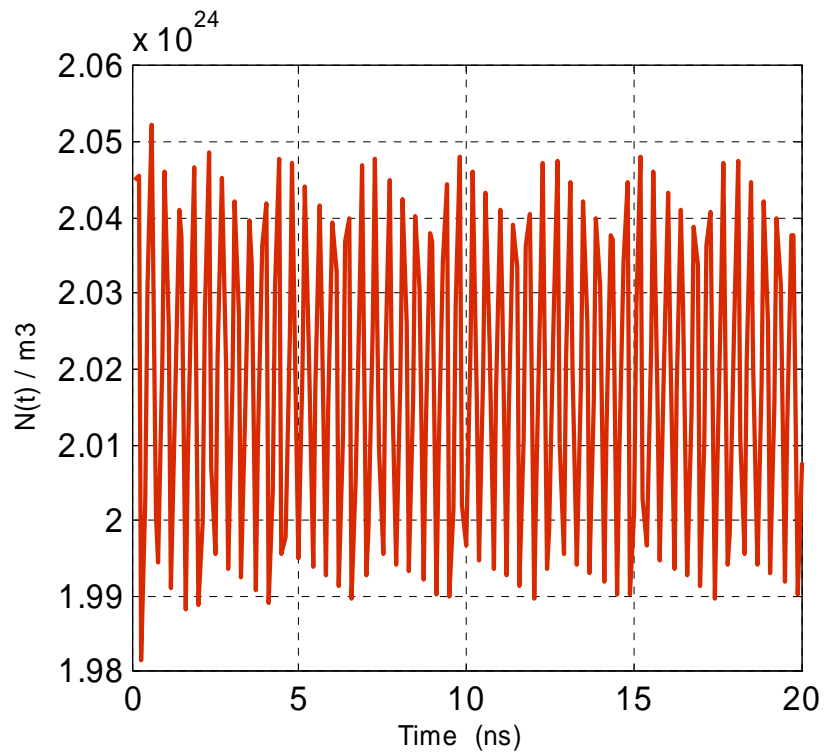
$$L=30\text{cm and } r=1.4\%$$

(a) Electric field (b) Phase of electric field (c) Output power (d) Carrier density

(e) Attractor.

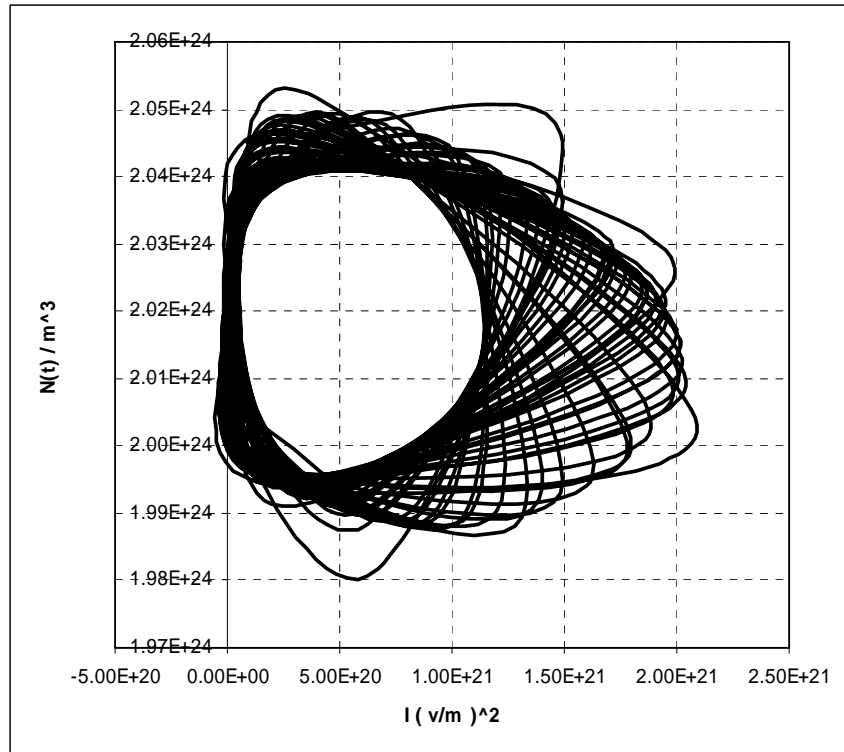


(c)



(d)

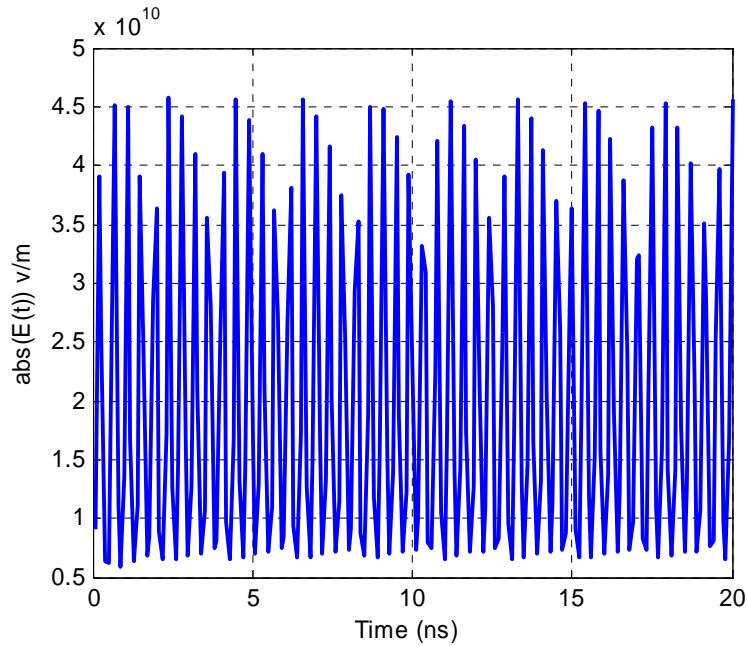
Fig. 4.11 (continued).



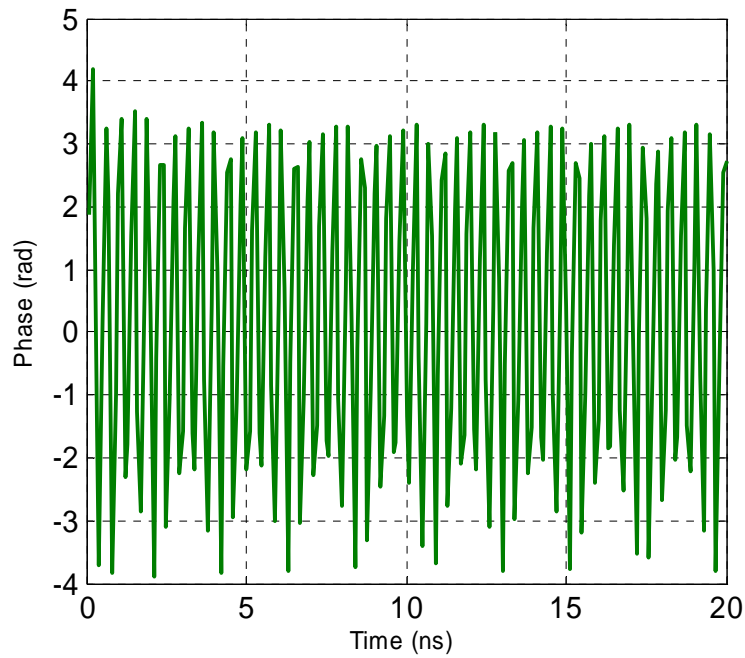
(e)

Fig. 4.9 (continued).

When L is fixed at 30cm, and the reflectivity r increases to 1.5% the parameters $|E(t)|$, $\phi(t)$, output power, $N(t)$, and the attractor are as shown in Figs. 4.12a-e.



(a)



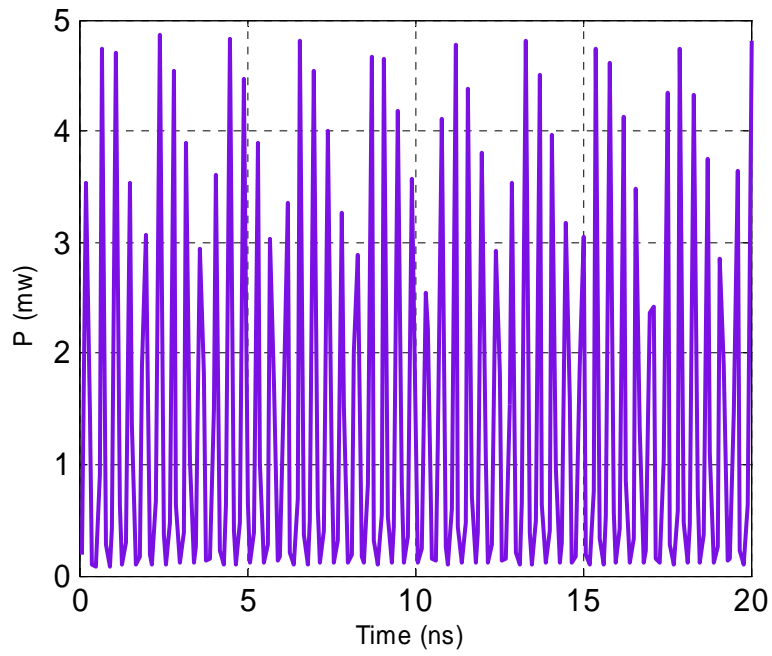
(b)

Fig.4.12. Characteristics of semiconductor laser with optical feedback when

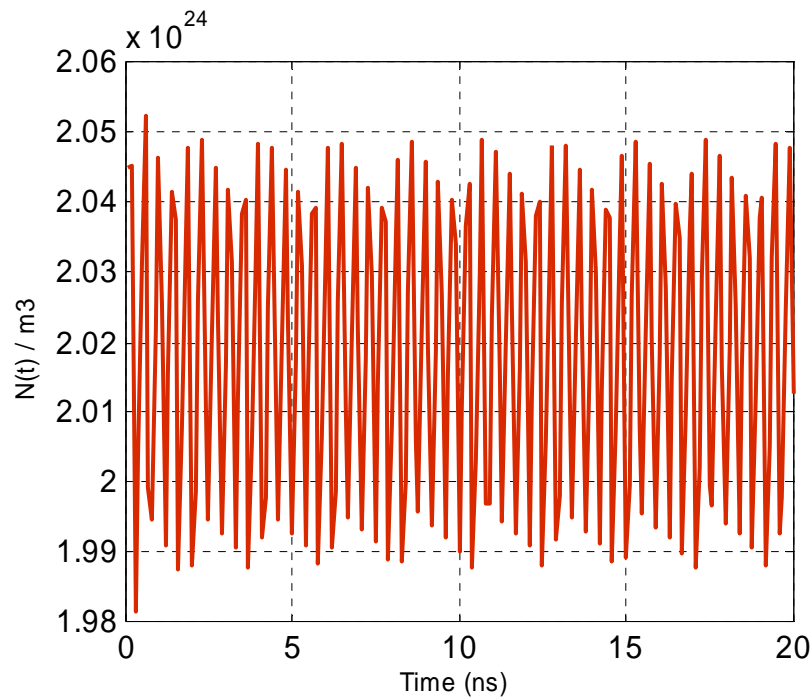
$$L=30\text{cm and } r=1.5\%$$

(a) Electric field (b) Phase of electric field (c) Output power (d) Carrier density

(e) Attractor.

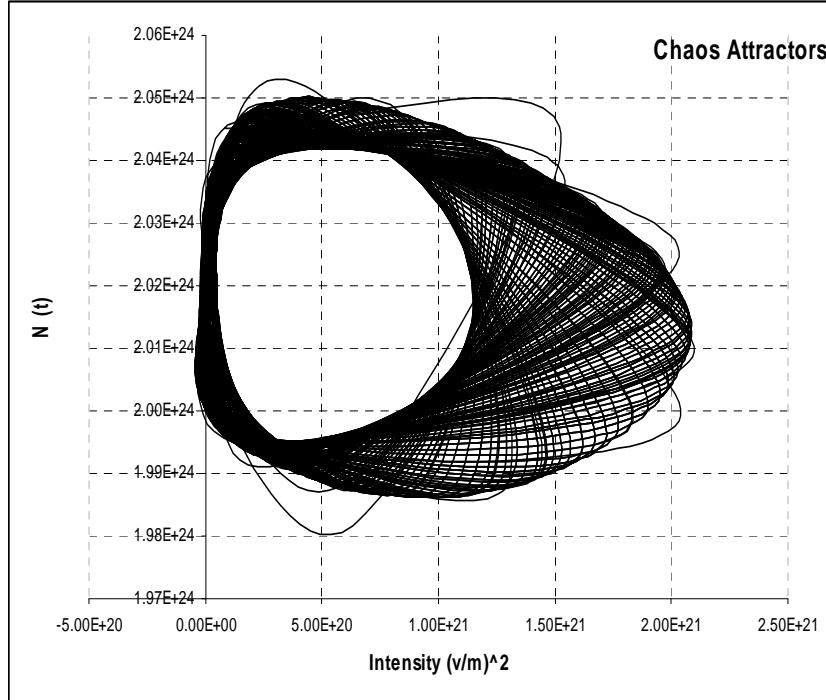


(c)



(d)

Fig. 4.12 (continued).



(e)

Fig. 4.12 (continued).

From Figs. 4.9-4.12, as one can see the amplitude of the external cavity reflectivity increased from 1% to 1.5%, one can observe continuous bifurcation from steady state to periodic state then quasiperiodic state and finally chaos. An incomplete period doubling bifurcation also occurs for certain values of r , which leads to the subharmonic periodic solutions. Quasiperiodic solutions emerge from the fundamental periodic solutions and the subharmonic periodic solutions or even the other limit cycles.

4.4 System Synchronization

This section is devoted to investigate the effect of various parameters on the synchronization between the transmitter and receiver lasers (see the flow chart in fig. 4.13. The parameters values used in this model are shown in Table 4.1.

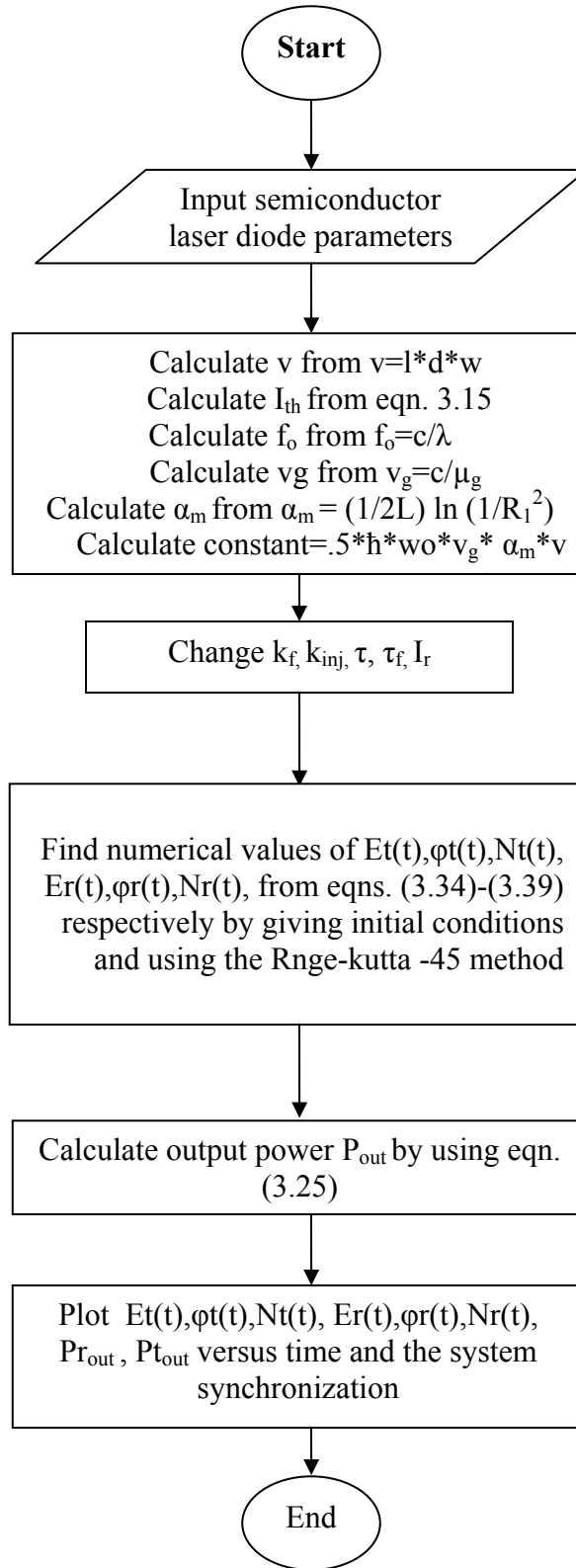
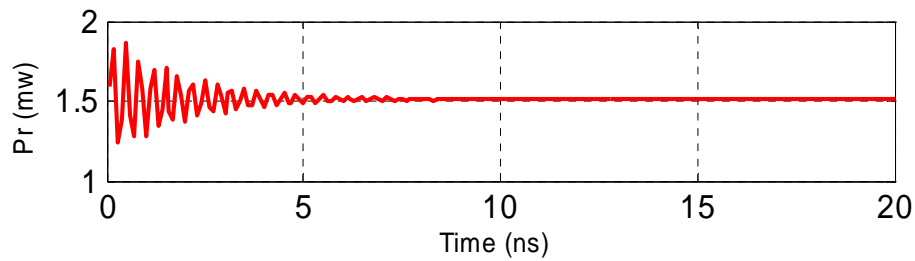
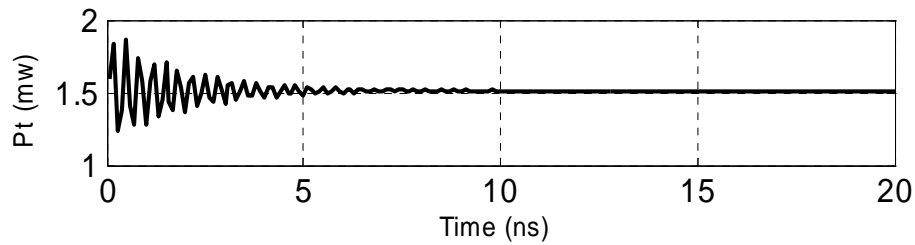


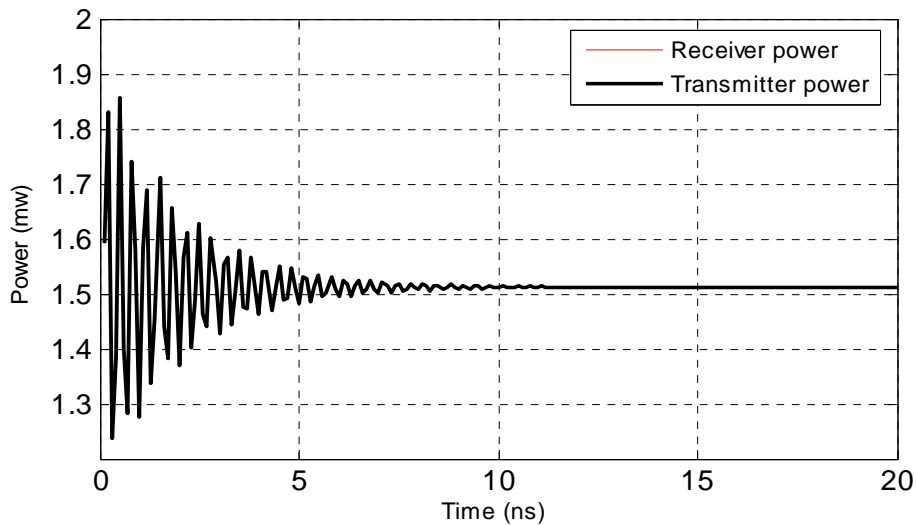
Fig. 4.13 Flowchart of the system model program.

4.4.1 Effect of Optical Feedback Coefficient

In this subsection, the effects of optical feedback on the system characteristics are addressed. When $k_f = 0$, $k_{inj} = 0$ and $\tau_f = 0$, the transmitter and receiver characteristics are shown in Figs. 4.14a-d.



(a)



(b)

Fig. 4.14. Transmitter and receiver characteristics when $k_f = k_{inj} = 0$

- (a) Transmitter and receiver power (b) System power (c) Carrier density
(d) System synchronization.

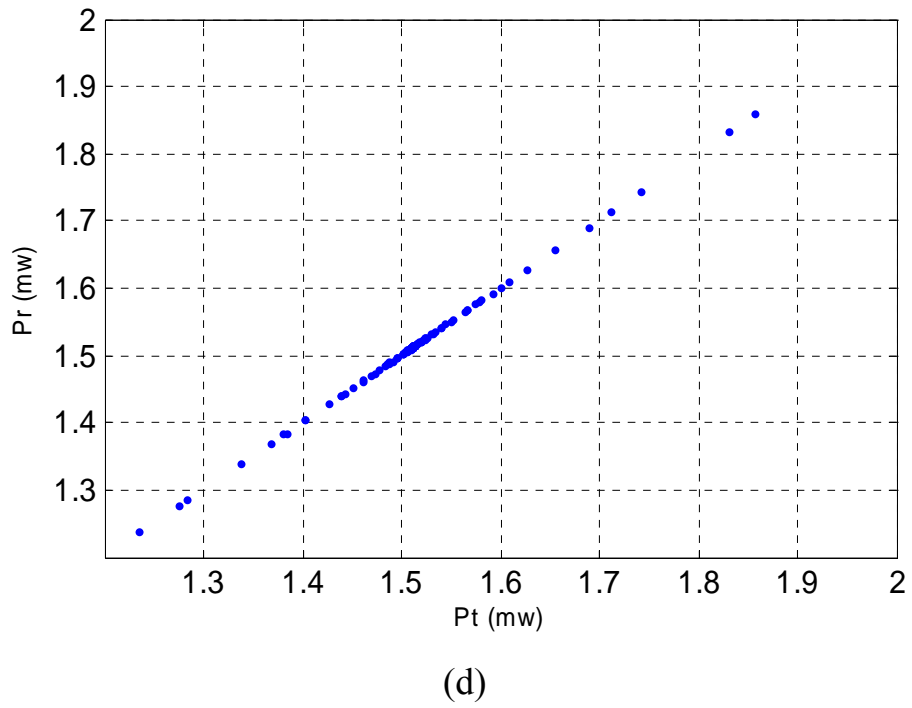
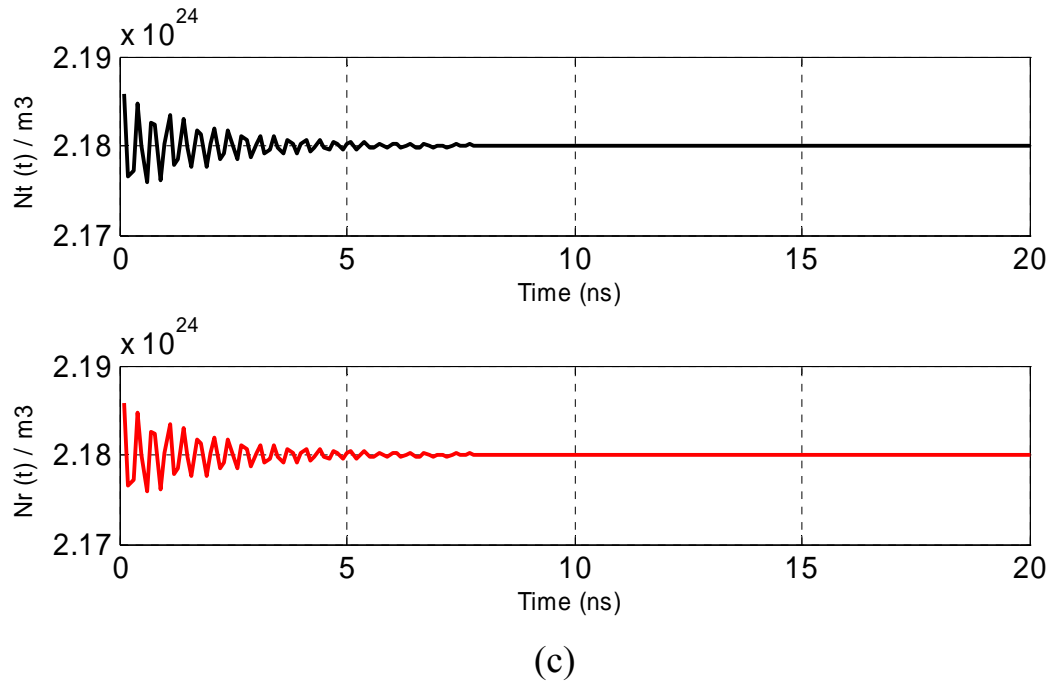


Fig. 4.14 (continued).

For the case when $k_f = k_{inj} = 0$, no effect is noticed on the transmitter/receiver system. This means that the system operates at free running operation and the system has complete synchronization.

When k_f increases to 0.1 while $k_{inj} = 0$ and $\tau_f = 0$, the transmitter and receiver characteristics are shown in Fig. 4.15a-d.

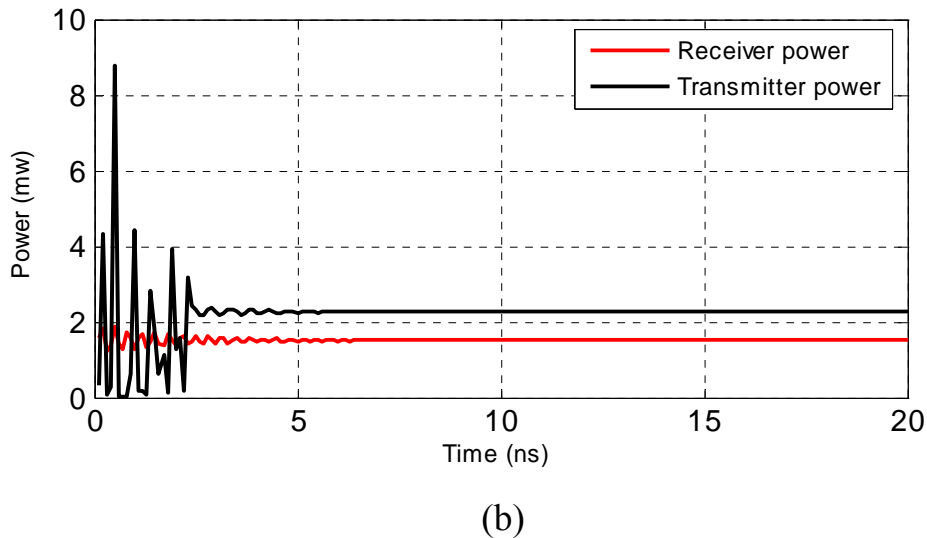
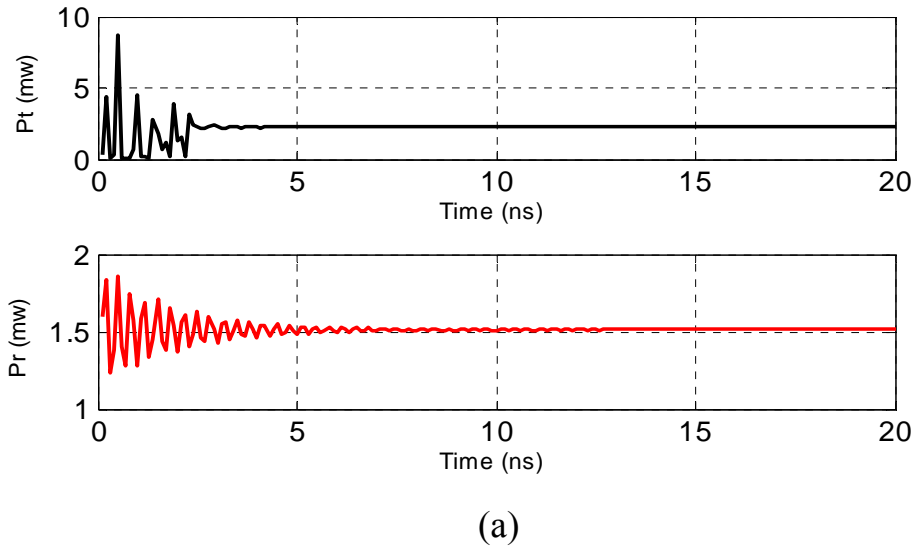


Fig. 4.15. Transmitter and receiver characteristics when $k_{inj}=0$ and $k_f=0.1$

- (a) Transmitter and receiver power
- (b) System power
- (c) Carrier density
- (d) System synchronization.

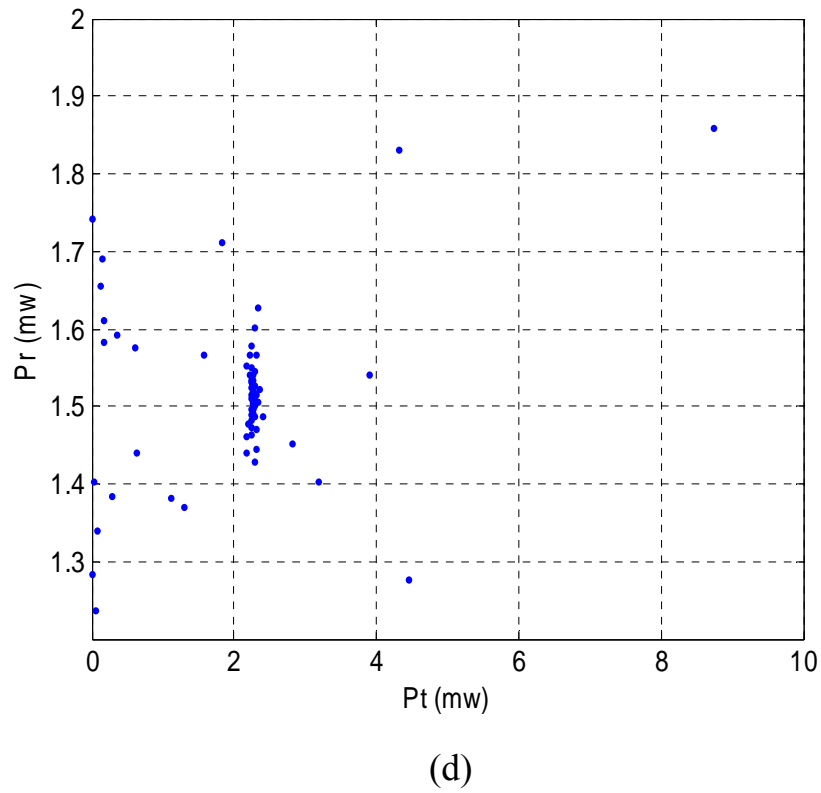
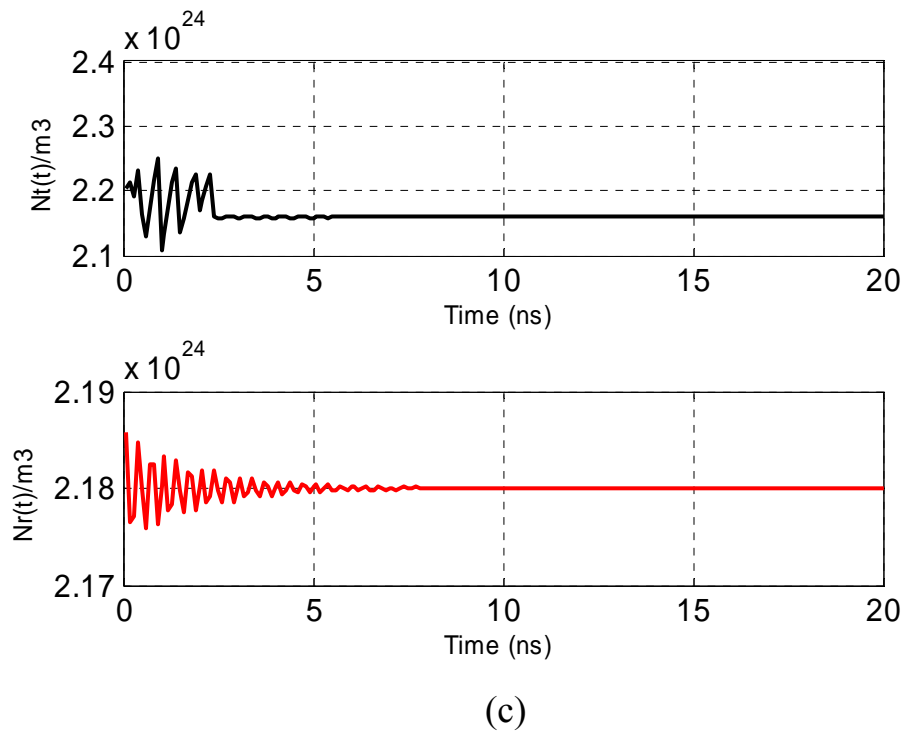
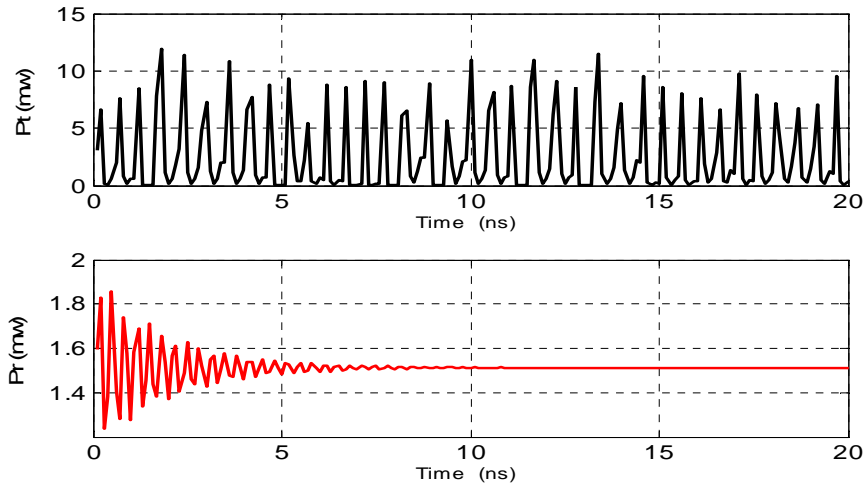


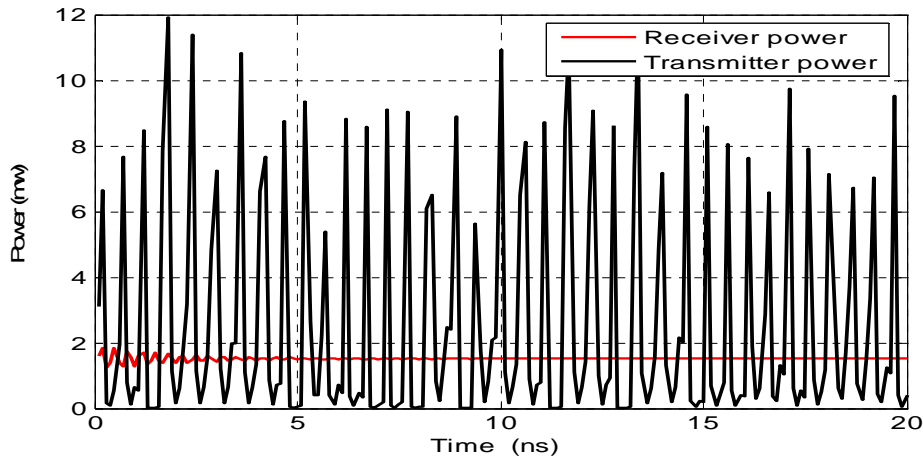
Fig. 4.15 (continued).

When the optical feedback coefficient increases to 0.1 in the transmitter system and no optical injection added to the receiver system, small effect on the transmitter output power and carrier density are appeared so that the transmitter output power increases and also the waveform is changed due to the presence of feedback on the transmitter.

Increasing k_f further to 0.2 yields the results shown in Figs. 4.16a-d.



(a)



(b)

Fig. 4.16. Transmitter and receiver characteristics when $k_{inj}=0$ and $k_f=0.2$

- (a) Transmitter and receiver power
- (b) System power
- (c) Carrier density
- (d) System synchronization.

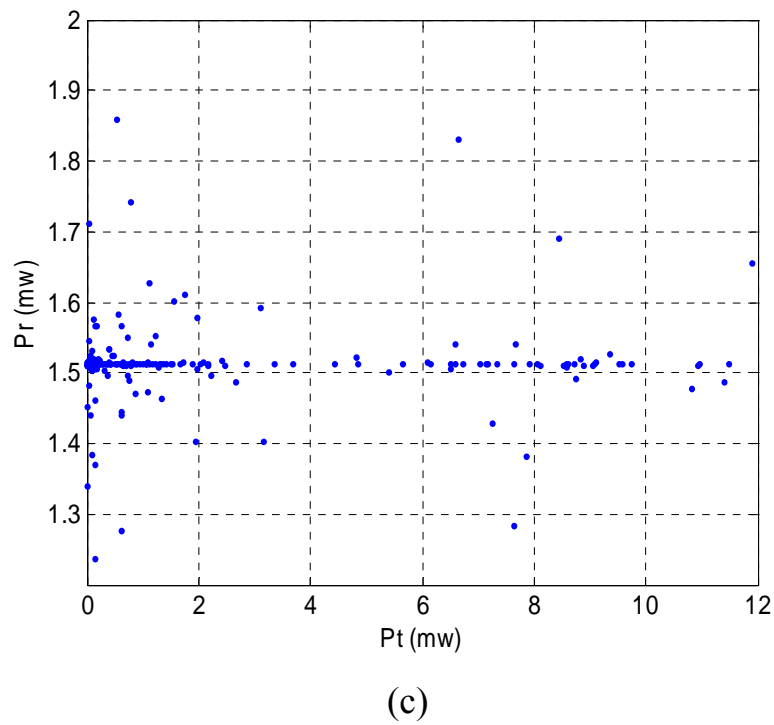
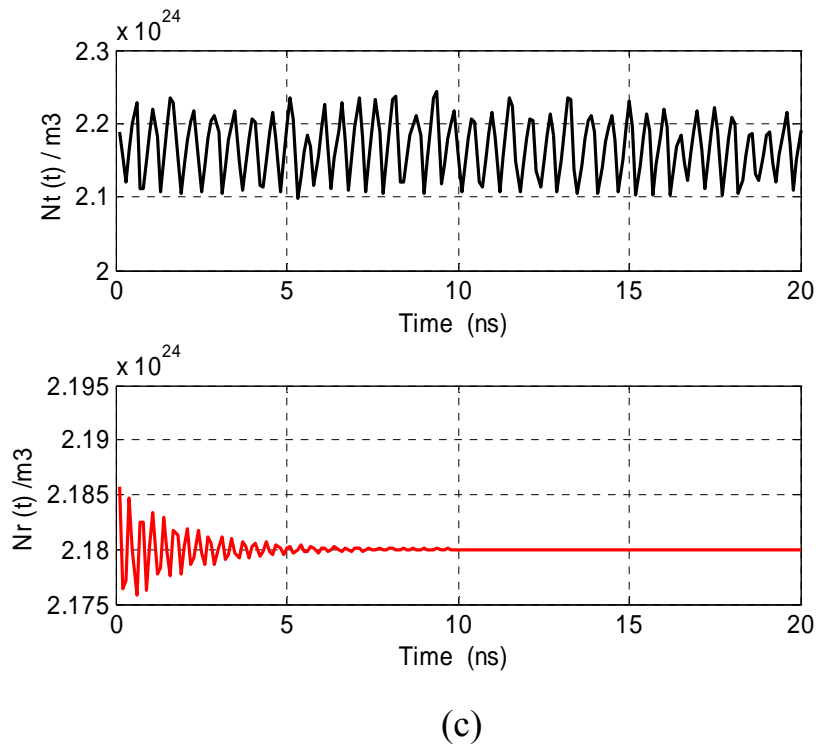
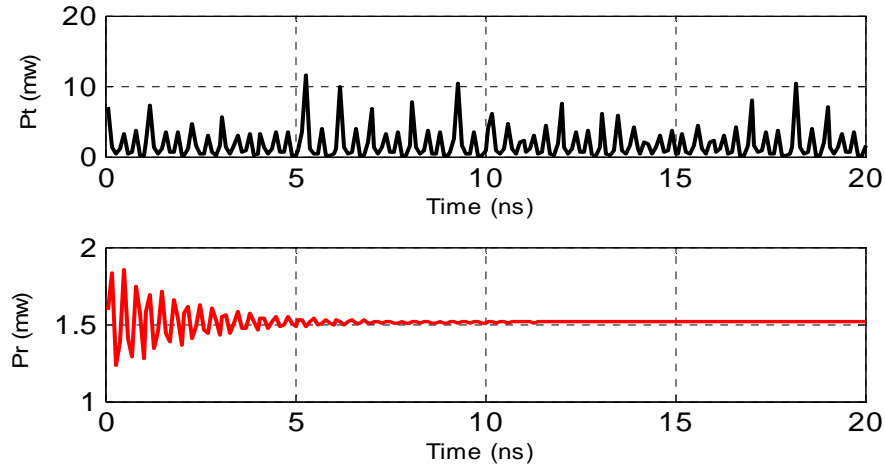
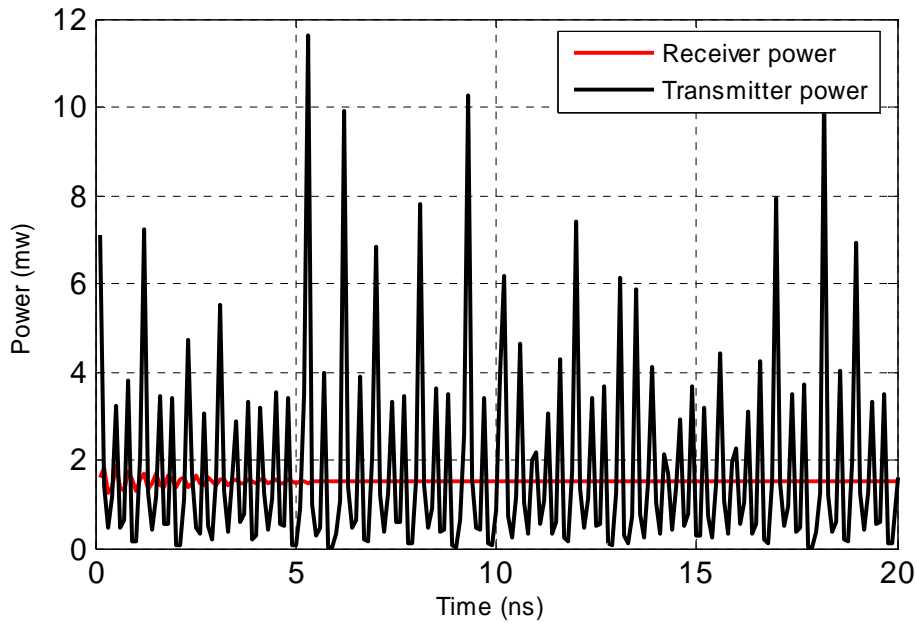


Fig. 4.16 (continued).

When $k_f = 0.3$, $k_{inj} = 0$ and $\tau_f = 0$, the transmitter and receiver characteristics are shown in Figs. 4.17a-d.



(a)

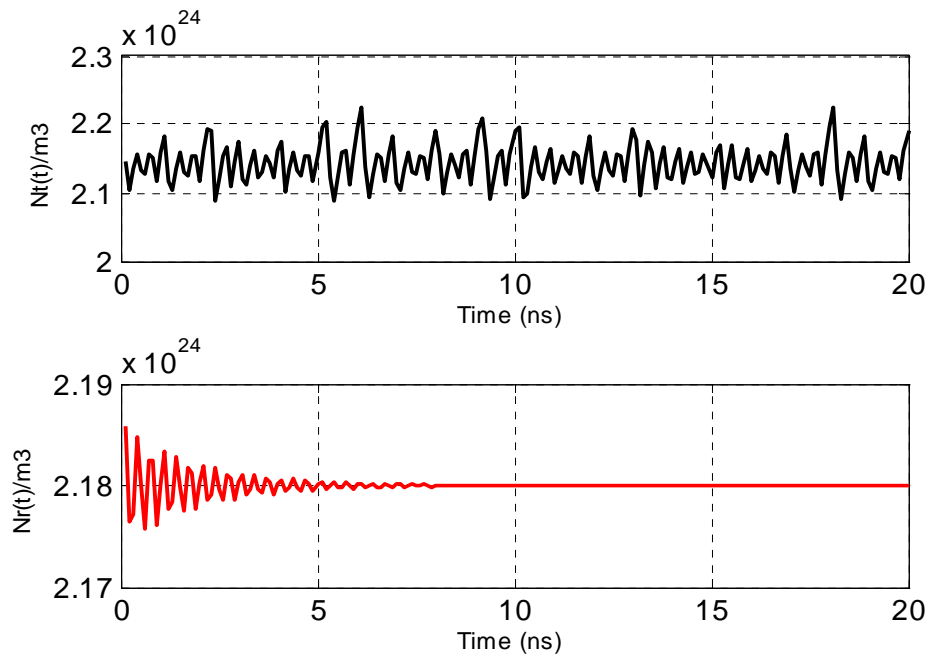


(b)

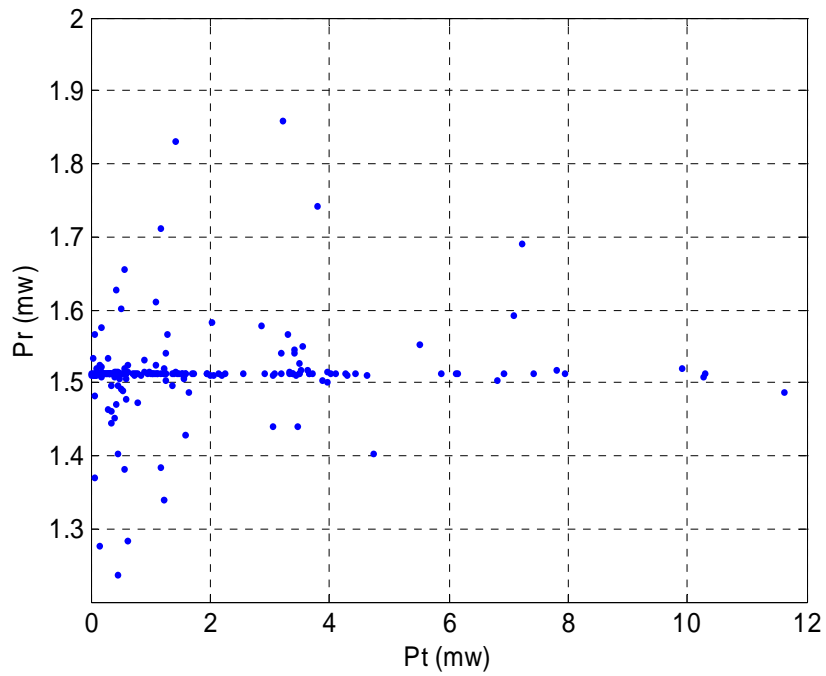
Fig. 4.17. Transmitter and receiver characteristics when $k_{inj}=0$ and $k_f=0.3$

(a) Transmitter and receiver power (b) System power (c) Carrier density

(d) System synchronization.



(c)



(d)

Fig. 4.17 (continued).

From these results, increasing the optical feedback coefficient has a noticeable effect on the transmitter waveforms. The waveforms are seemed to be more perturbation than the previous state. Due to the increase of optical feedback, the transmitter system starts to generate chaotic signals because of increasing effect on the laser cavity, whereas the characteristics of the receiver system stay without any change. Therefore there is no synchronization between the transmitter and receiver systems as shown in Fig. 4.17d.

4.4.2 Effect of Optical Injection Coefficient

In this section, the values of k_f and τ_f are fixed at zero while k_{inj} is varied from 0.1 to 0.3. When $k_{inj} = 0.1$, the transmitter and receiver characteristics are as shown in Figs. 4.18a-d.

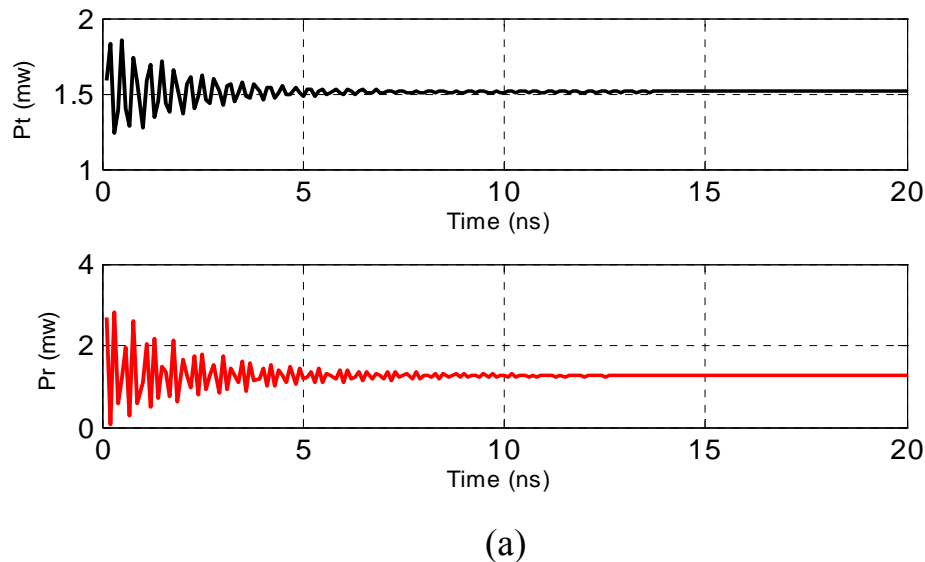
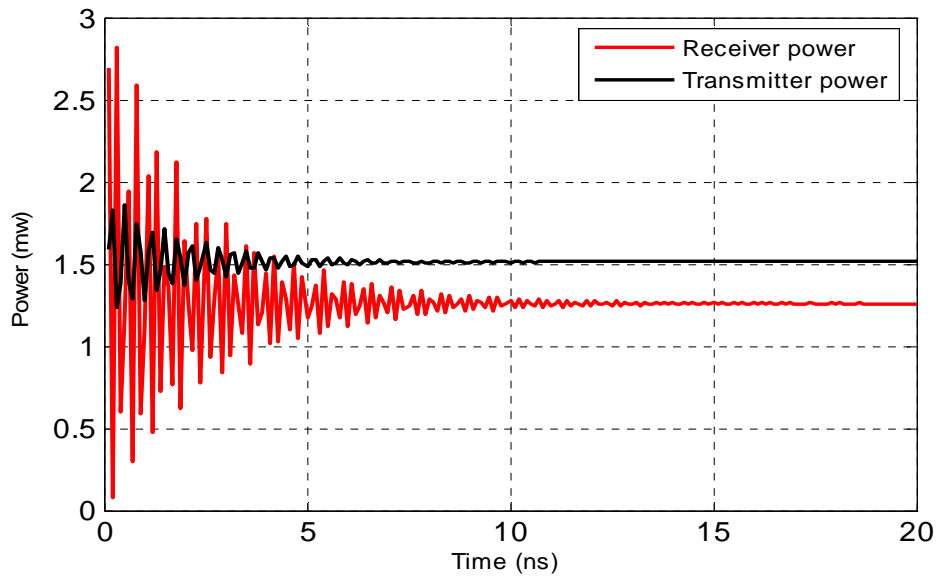
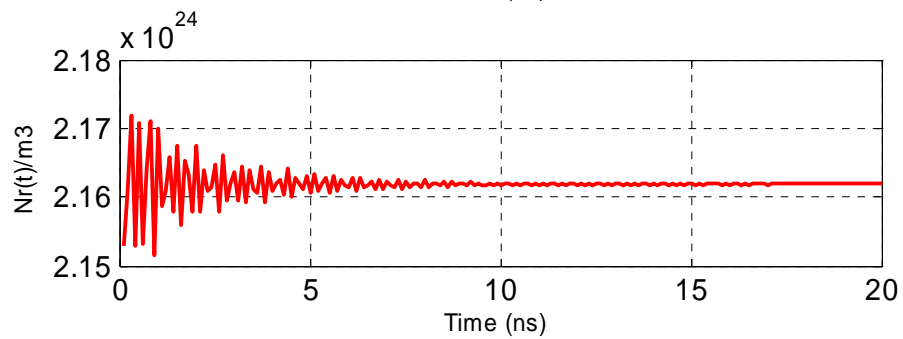
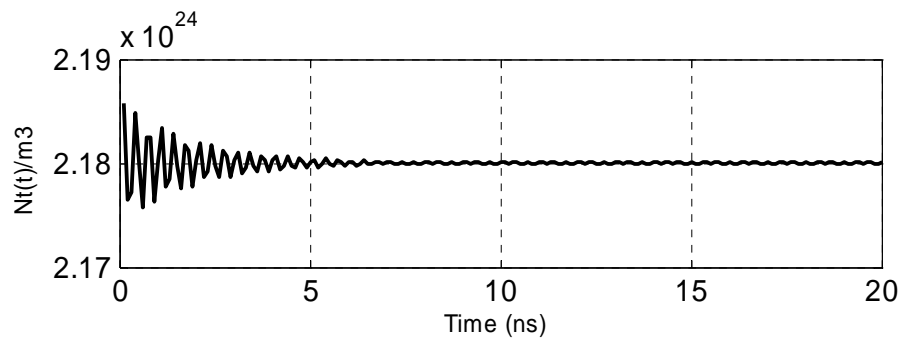


Fig. 4.18. Transmitter and receiver characteristics when $k_f=0$ and $k_{inj}=0.1$

- (a) Transmitter and receiver power (b) System power (c) Carrier density
(d) System synchronization.

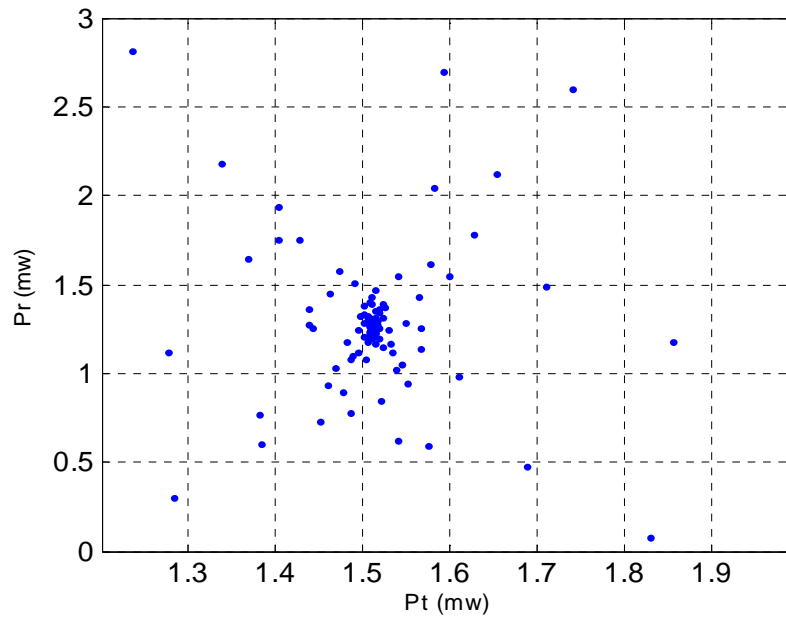


(b)



(c)

Fig. 4.18 (continued).

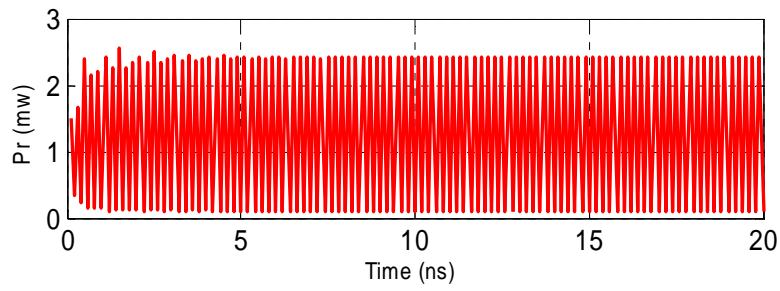
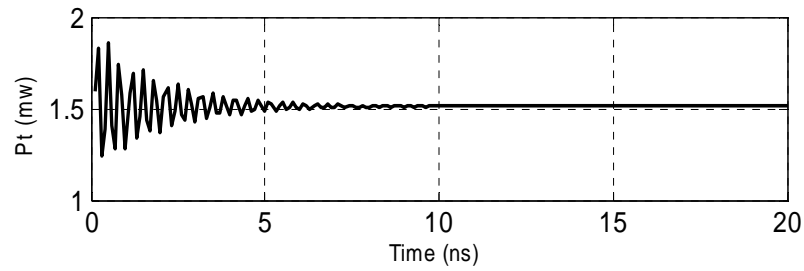


(d)

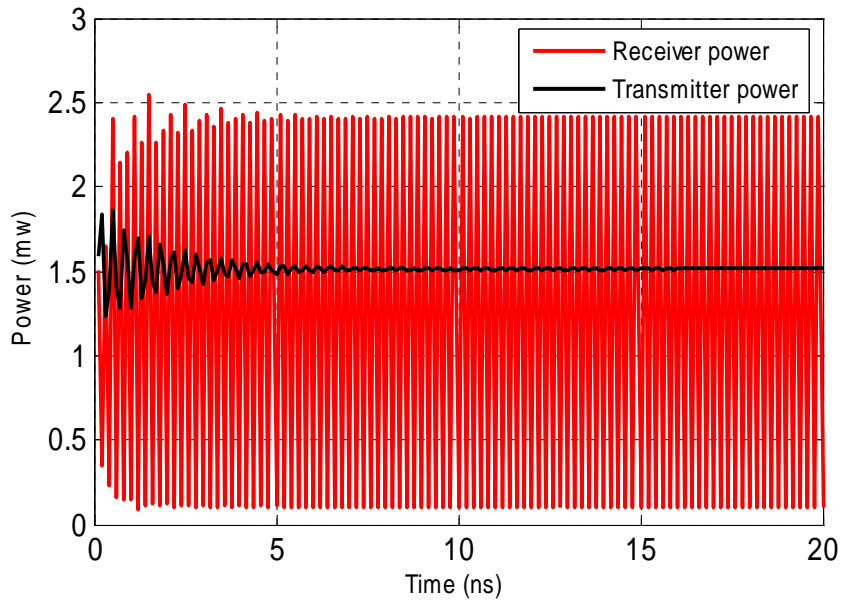
Fig. 4.18 (continued).

In the case of presence injection coefficient on the receiver system, the waveforms starts to change and the receiver power increases. The transmitter output does not change since there is no effect on it ($k_f=0$). This means that the system is unsynchronized because the transmitter system is not compatible with the receiver system as shown in Fig. 4.18d.

As k_{inj} increases to 0.2, the change on the receiver characteristics are very clear as shown in Fig. 4.19a-d, and the system stays unsynchronized.



(a)



(b)

Fig. 4.19. Transmitter and receiver characteristics when $k_f=0$ and $k_{inj}=0.2$

(a) Transmitter and receiver power (b) System power (c) Carrier density

(d) System synchronization.

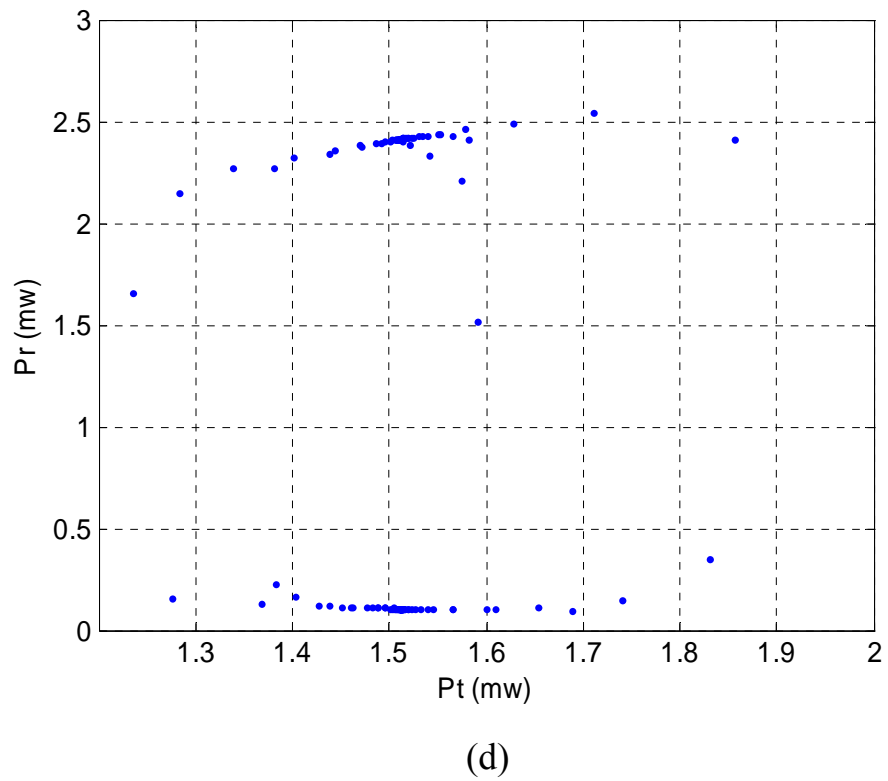
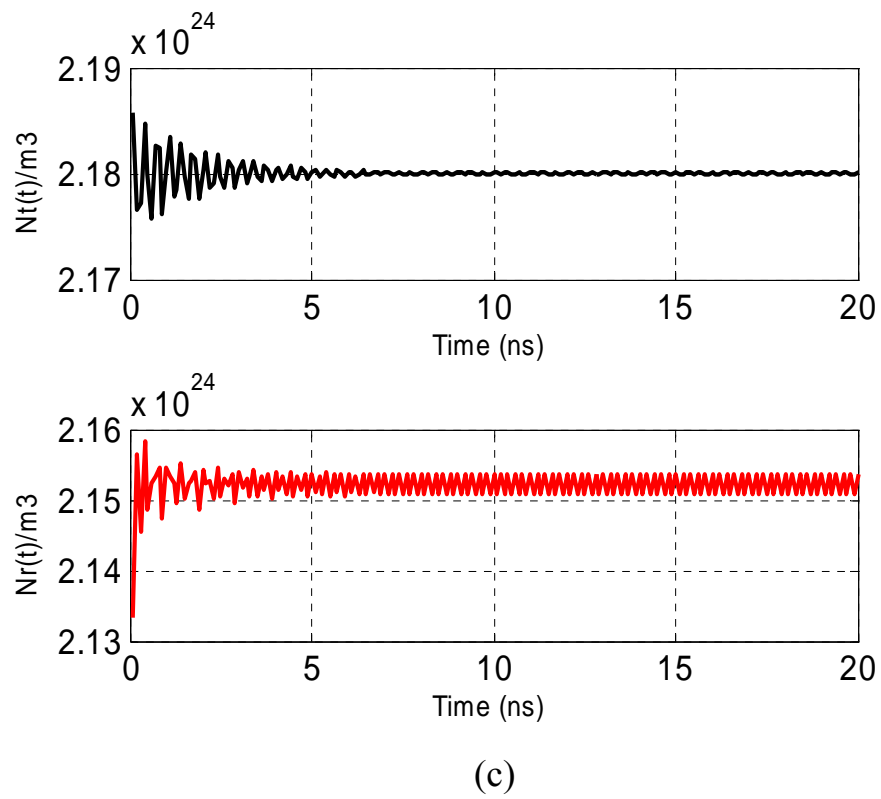


Fig. 4.19 (continued).

When k_{inj} increases to 0.3 the transmitter and receiver characteristics are as shown in Figs. 4.20a-d.

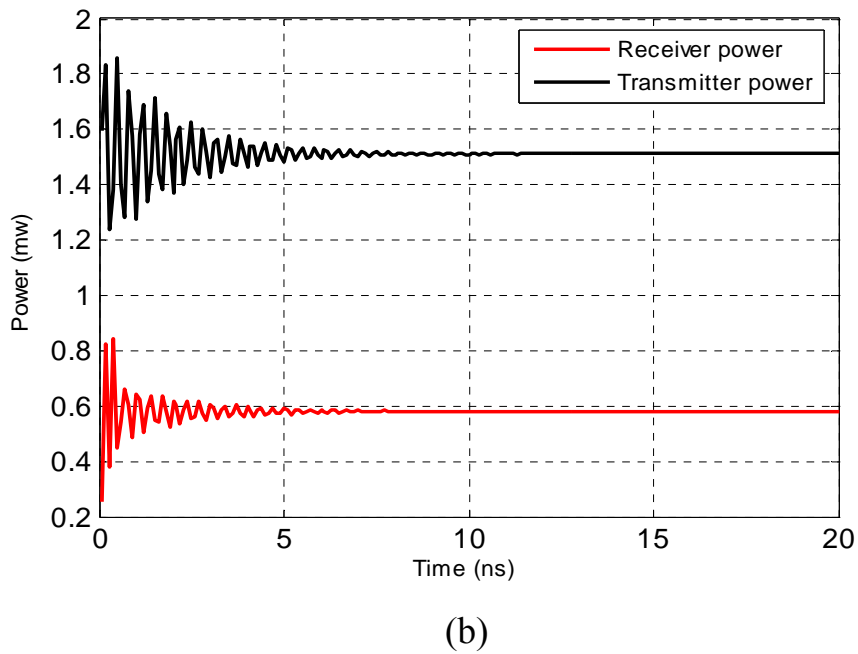
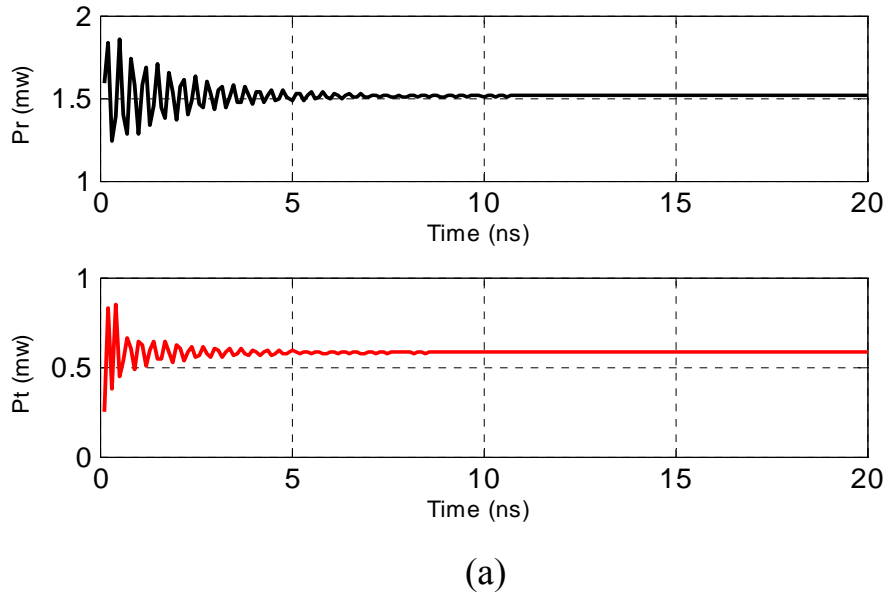
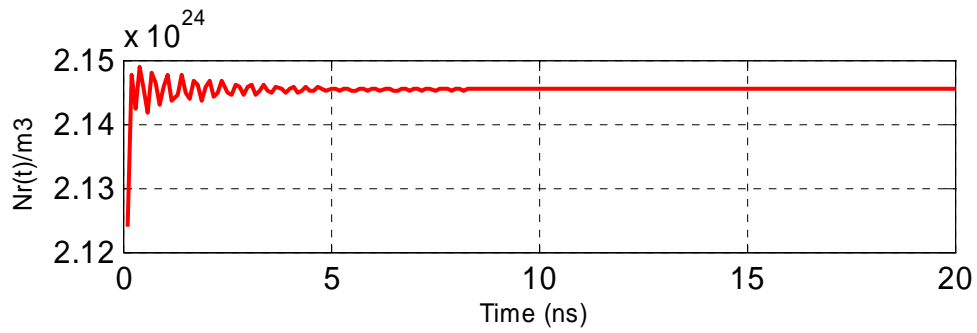
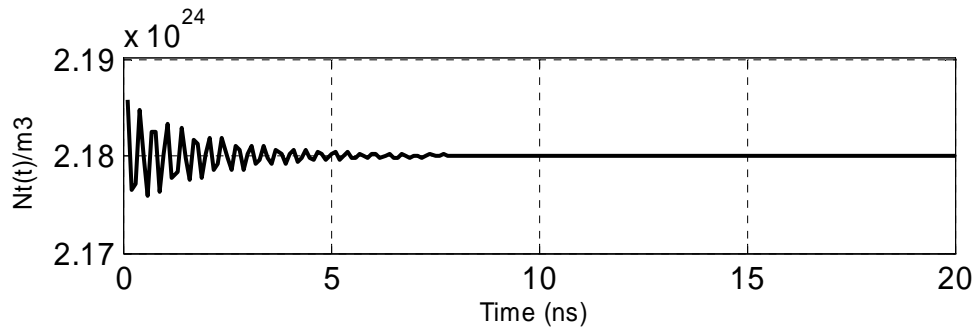
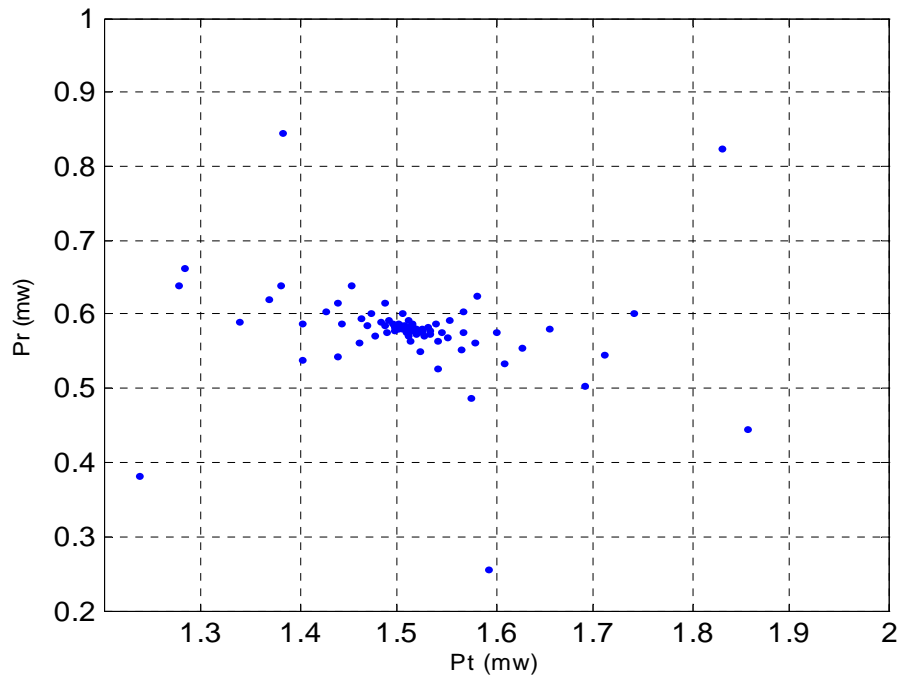


Fig. 4.20. Transmitter and receiver characteristics when $k_f=0$ and $k_{inj}=0.3$

- (a) Transmitter and receiver power
- (b) System power
- (c) Carrier density
- (d) System synchronization.



(c)



(d)

Fig. 4.20 (continued).

It is observed from the previous figures that when k_{inj} increases to 0.3 without any feedback, the system stays unsynchronized and arrives to a case similar to a steady-state case.

For the case when $k_f = k_{inj} = 0.3$ while $\tau_f = 0$, the transmitter and receiver characteristics are as shown in Figs. 4.21a-d.

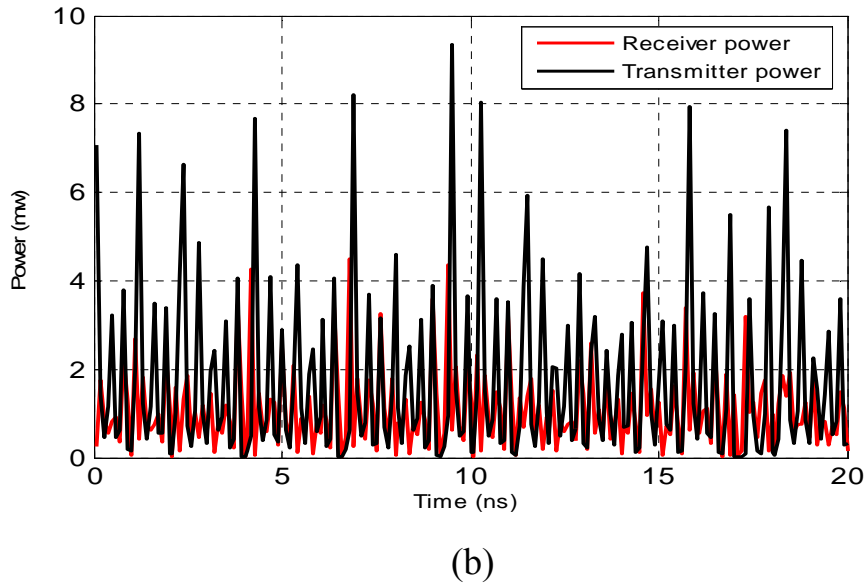
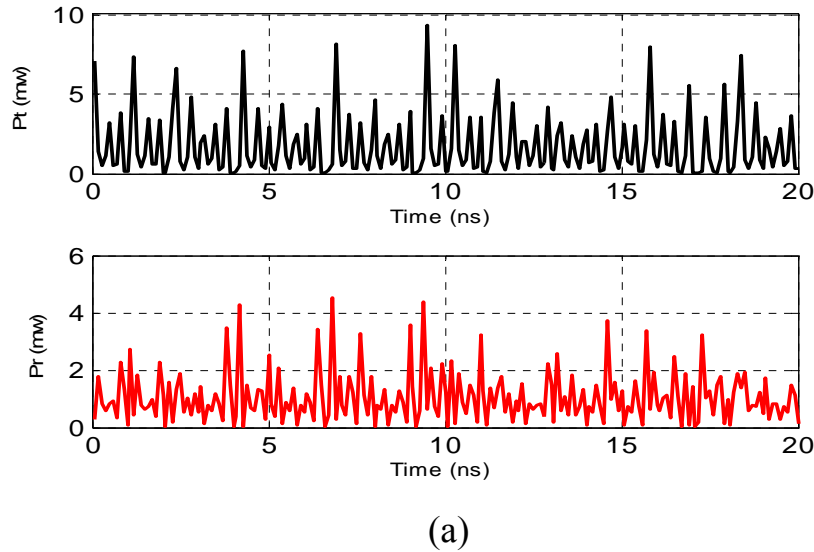
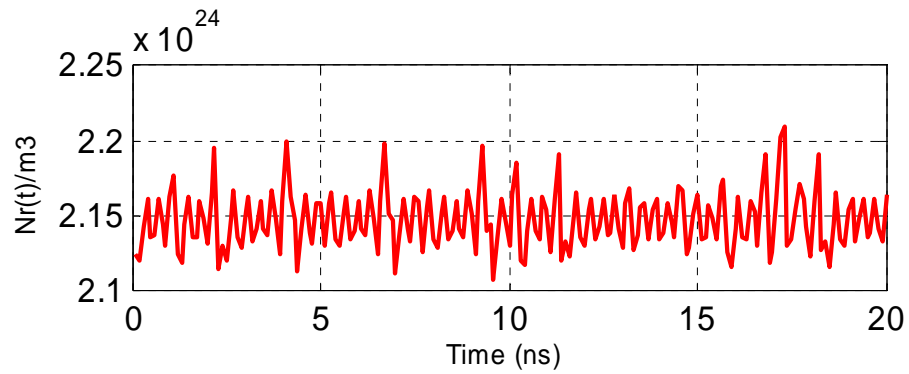
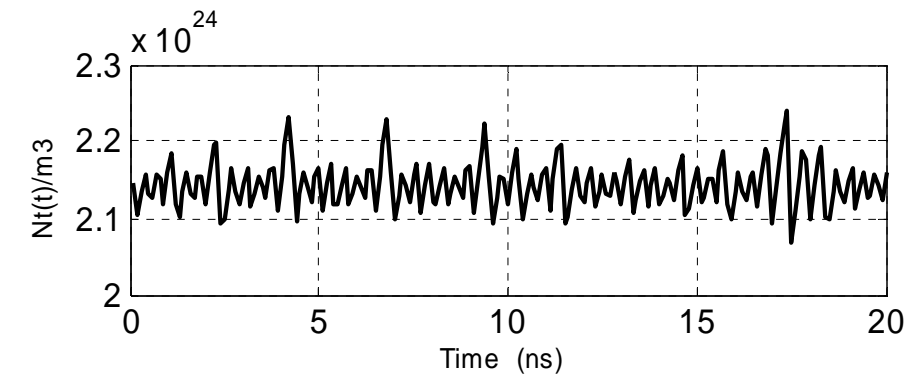
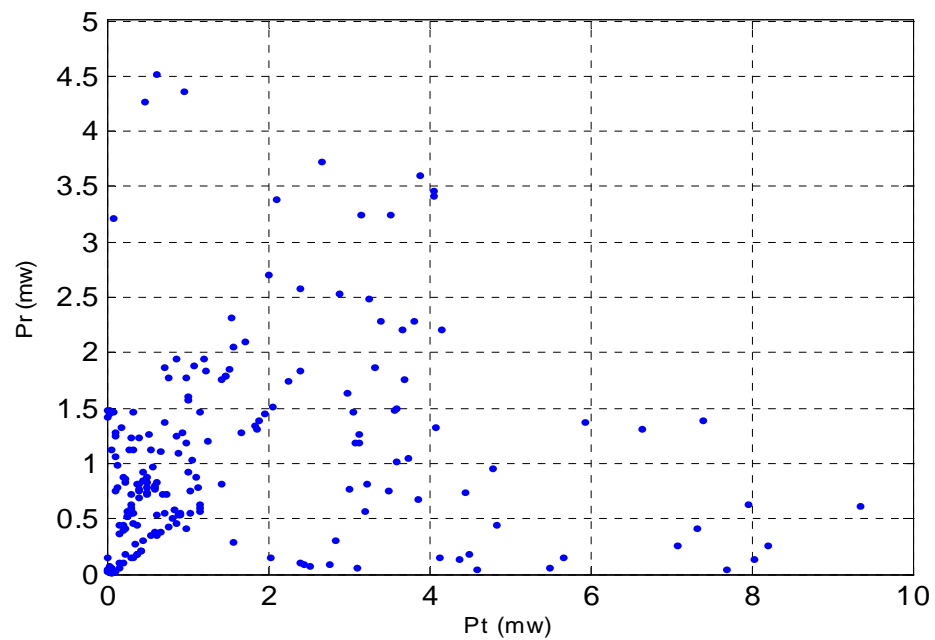


Fig. 4.21. Transmitter and receiver characteristics when $k_f = 0.3$ and $k_{inj} = 0.3$

- (a) Transmitter and receiver power
- (b) System power
- (c) Carrier density
- (d) System synchronization.



(c)



(d)

Fig. 4.21 (continued)

These results refer to the case where the transmitter waveforms are approximately similar to the receiver waveforms. This means that the effect of optical feedback is appeared on the system while the system is still unsynchronized as shown in Fig. 4.21d.

When $k_f = 0.4$ and $k_{inj} = 0.3$, the transmitter and receiver characteristics are as shown in Fig. 4.22a-d.

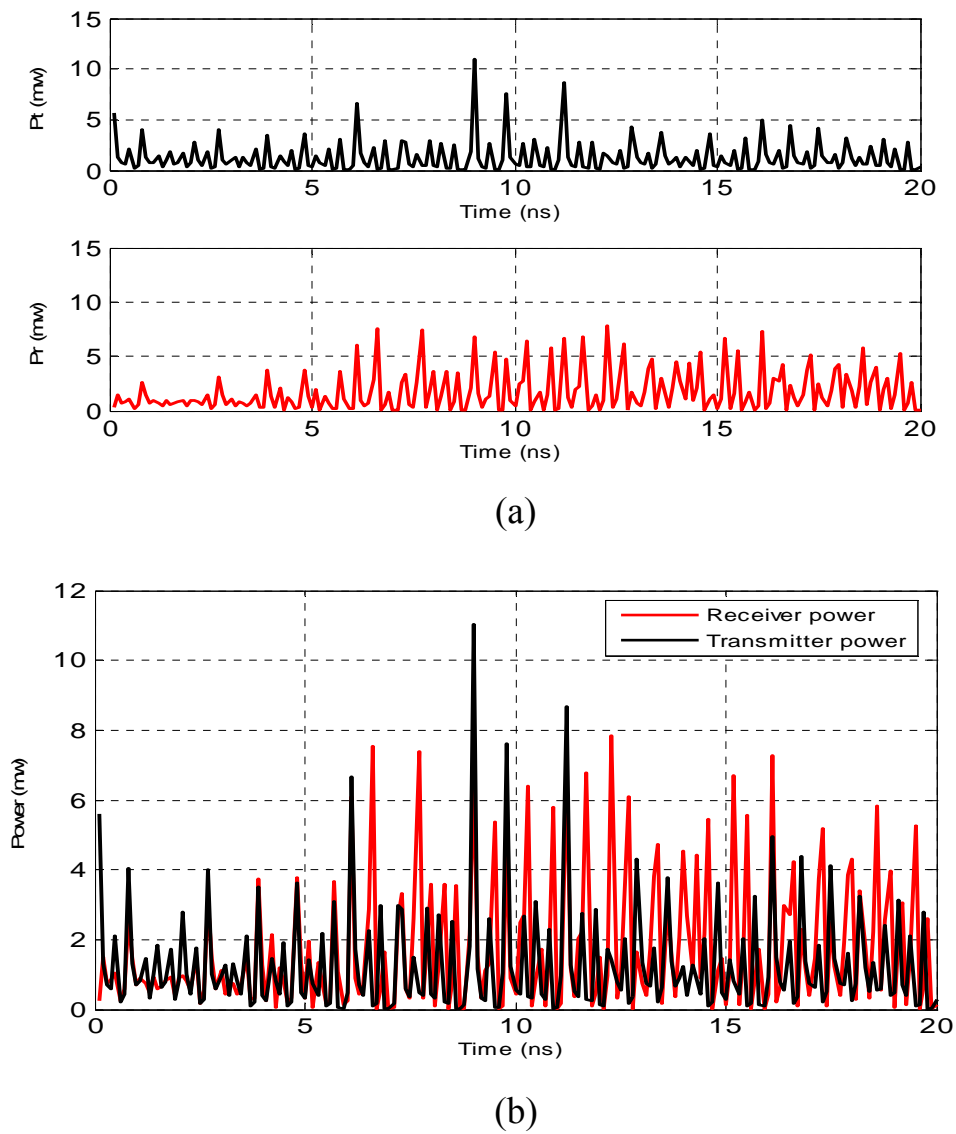
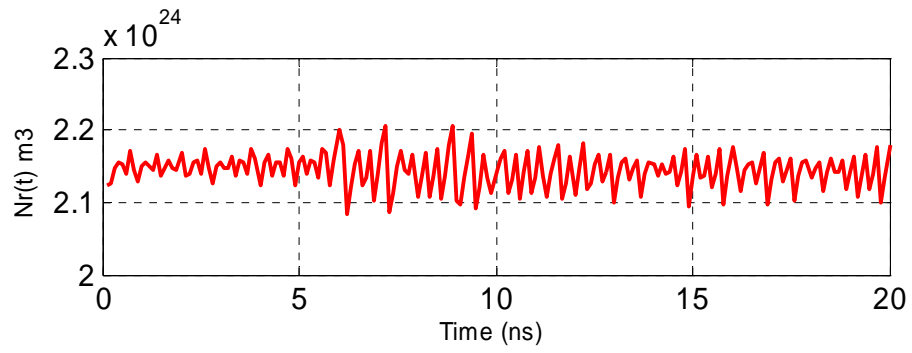
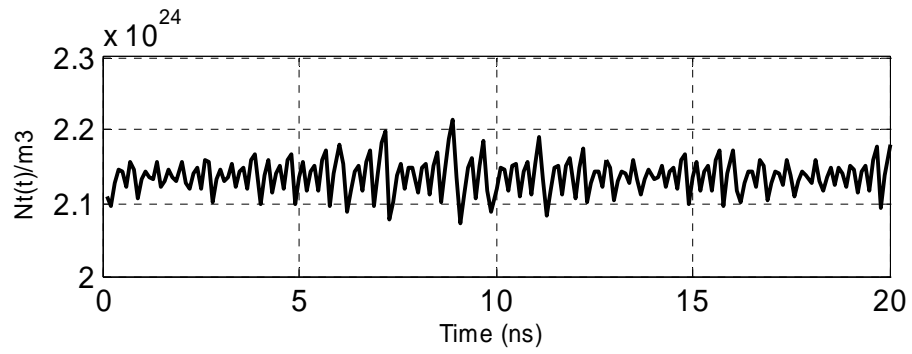
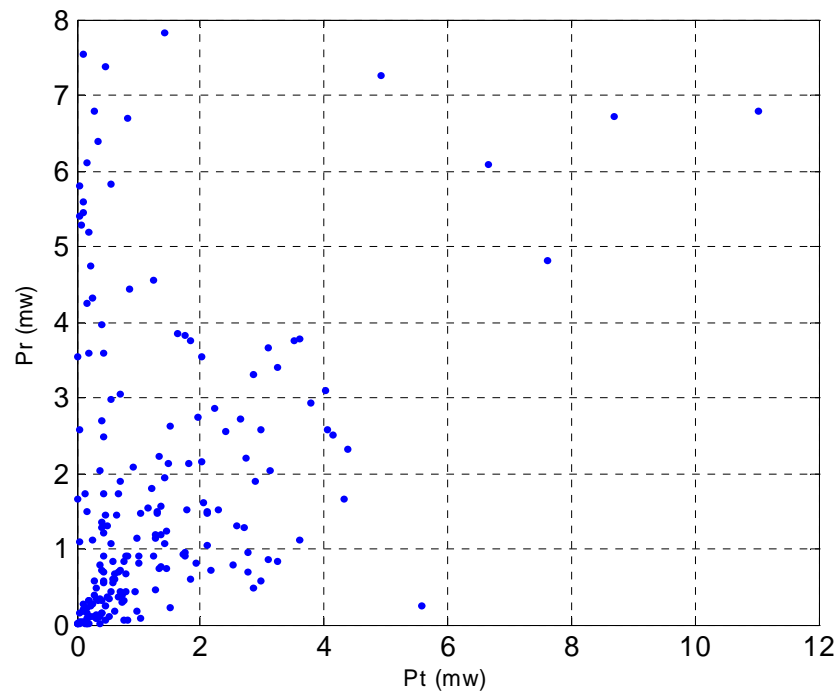


Fig. 4.22. Transmitter and receiver characteristics when $k_f=0.4$ and $k_{inj}=0.3$

- (a) Transmitter and receiver power
- (b) System power
- (c) Carrier density
- (d) System synchronization.



(c)



(d)

Fig. 4.22 (continued).

When $k_f = 0.3$ and $k_{inj} = 0.4$, the transmitter and receiver characteristics are as shown in Figs. 4.23a-d.

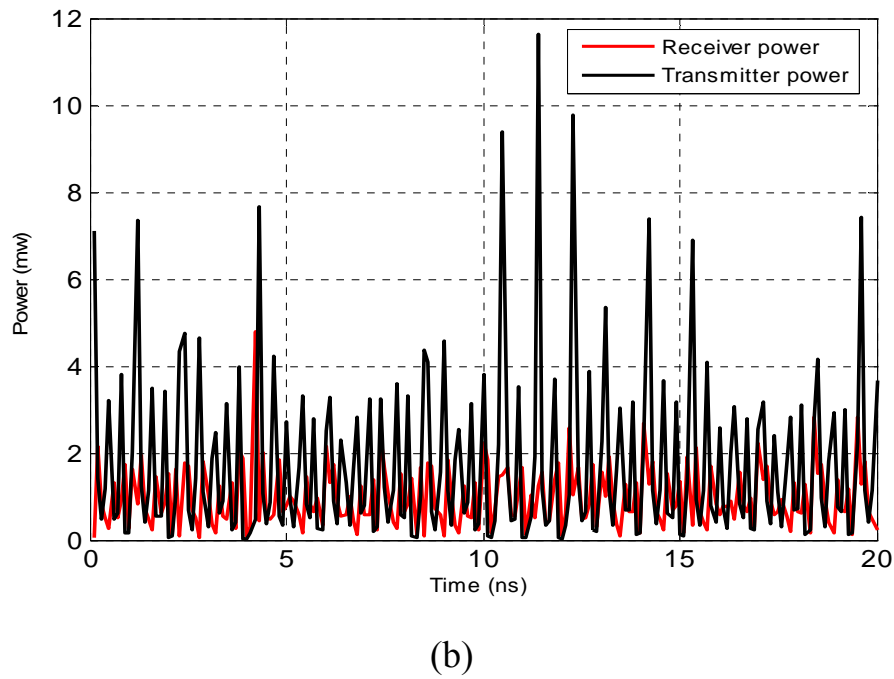
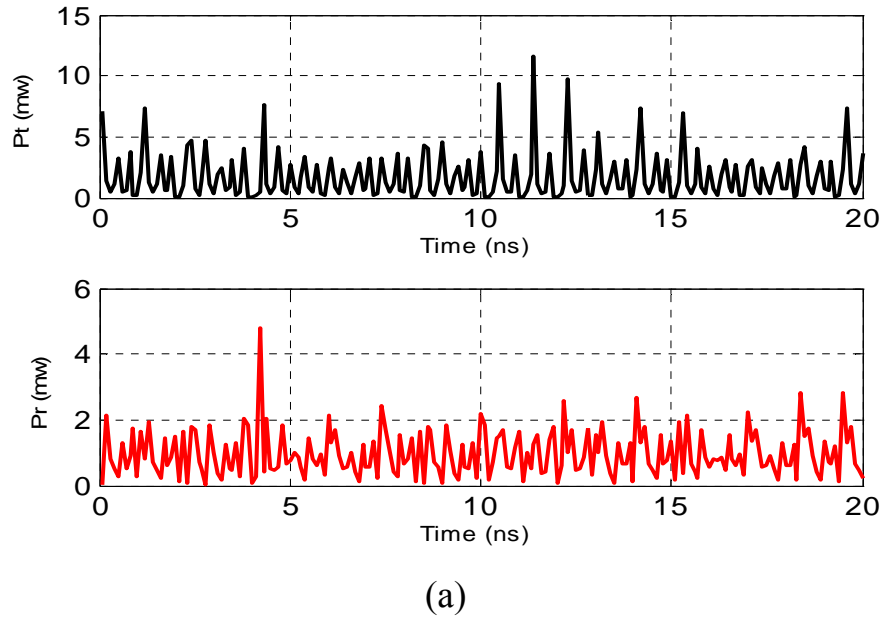
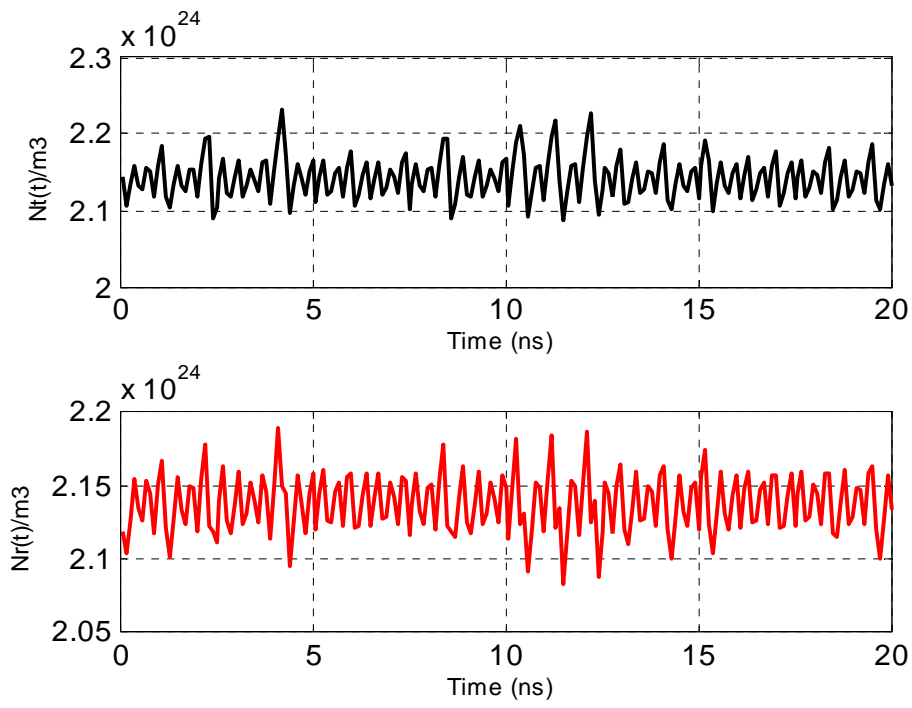
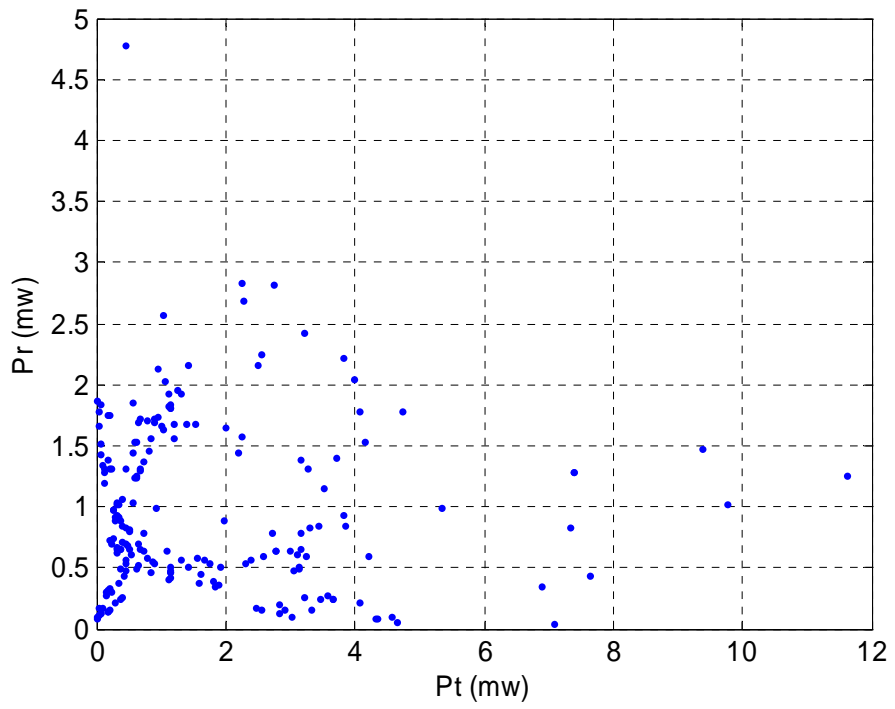


Fig. 4.23. Transmitter and receiver characteristics when $k_f = 0.3$ and $k_{inj} = 0.4$

- (a) Transmitter and receiver power
- (b) System power
- (c) Carrier density
- (d) System synchronization.



(c)



(d)

Fig. 4.23 (continued).

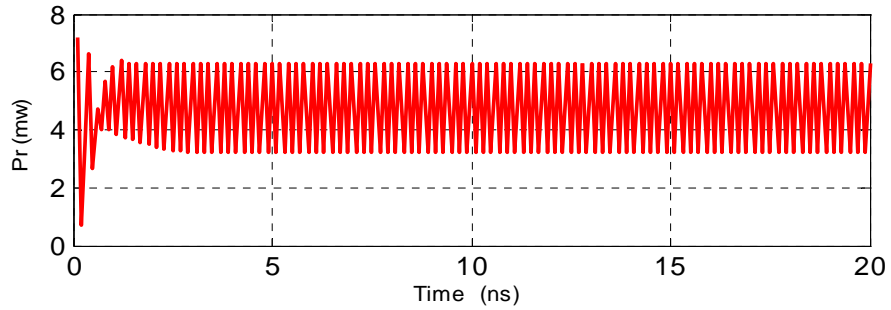
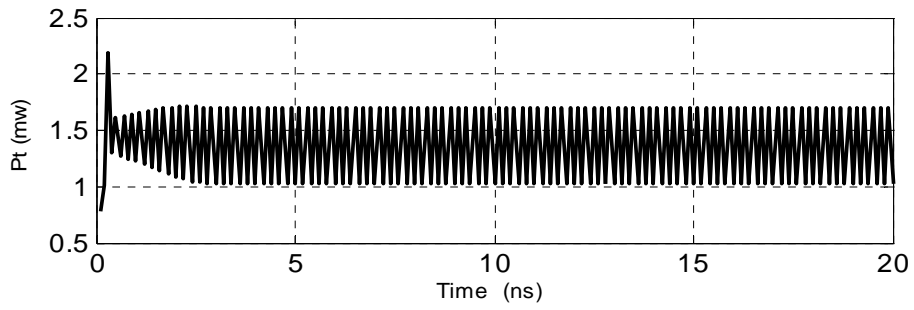
It is clear that when the optical injection is near to the optical feedback, the transmitter and receiver characteristics are approximately similar in waveforms and the system operates approximately in synchronization. From all the figures shown, before one can observe that the best values of the optical feedback and optical injection coefficients that make the system generates chaotic signals are $k_f = k_{inj} = 0.3$, and when $I_t = I_r = 1.4I_{th}$.

In the next subsection, the effects of the time of flight between the transmitter and receiver τ_f and the round trip time in the external cavity (τ) are discussed.

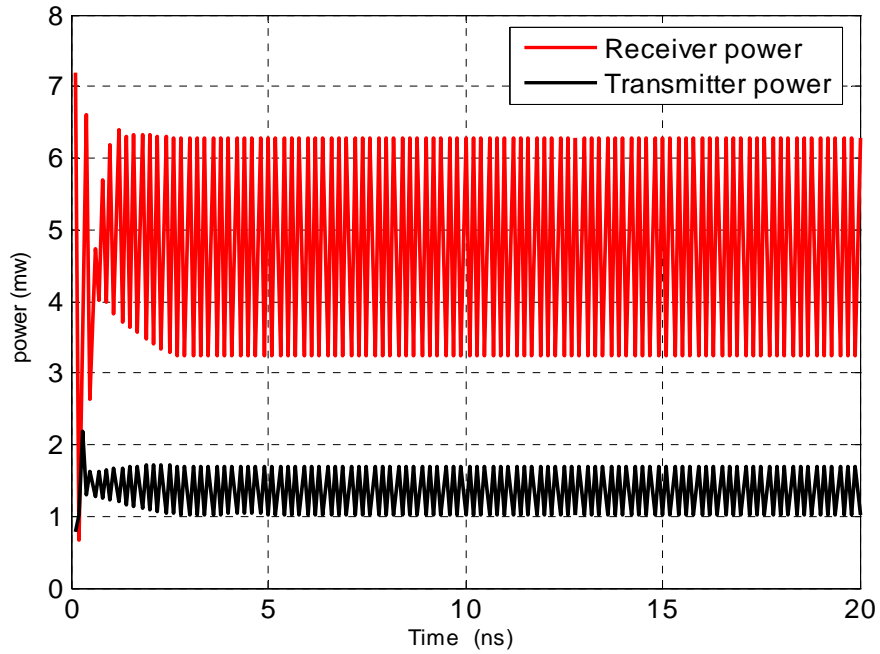
4.4.3 Effect of τ_f and τ

When the transmission time of flight between the transmitter and the receiver τ_f is varied, many of characteristics parameters system are affected such as $N(t)$, transmitter and receiver power, and system synchronization. In this section, it will be shown that for full synchronization, τ_f must be equal to τ . Figs. 4.21-4.26 show the variation of each of these parameters with some values of τ_f and τ . For the optimum values of k_f and $k_{inj} = 0.3$, $I_t = I_r = 1.4I_{th}$ and $\tau_f = 0.5\text{ns}$, the effect of τ is considered first.

When $\tau = 0.2\text{ns}$, the transmitter and receiver characteristics are as shown in Figs. 4.24a-d.



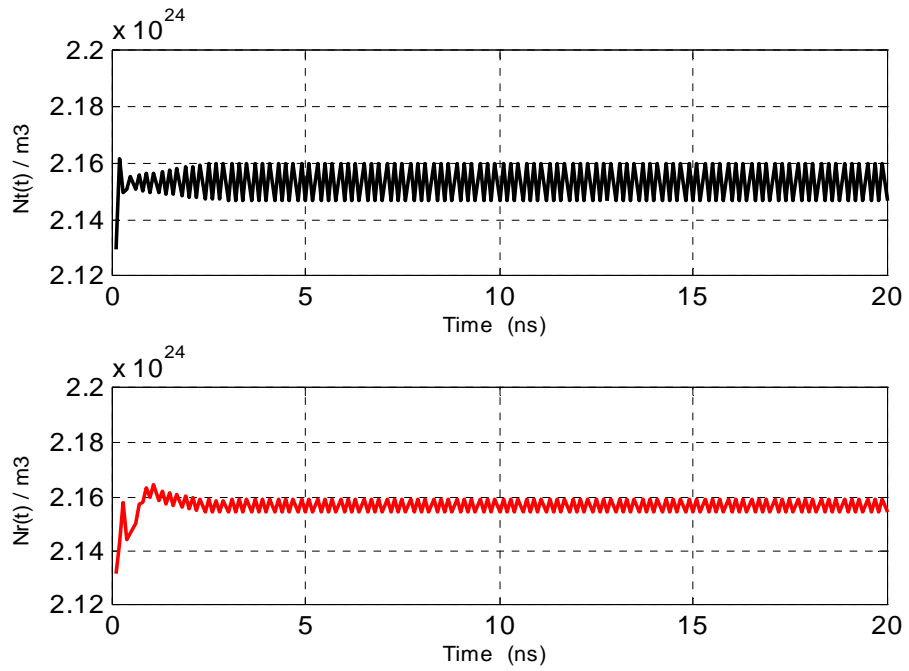
(a)



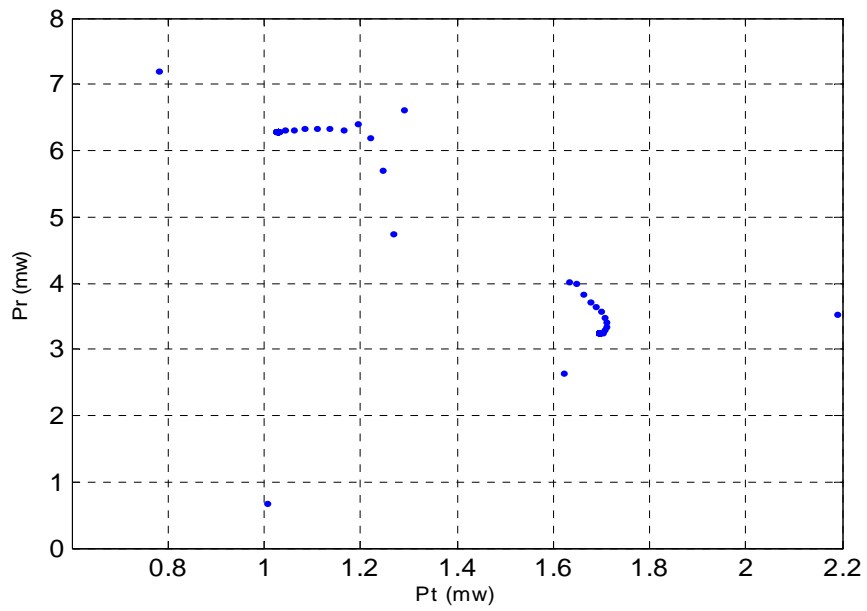
(b)

Fig. 4.24. Transmitter and receiver characteristics when $\tau_f = 0.5\text{ns}$ and $\tau = 0.2\text{ns}$

- (a) Transmitter and receiver power
- (b) System power
- (c) Carrier density
- (d) System synchronization.



(c)



(d)

Fig. 4.24 (continued).

When the round trip time in the external cavity τ increases to 0.3ns, the transmitter and receiver characteristics are as shown in Figs. 4.25a-d.

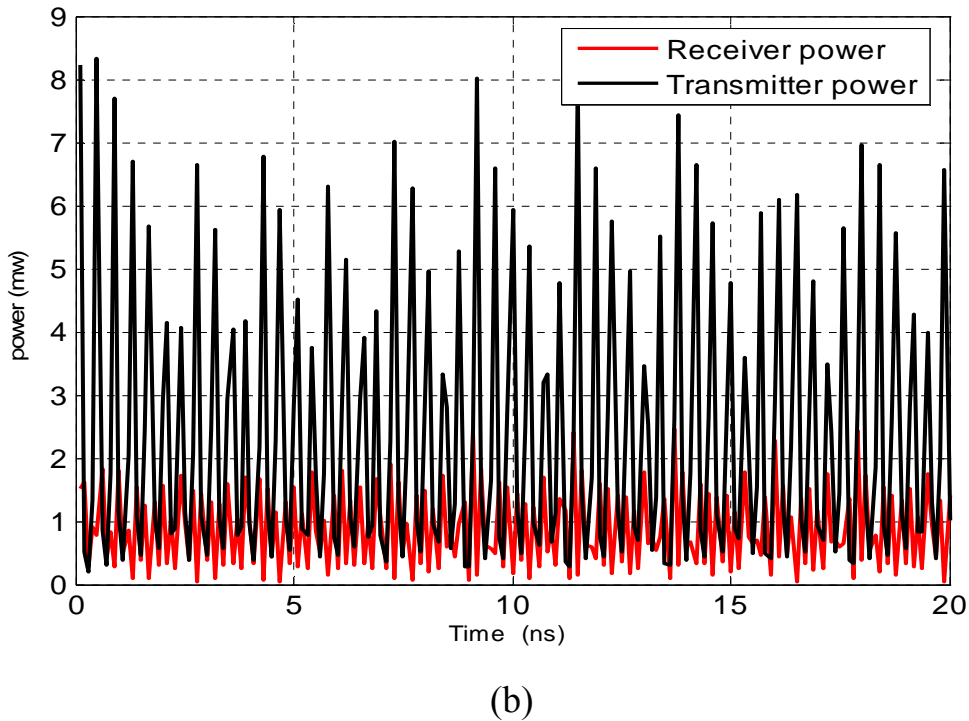
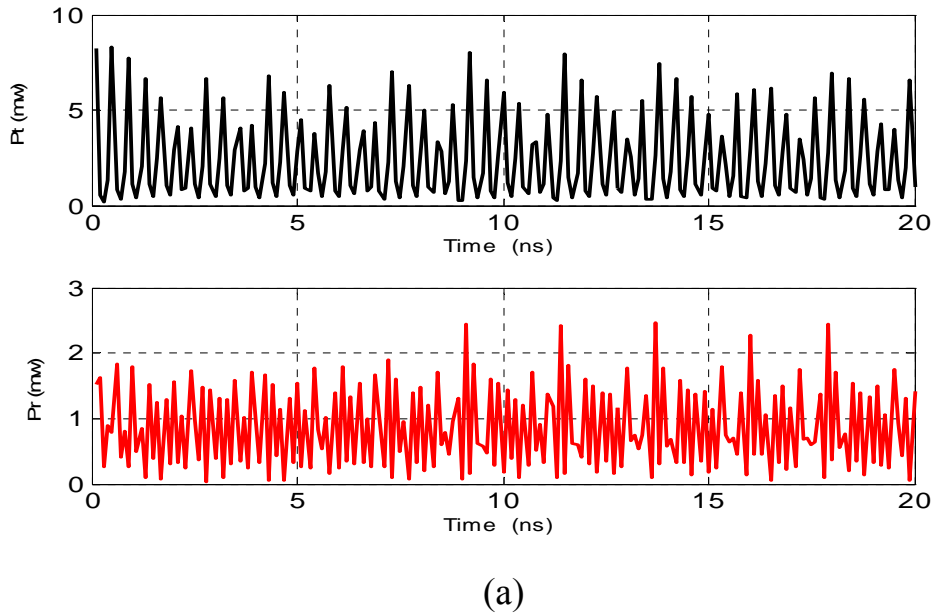


Fig. 4.25. Transmitter and receiver characteristics when $\tau_f = 0.5\text{ns}$ and $\tau = 0.3\text{ns}$

- (a) Transmitter and receiver power
- (b) System power
- (c) Carrier density
- (d) System synchronization.

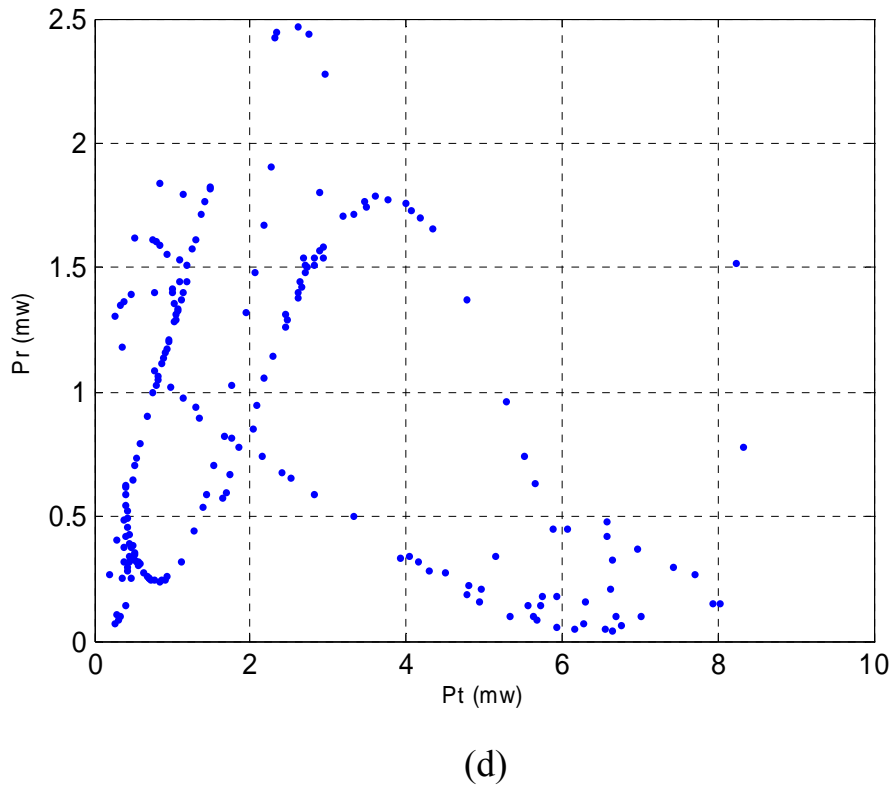
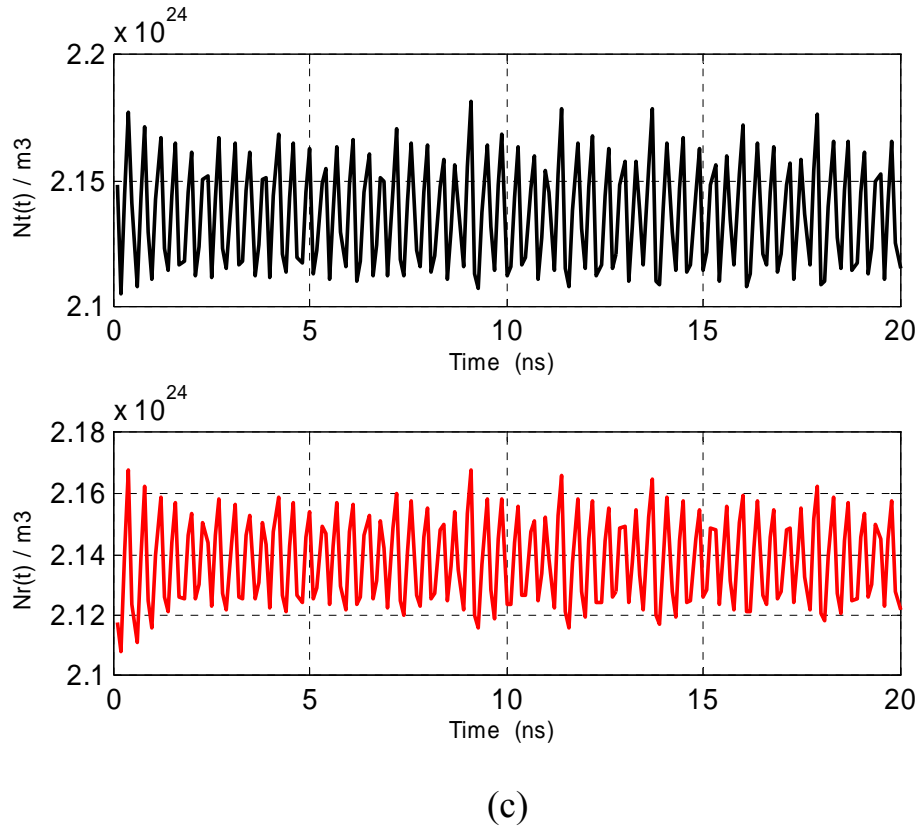


Fig. 4.25 (continued).

If $\tau_f = \tau = 0.5\text{ns}$, the transmitter and receiver characteristics are as shown in Figs. 4.26a-d.

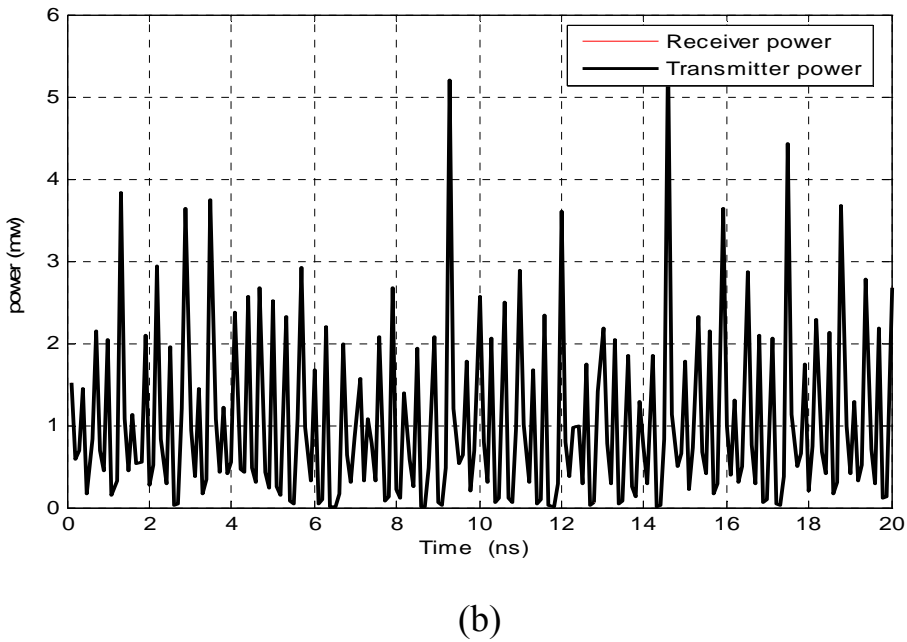
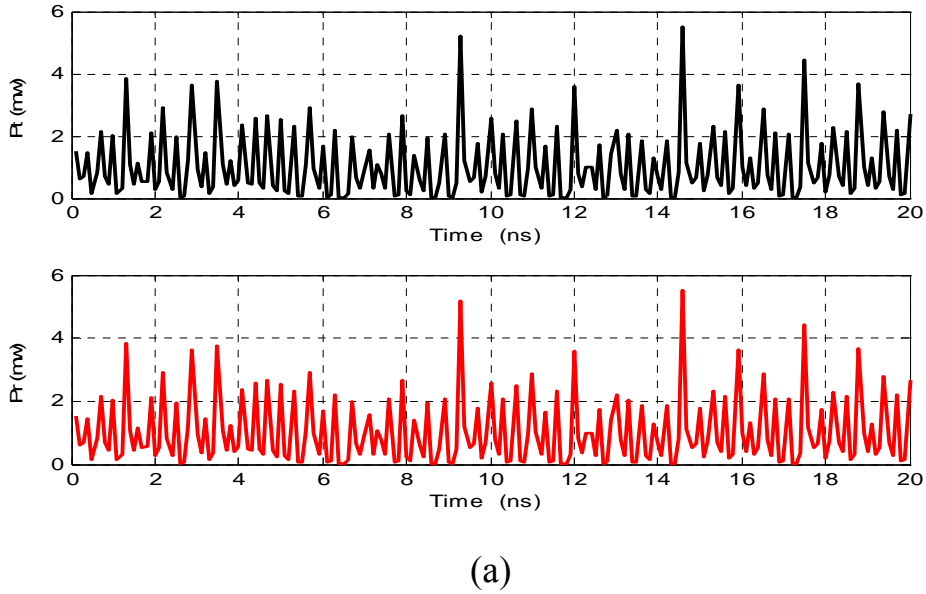
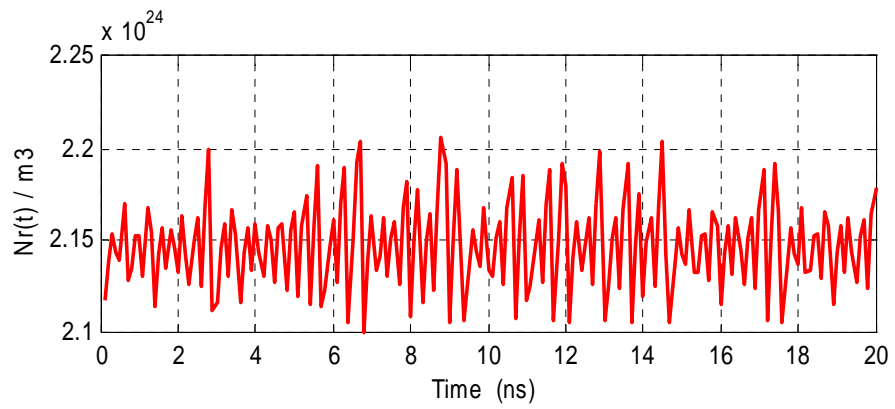
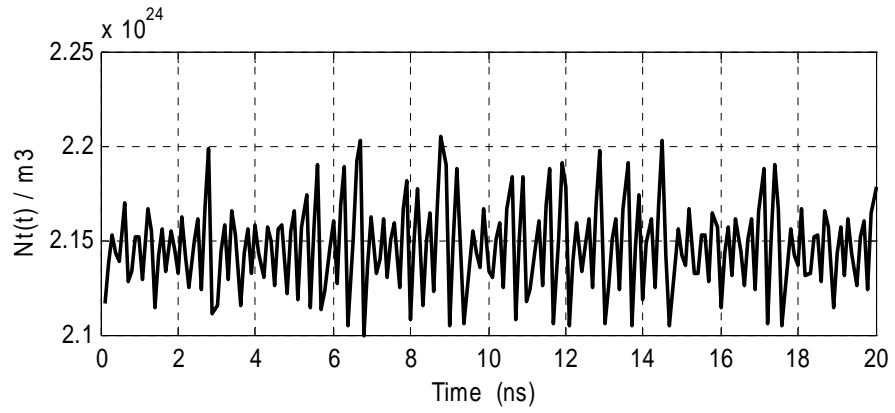
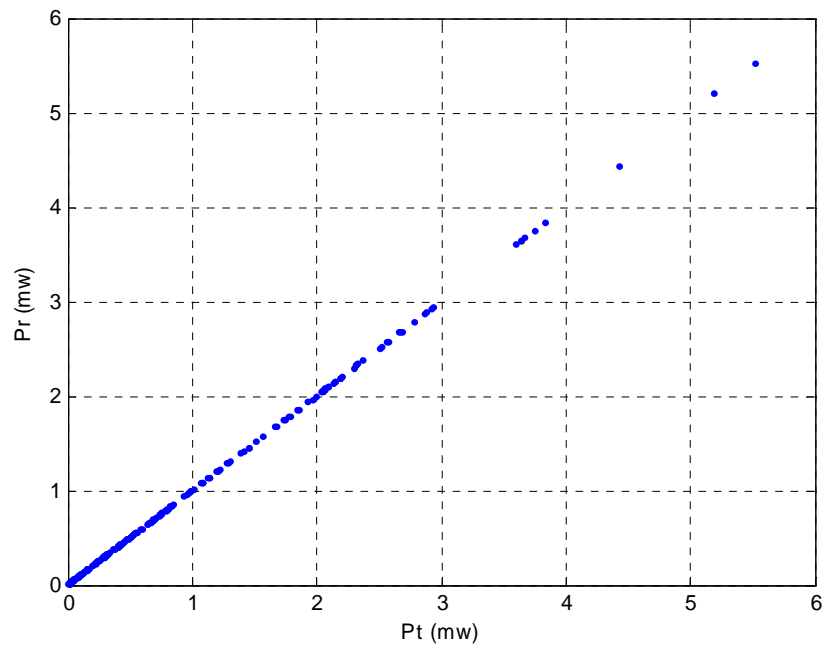


Fig. 4.26. Transmitter and receiver characteristics when $\tau_f = \tau = 0.5\text{ns}$
 (a) Transmitter and receiver power (b) System power (c) Carrier density
 (d) System synchronization.



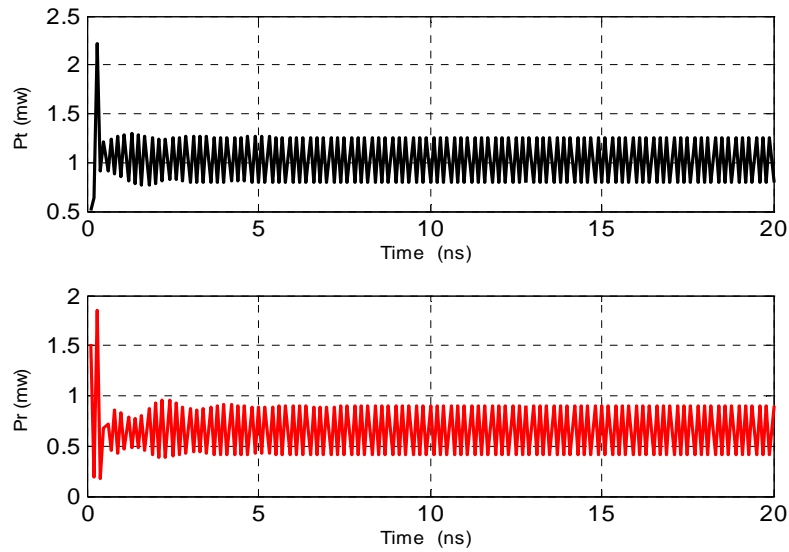
(c)



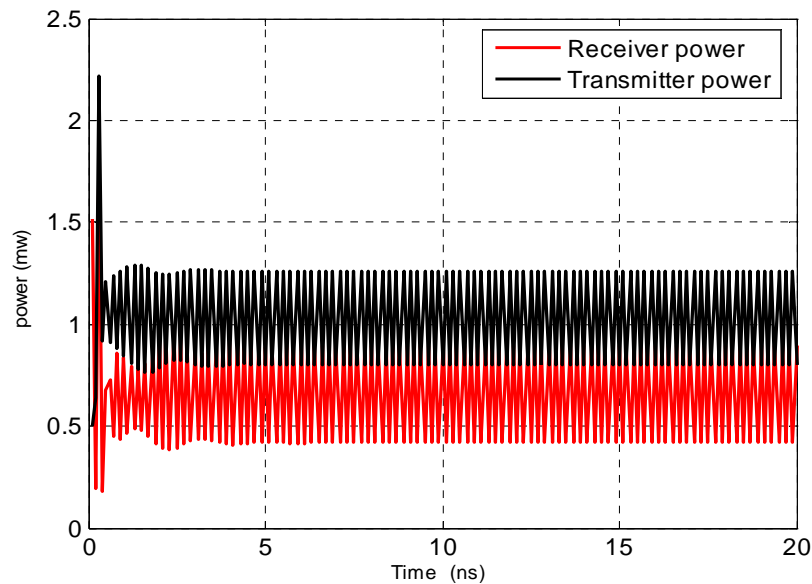
(d)

Fig. 4.26 (continued).

When $\tau_f = 0.5\text{ns}$ and $\tau = 0.7\text{ns}$, the transmitter and receiver characteristics are as shown in Figs. 4.27a-d.



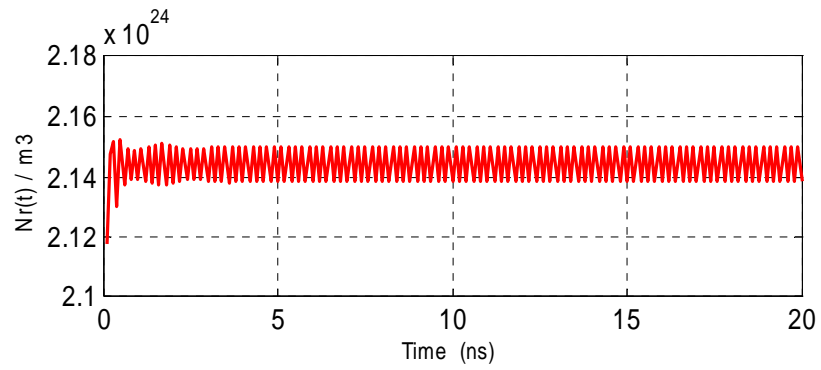
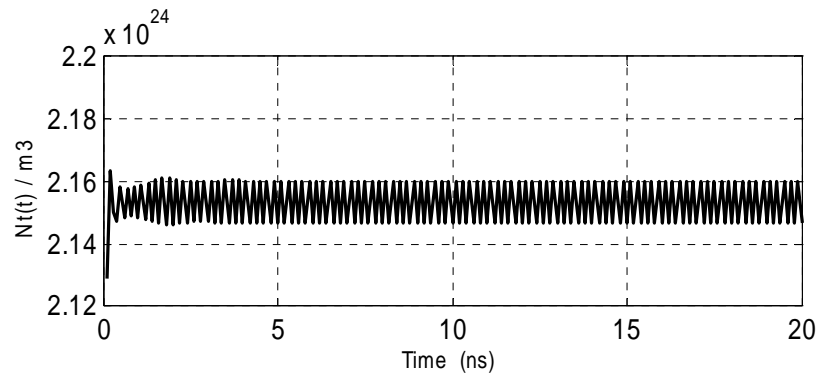
(a)



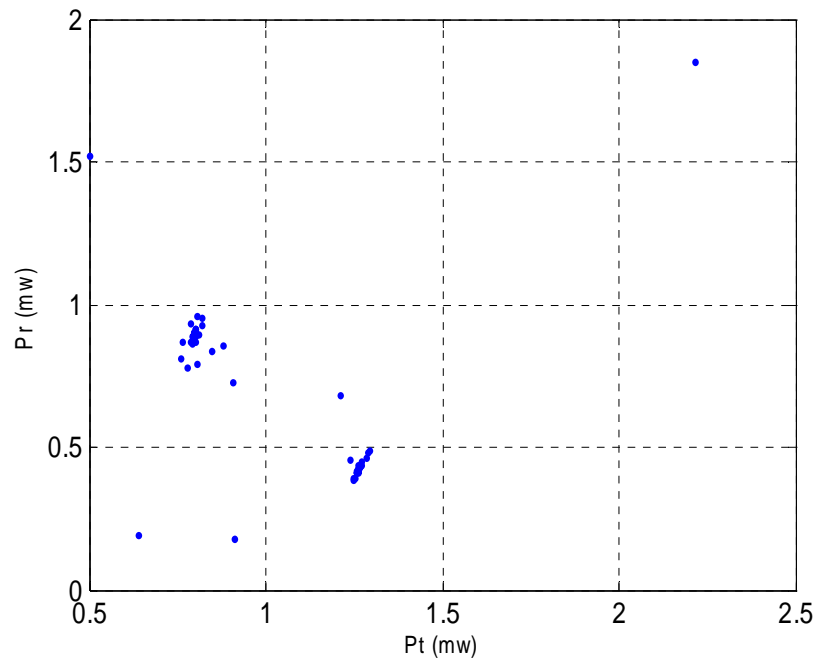
(b)

Fig. 4.27. Transmitter and receiver characteristics when $\tau_f = 0.5\text{ns}$ and $\tau = 0.7\text{ns}$

- (a) Transmitter and receiver power (b) System power (c) Carrier density
(d) System synchronization.



(c)



(d)

Fig. 4.27 (continued).

When $\tau = 1\text{ns}$, and $\tau_f = 0.5 \text{ ns}$ the transmitter and receiver characteristics are as shown in Figs. 4.28a-d.

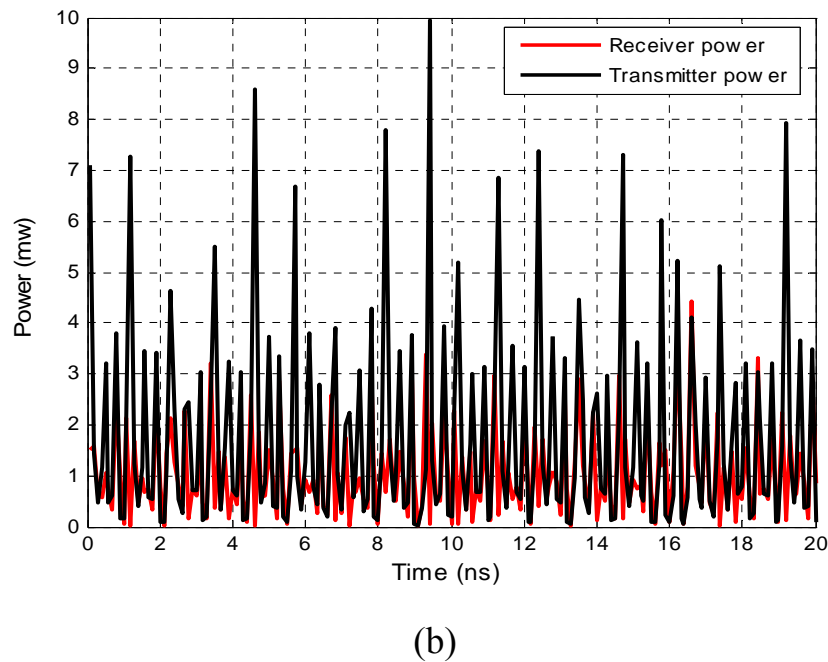
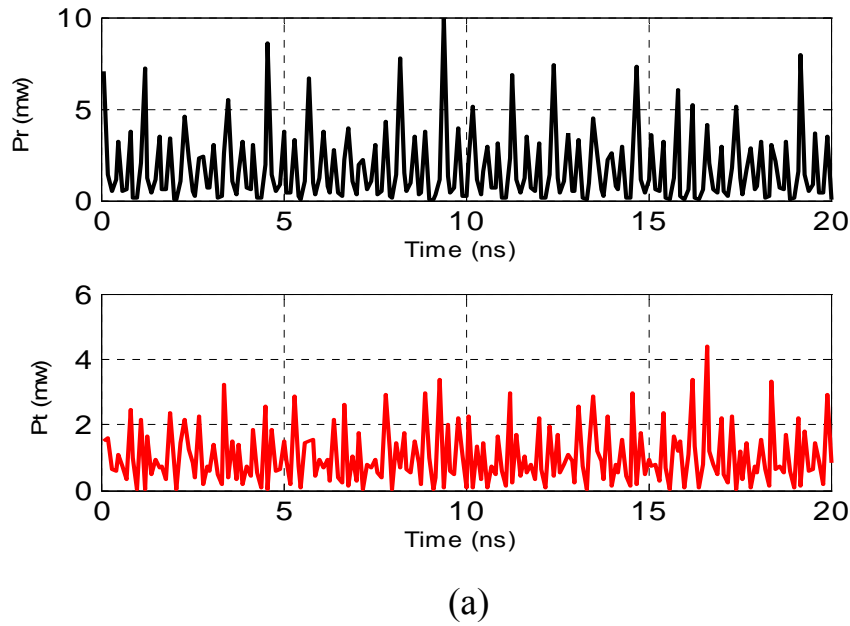
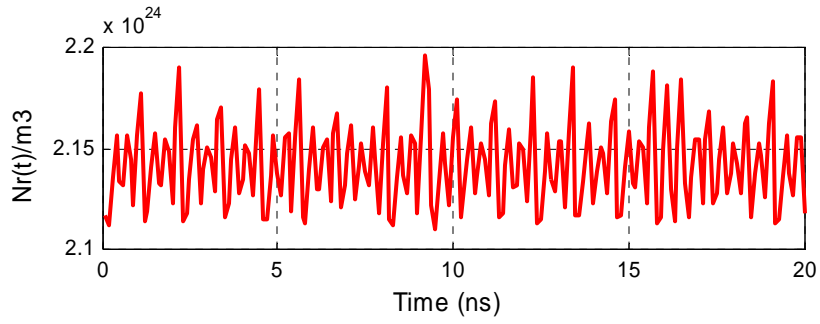
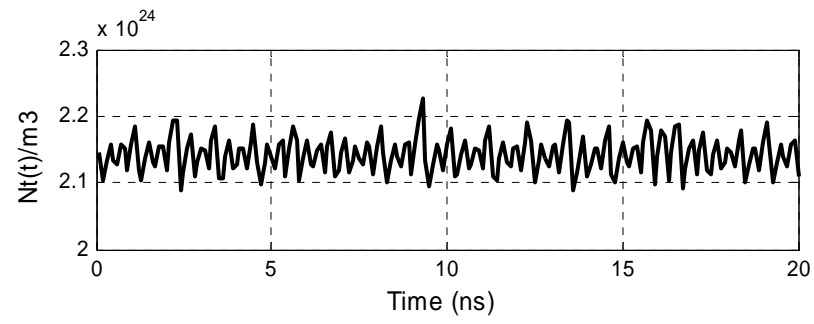
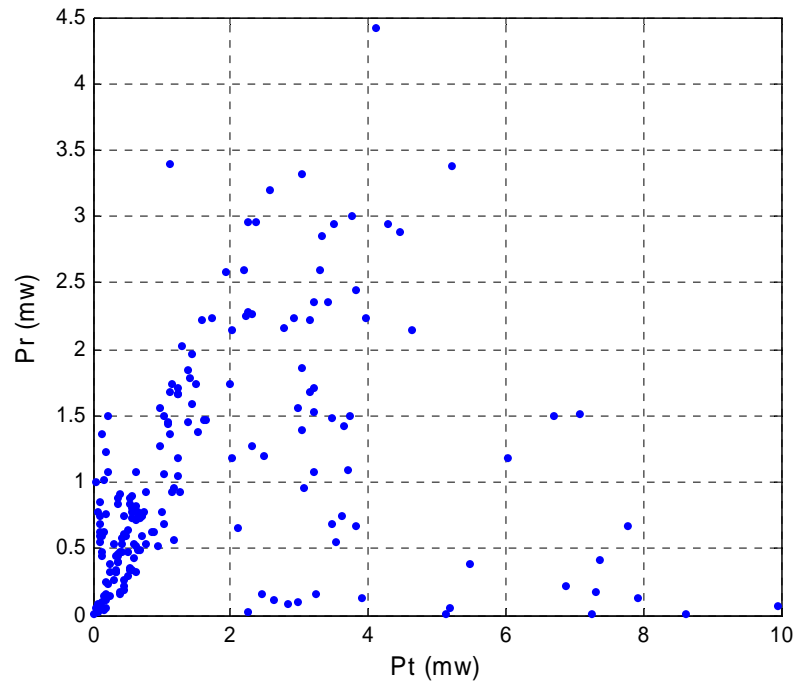


Fig. 4.28. Transmitter and receiver characteristics when $\tau_f = 0.5\text{ns}$ and $\tau = 1\text{ns}$

- (a) Transmitter and receiver power (b) System power (c) Carrier density
 (d) System synchronization.



(c)



(d)

Fig. 4.28 (continued).

When $\tau = \tau_f = 1\text{ns}$, the transmitter and receiver characteristics are as shown in Figs. 4.29a-d.

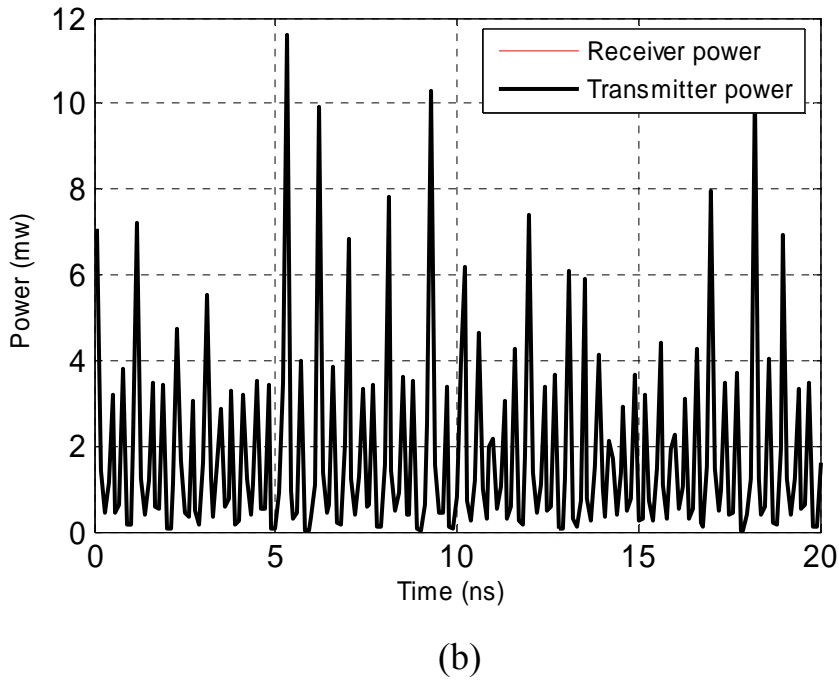
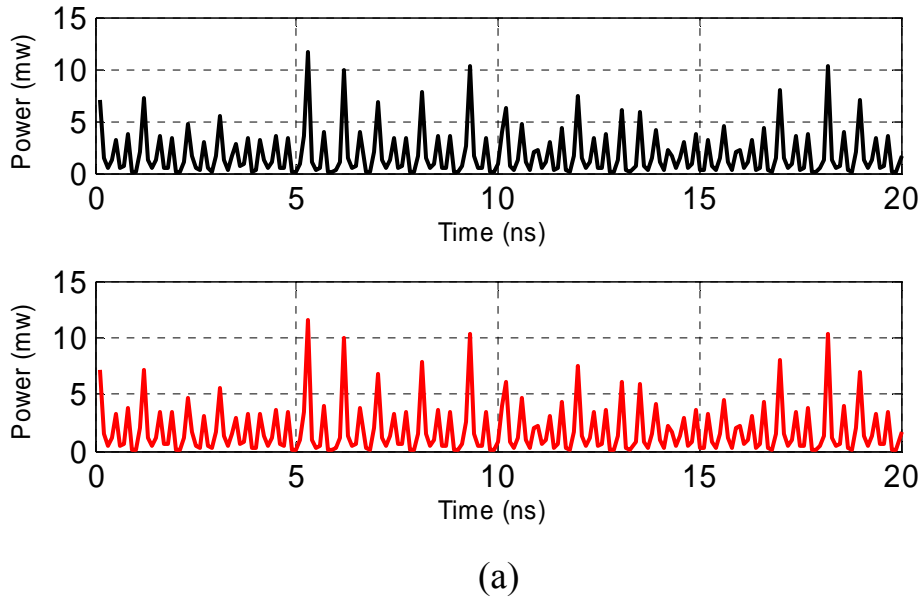
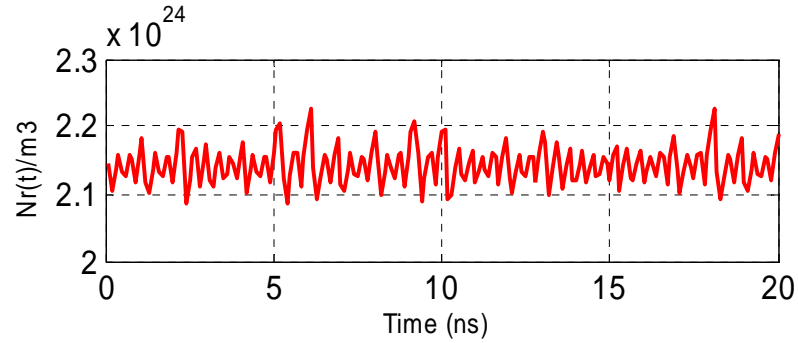
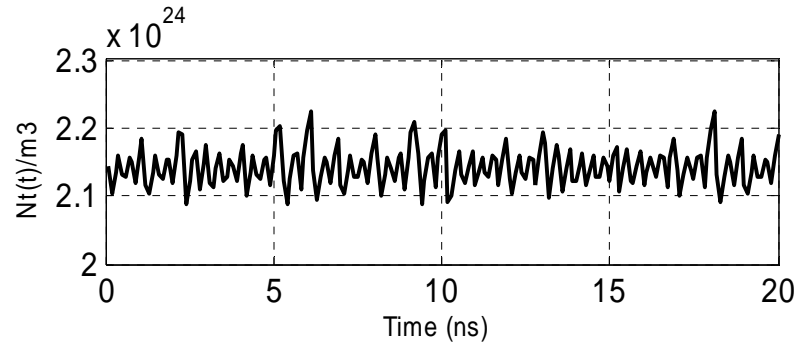
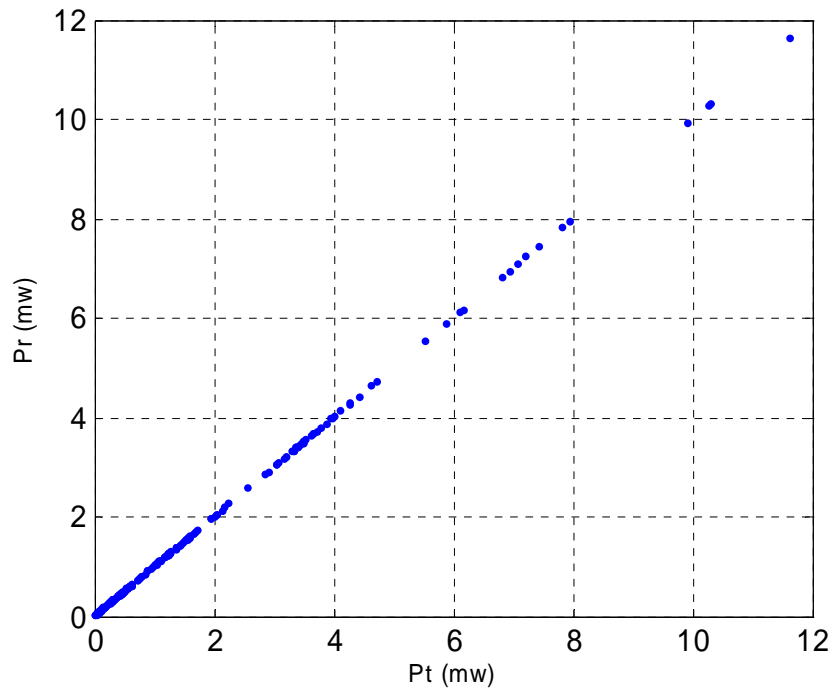


Fig. 4.29. Transmitter and receiver characteristics when $\tau_f = 1\text{ns}$ and $\tau = 1\text{ns}$

- (a) Transmitter and receiver power
- (b) System power
- (c) Carrier density
- (d) System synchronization.



(c)



(d)

Fig. 4.29 (continued).

From Figs. 4.24 to 4.29, it is clear that there are high effects on the system synchronization when τ_f varies from 0.2ns to 1ns and the system is synchronized only when τ_f equals to τ and the best case is that when $\tau_f = \tau = 1ns$.

4.4.4 Effect of Receiver Injection Current

In this subsection, the effect of changing the receiver current is discussed for optimum values of synchronization $k_f = k_{inj} = 0.3, \tau = \tau_f = 1ns$, and $I_t = 1.4I_{th}$. Figs. 4.30a-d show the characteristic waveforms of the transmitter and receiver for each value of I_r .

When $I_r = 1.2I_{th}$, the characteristics of the transmitter and the receiver are as shown in Figs. 4.30a-d.

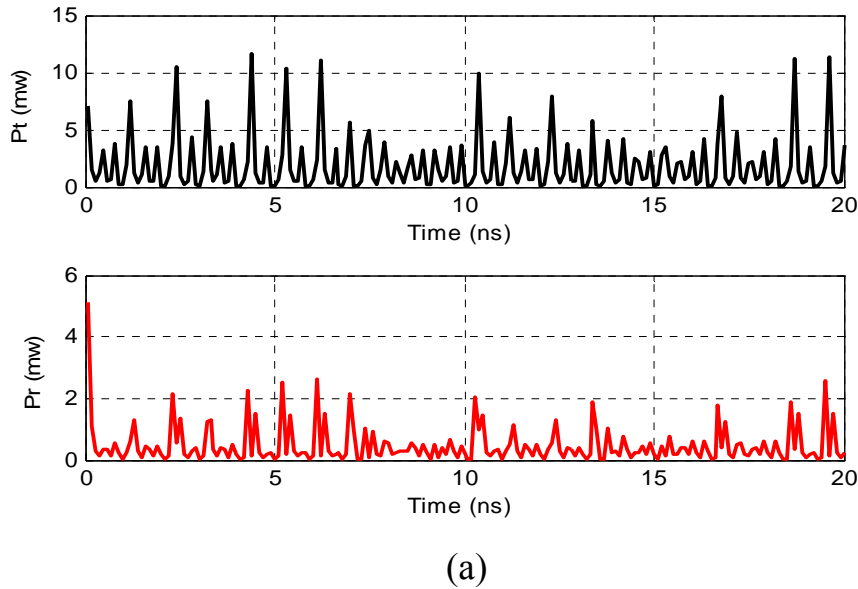
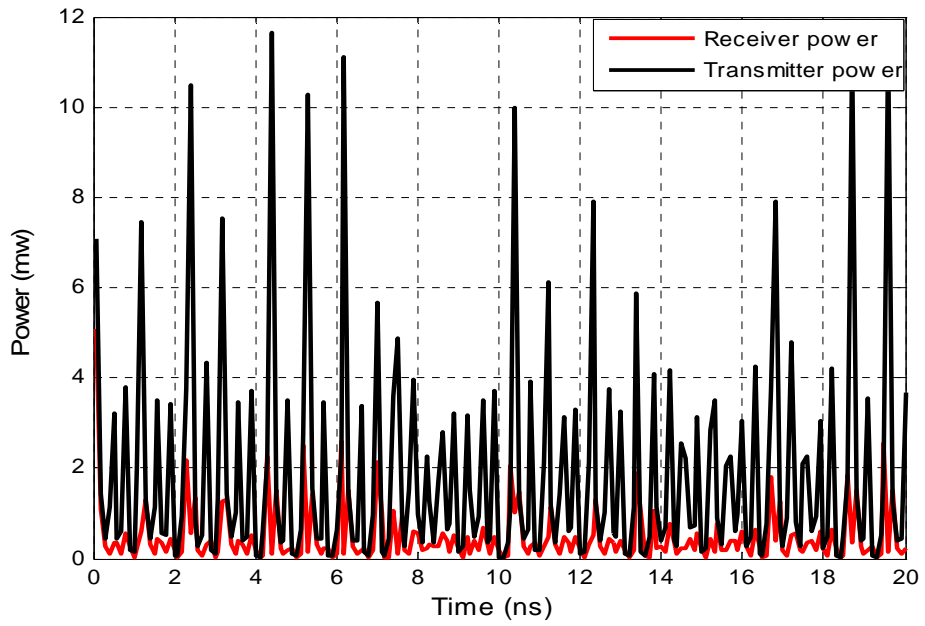
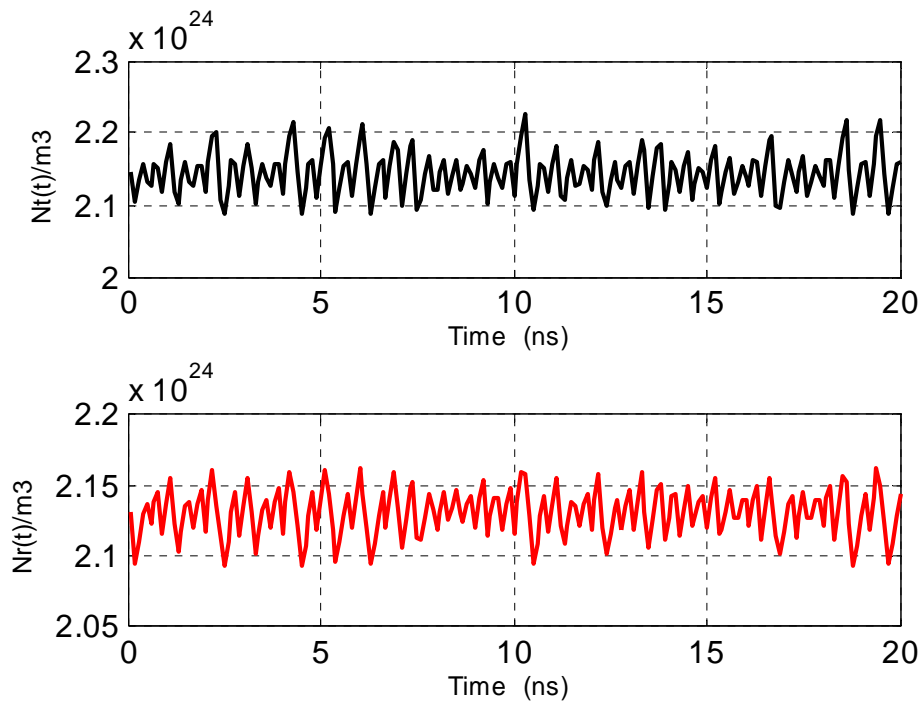


Fig. 4.30. Transmitter and receiver characteristics when $k_f = k_{inj} = 0.3, \tau = \tau_f = 1ns$, and $I_r = 1.2I_{th}$ (a) Transmitter and receiver power (b) System power (c) Carrier density (d) System synchronization.

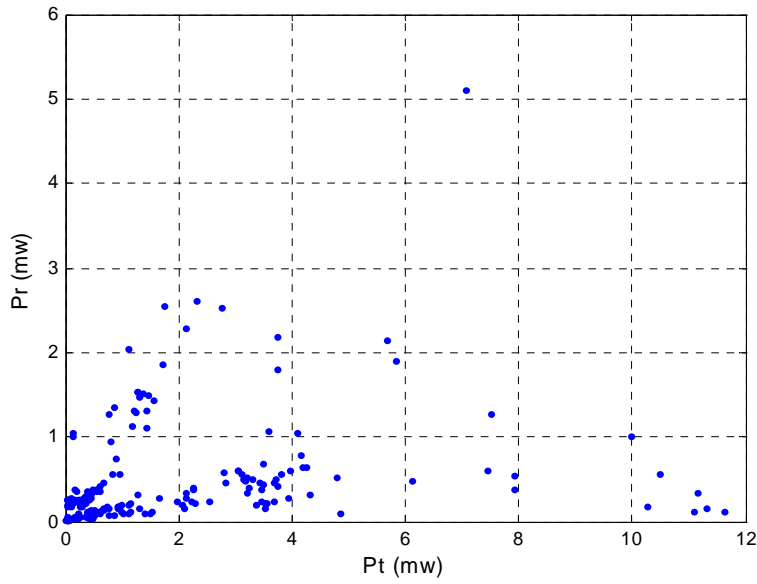


(b)



(c)

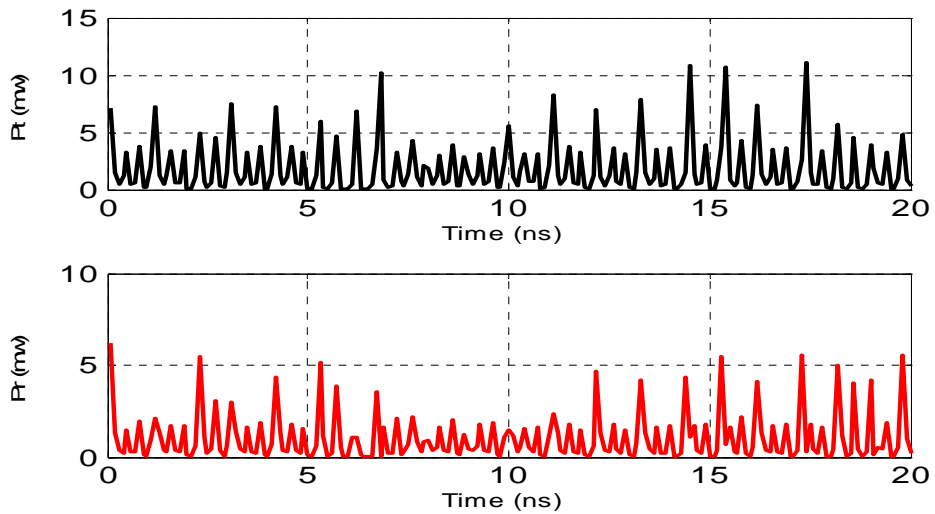
Fig. 4.30 (continued).



(d)

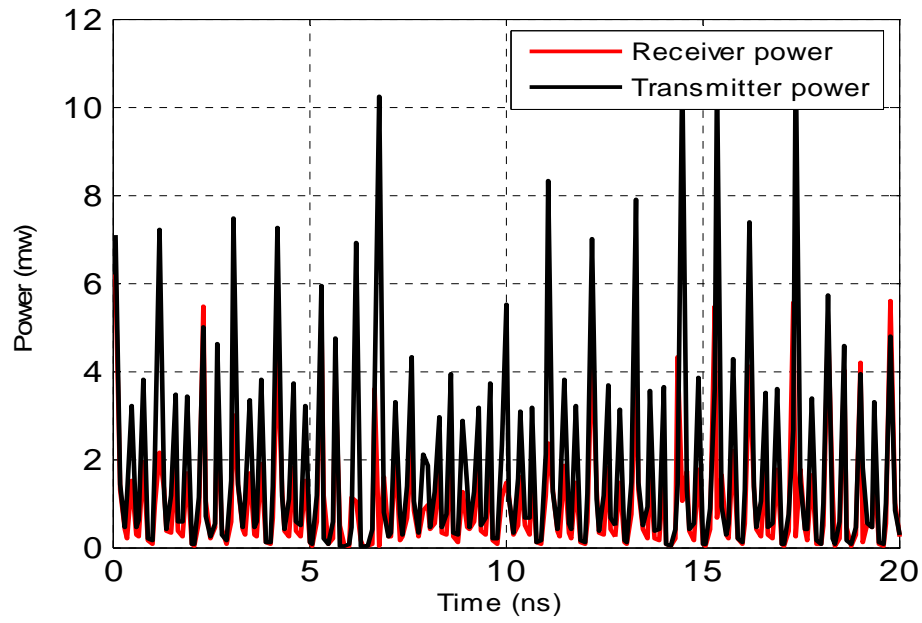
Fig. 4.30 (continued).

When $I_r = 1.3I_{th}$, the characteristics of the transmitter and receiver are as shown in Figs. 4.31a-d.

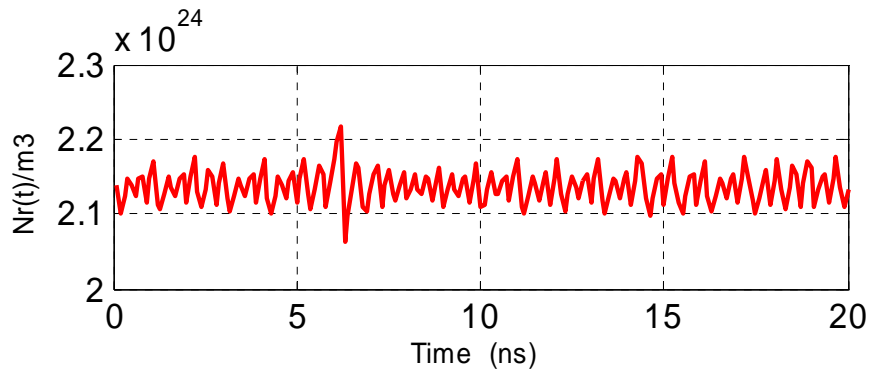
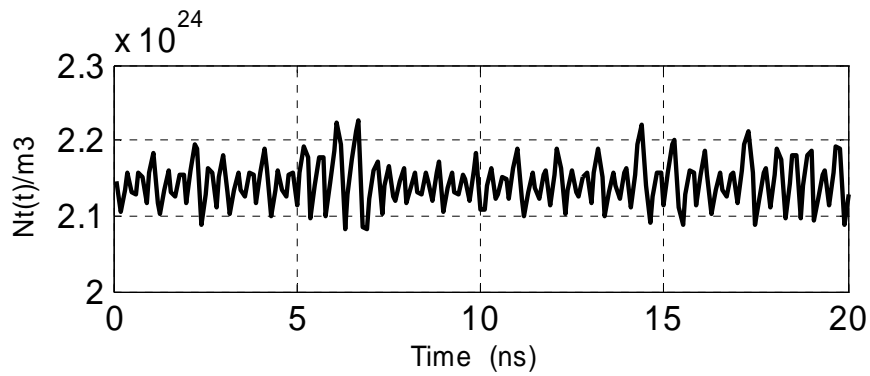


(a)

Fig. 4.31. Transmitter and receiver characteristics when $k_f = k_{inj} = 0.3$, $\tau = \tau_f = 1$ ns, and $I_r = 1.3I_{th}$ (a) Transmitter and receiver power (b) System power (c) Carrier density (d) System synchronization.

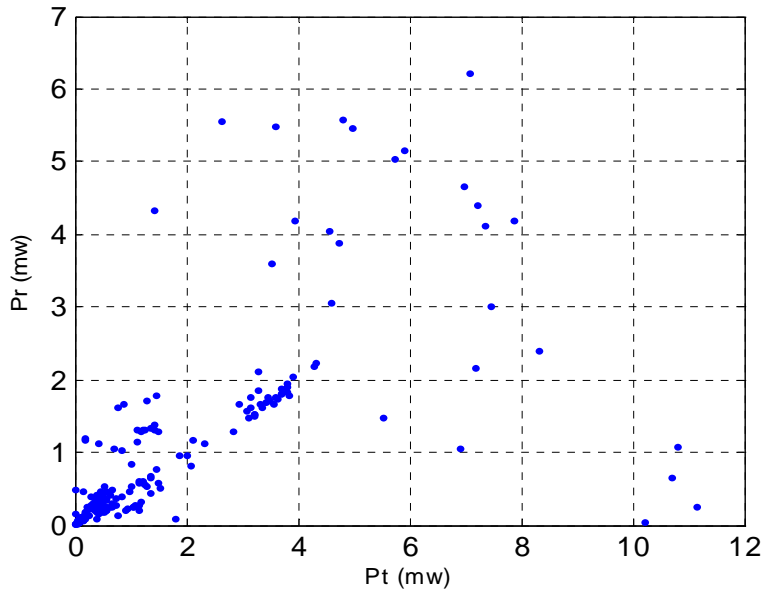


(b)



(c)

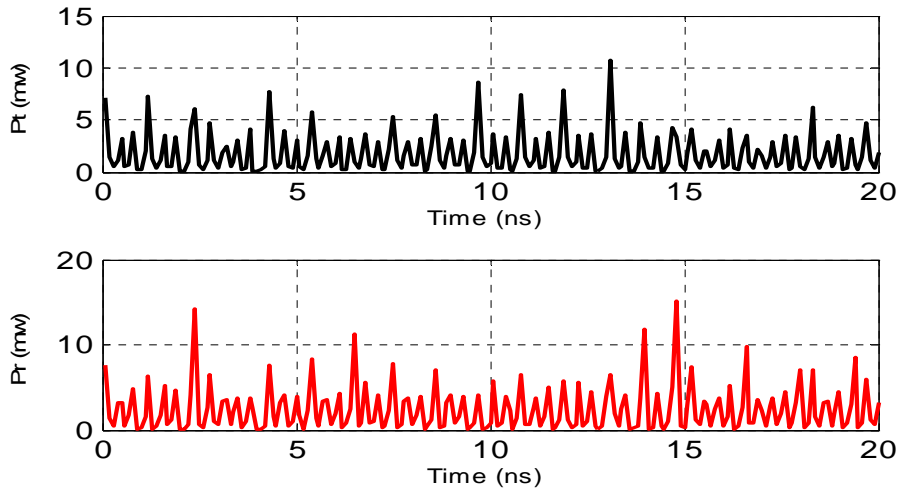
Fig. 4.31 (continued).



(d)

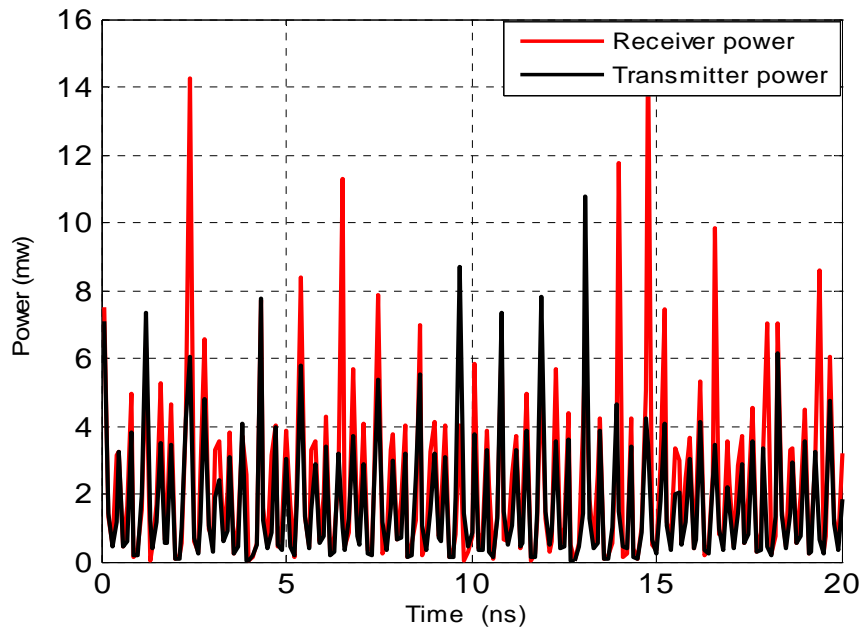
Fig. 4.31 (continued).

When $I_r = 1.5I_{th}$, the characteristics of the transmitter and receiver are shown in Figs. 4.32a-d.

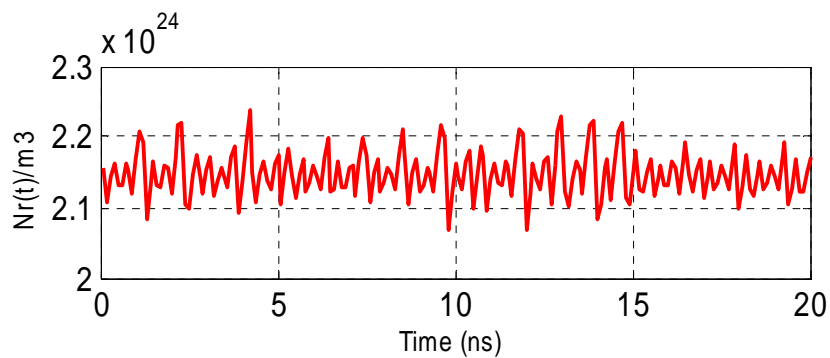
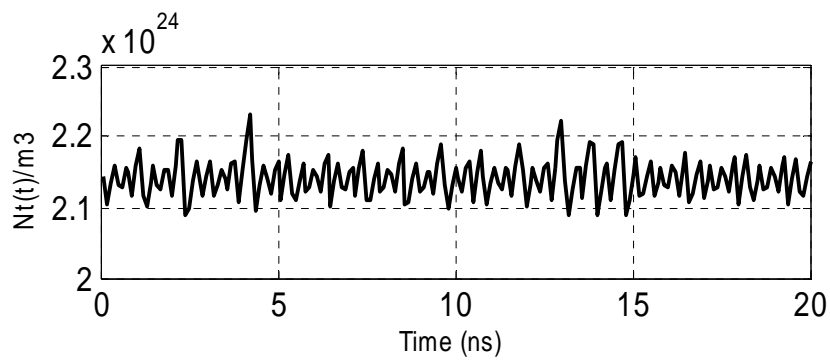


(a)

Fig. 4.32. Transmitter and receiver characteristics when $k_f = k_{inj} = 0.3, \tau = \tau_f = 1\text{ns}$ and $I_r = 1.5I_{th}$ (a) Transmitter and receiver power (b) System power (c) Carrier density (d) System synchronization.

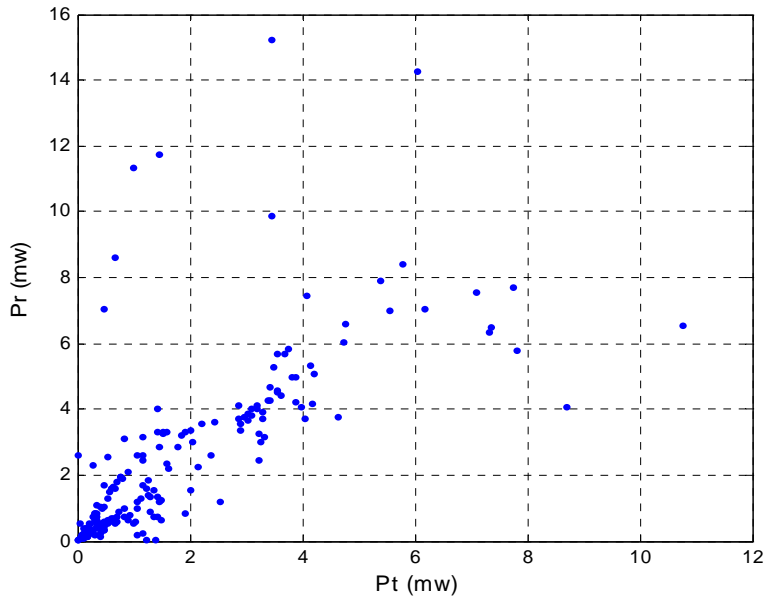


(b)



(c)

Fig. 4.32 (continued)



(d)

Fig. 4.32 (continued)

It is observed that when the receiver injection current is less or more than the transmitter injection current, the system stays unsynchronized as shown in Fig. 4.32d. Therefore, to achieve system synchronization, the optimum value of receiver injection current must be equal to transmitter injection current.

4.4.5 Effect of Frequency Detuning

In the previous subsections, all the calculations have been carried out at zero frequency detuning ($\Delta\omega = 0$). For the best values of k_f , k_{inj} , I_t , I_r , τ and τ_f , which make the system at complete synchronization, if the frequency detuning does not equal to zero, the system will be unsynchronized as shown in the following pages.

When $\Delta\omega = -13\text{GHz}$ the transmitter and receiver characteristics are shown in Figs. 4.33a-d.

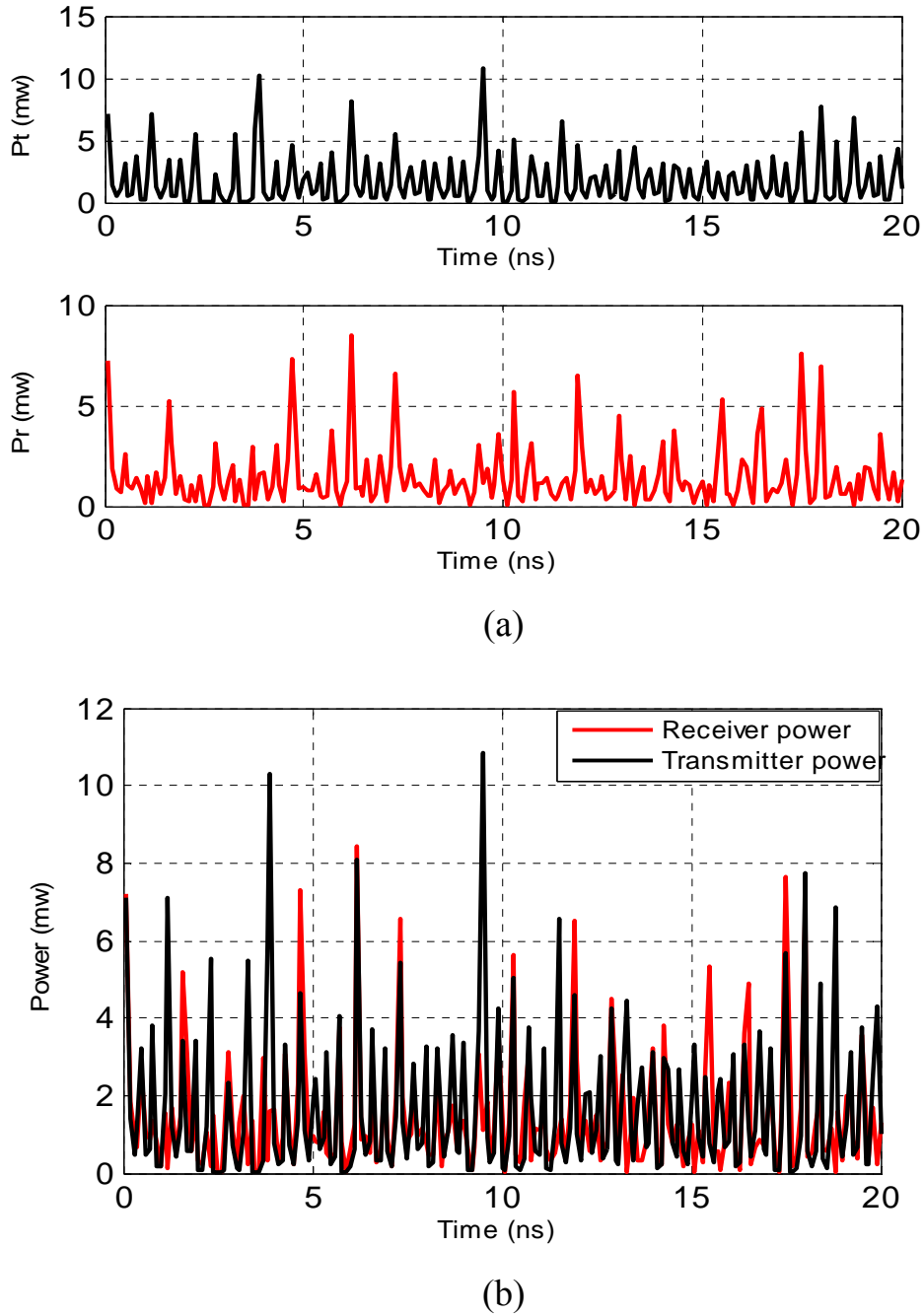


Fig. 4.33. Transmitter and receiver characteristics when $k_f = k_{inj} = 0.3, \tau = \tau_f = 1\text{ns}$ and $I_r = 1.4I_{th}$ and $\Delta\omega = -13\text{GHz}$. (a) Transmitter and receiver power (b) System power (c) Carrier density (d) System synchronization.

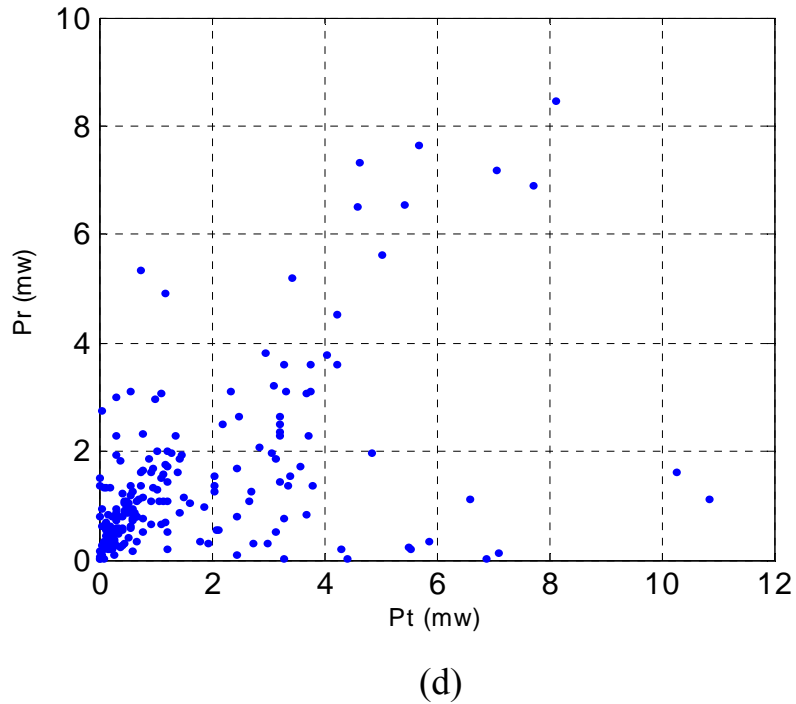
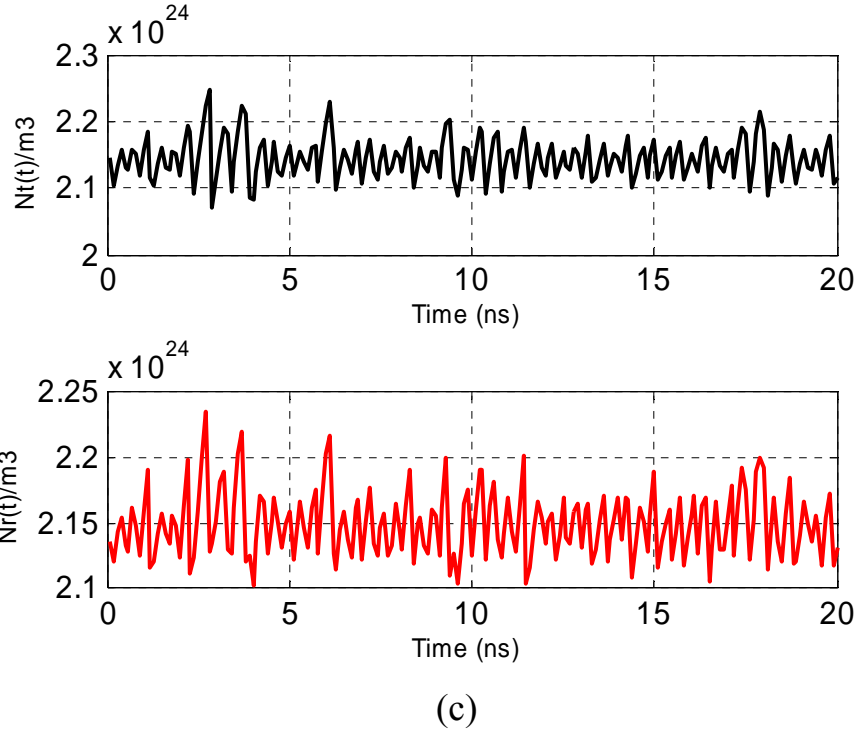


Fig. 4.33 (continued).

The simulation results are presented in Figs. (4.14-4.33), in each figures, the value of one parameter is changed with respect to the rest of figures.

Table 4.2 Parameters values used in producing Figs. (4.11-4.30)

Figure Number	Parameters Values							Remark
	k_f	k_{inj}	τ (ns)	τ_f (ns)	I_i (mA)	I_r (mA)	$\Delta\omega$ (GHz)	
4.14	0	0	1	0	$1.4I_{th}$	$1.4I_{th}$	0	synchronization
4.15	0.1	0	1	0	$1.4I_{th}$	$1.4I_{th}$	0	unsynchronized
4.16	0.2	0	1	0	$1.4I_{th}$	$1.4I_{th}$	0	unsynchronized
4.17	0.3	0	1	0	$1.4I_{th}$	$1.4I_{th}$	0	unsynchronized
4.18	0	0.1	1	0	$1.4I_{th}$	$1.4I_{th}$	0	unsynchronized
4.19	0	0.2	1	0	$1.4I_{th}$	$1.4I_{th}$	0	unsynchronized
4.20	0	0.3	1	0	$1.4I_{th}$	$1.4I_{th}$	0	unsynchronized
4.21	0.3	0.3	1	0	$1.4I_{th}$	$1.4I_{th}$	0	unsynchronized
4.22	0.4	0.3	1	0	$1.4I_{th}$	$1.4I_{th}$	0	unsynchronized
4.23	0.3	0.4	1	0	$1.4I_{th}$	$1.4I_{th}$	0	unsynchronized
4.24	0.3	0.3	0.2	0.5	$1.4I_{th}$	$1.4I_{th}$	0	unsynchronized
4.25	0.3	0.3	0.3	0.5	$1.4I_{th}$	$1.4I_{th}$	0	unsynchronized
4.26	0.3	0.3	0.5	0.5	$1.4I_{th}$	$1.4I_{th}$	0	synchronization
4.27	0.3	0.3	0.7	0.5	$1.4I_{th}$	$1.4I_{th}$	0	unsynchronized
4.28	0.3	0.3	1	0.5	$1.4I_{th}$	$1.4I_{th}$	0	unsynchronized
4.29	0.3	0.3	1	1	$1.4I_{th}$	$1.4I_{th}$	0	synchronization
4.30	0.3	0.3	1	1	$1.4I_{th}$	$1.2I_{th}$	0	unsynchronized
4.31	0.3	0.3	1	1	$1.4I_{th}$	$1.3I_{th}$	0	unsynchronized
4.32	0.3	0.3	1	1	$1.4I_{th}$	$1.5I_{th}$	0	unsynchronized
4.33	0.3	0.3	1	1	$1.4I_{th}$	$1.4I_{th}$	-13	unsynchronized

4.5 Message Encoding and Decoding

This section shows the transmission of the message with secret key through the system operating under the conditions reported in previous sections ($k_f = k_{inj} = 0.3, I_t = I_r = 1.4I_{th}, \tau = \tau_f = 1ns$ and $\Delta\omega = 0$) and examines the system synchronization through the transmission process. The results are reported to chaos masking method (CMA).

Fig. 4.34 shows the digital message $m(t)$ which is transmitted to the receiver, while Fig. 4.35 shows the secret key which is used with this message. The flowchart of this process is shown in Fig. 4.36.

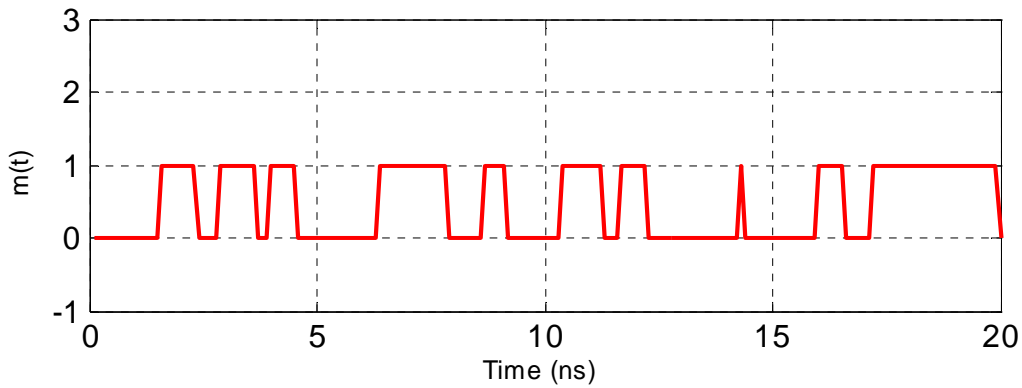


Fig. 4.34 Transmit message $m(t)$.

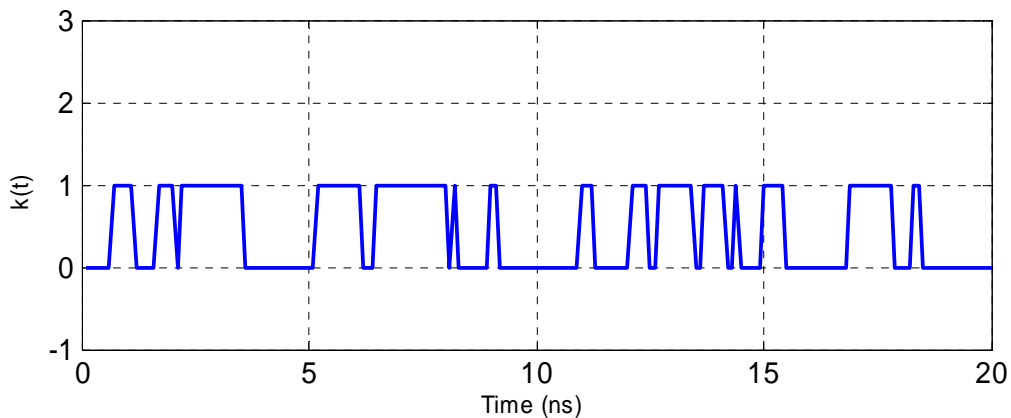


Fig. 4.35 Secret key $k(t)$.

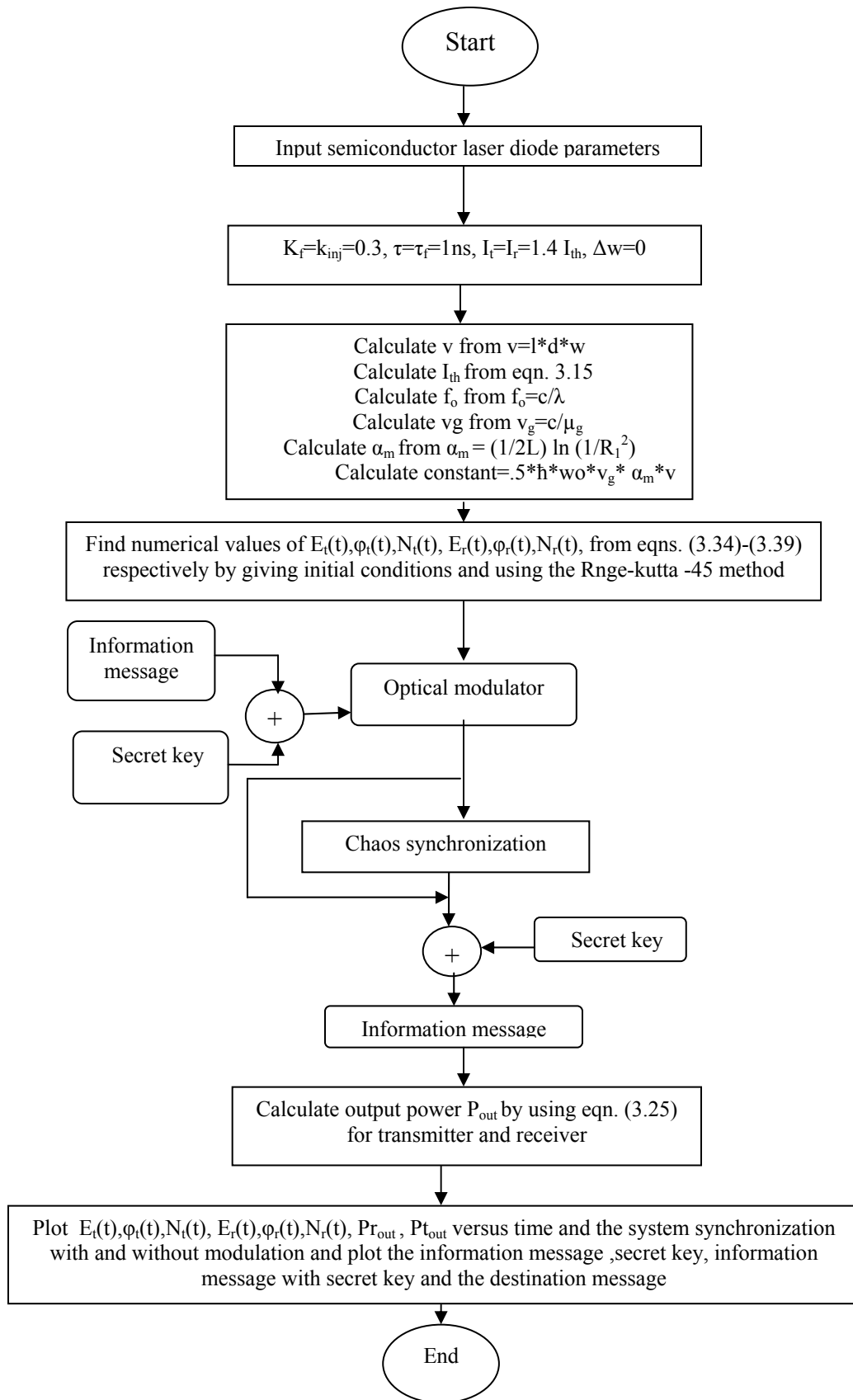


Fig. 4.36 Flowchart of coding and decoding program.

The transmitted message after Ex-ORed with the secret key is shown in Fig. 4.37.

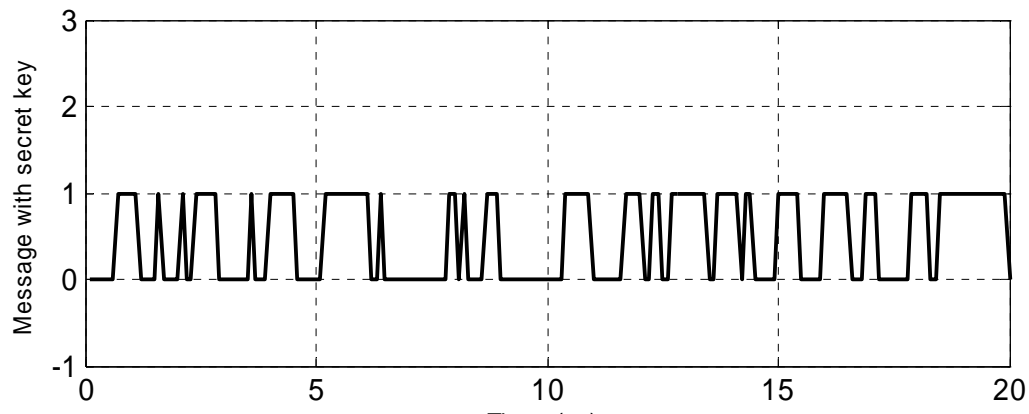


Fig. 4.37 Transmitted message after Ex-ORed with secret key

The transmitter output power waveform when the system is operating under modulation with $(m(t) \text{ Ex-ORed } k(t))$ is shown in Fig. 4.38.

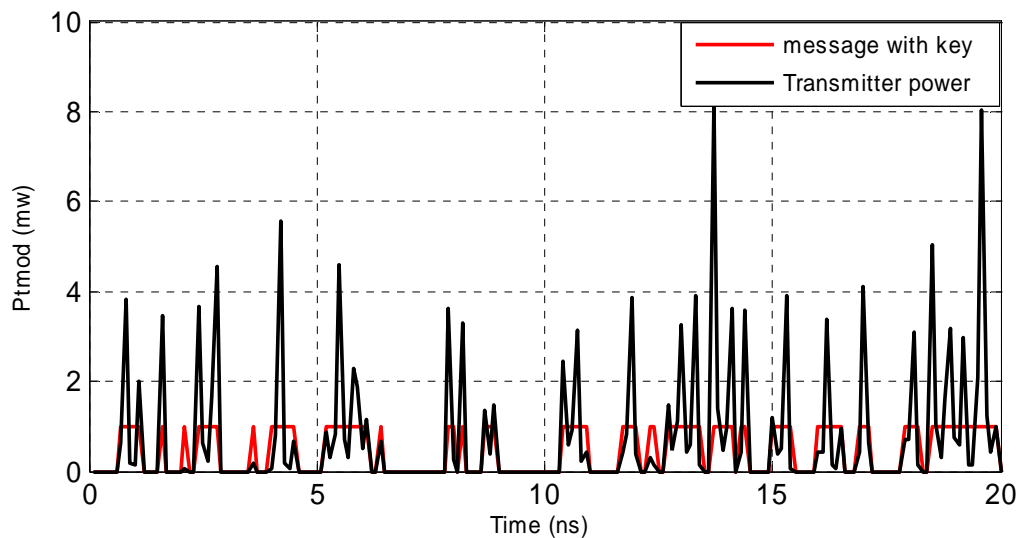


Fig.4.38 Transmitter output power when the laser is directly modulated with $(m(t) \text{ Ex-ORed } k(t))$.

Note that after modulation, the output power of the transmitter and the output power of the receiver take another shape as shown in Fig. 4.40.

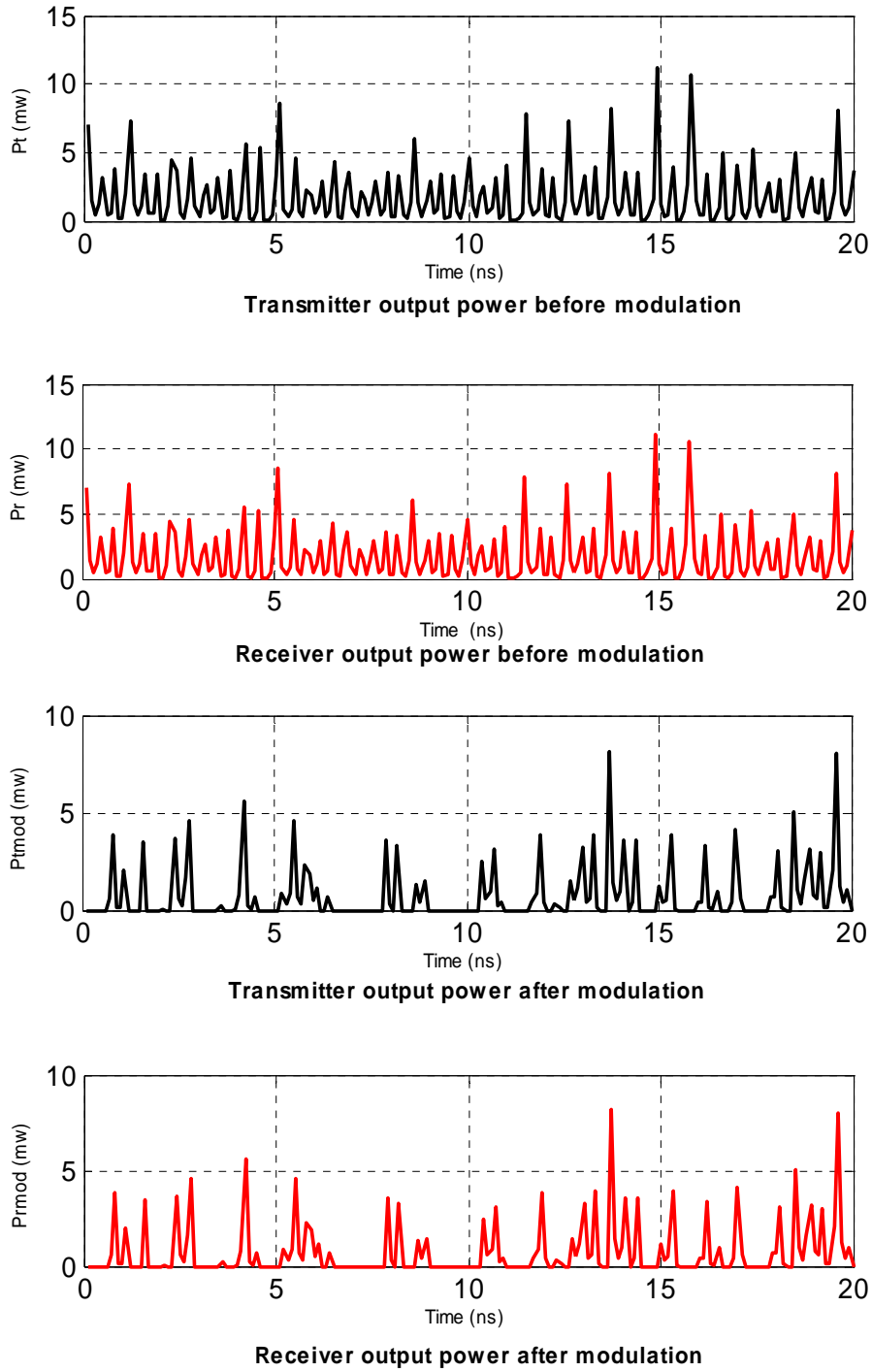


Fig.4.39 Transmitter and receiver output power without and with modulation.

To recover the original message at the receiver, the output of the receiver is subtracted from the output of the transmitter and the resultant message is then Ex-ORed with the secret key, as shown in Fig. 4.41.

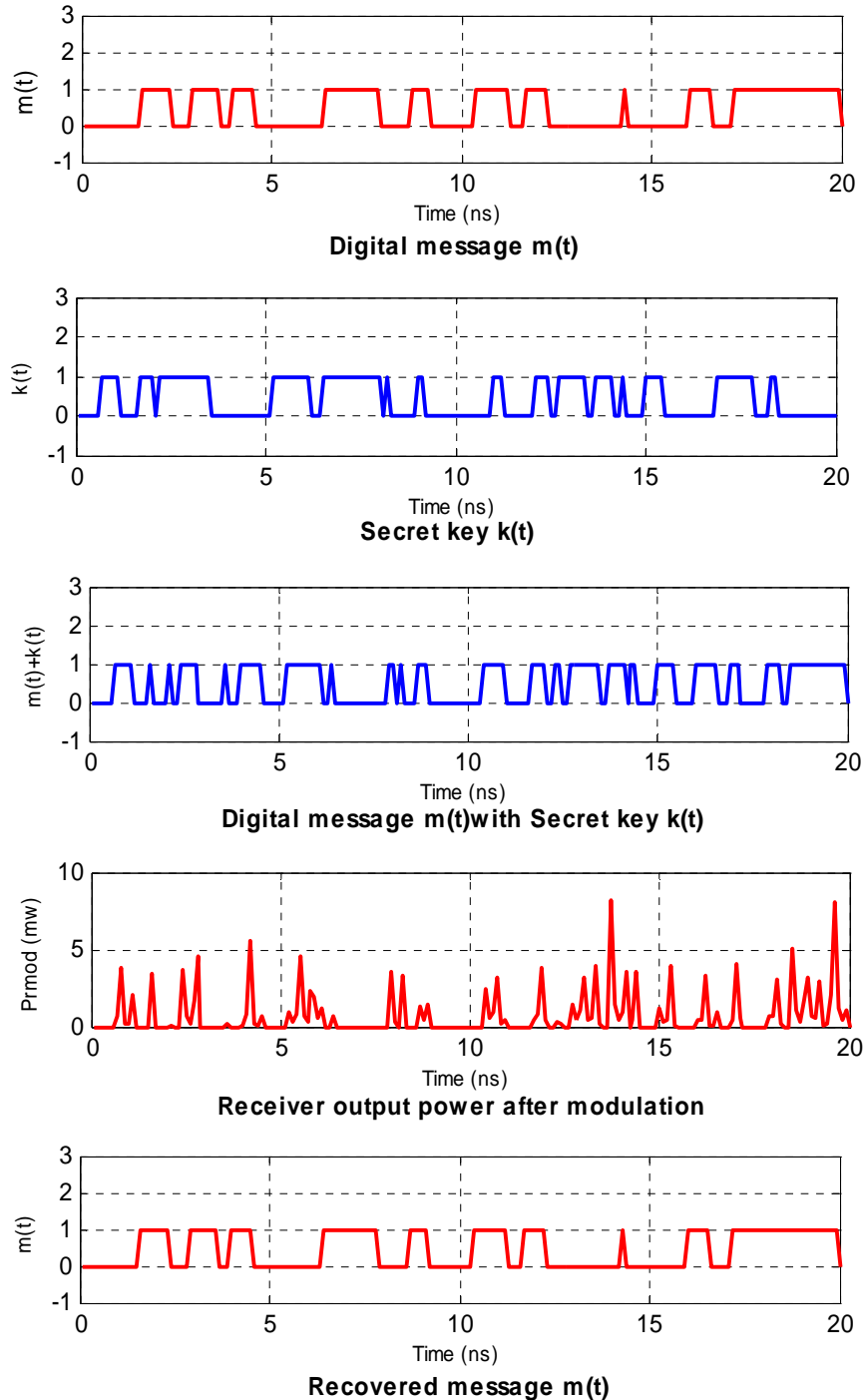
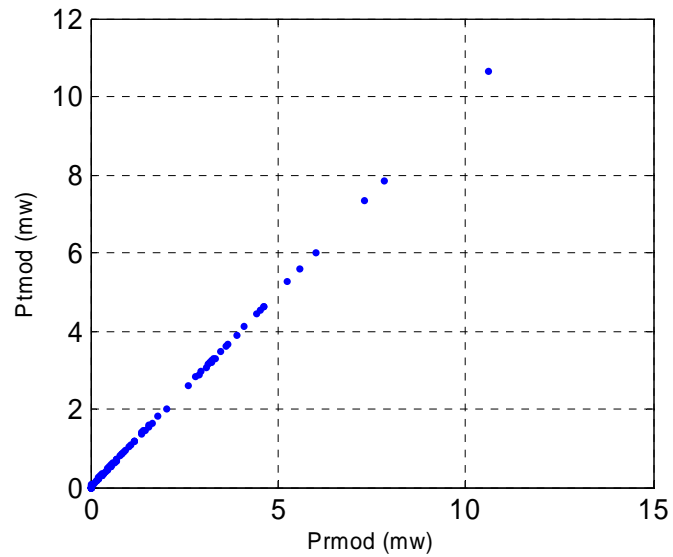
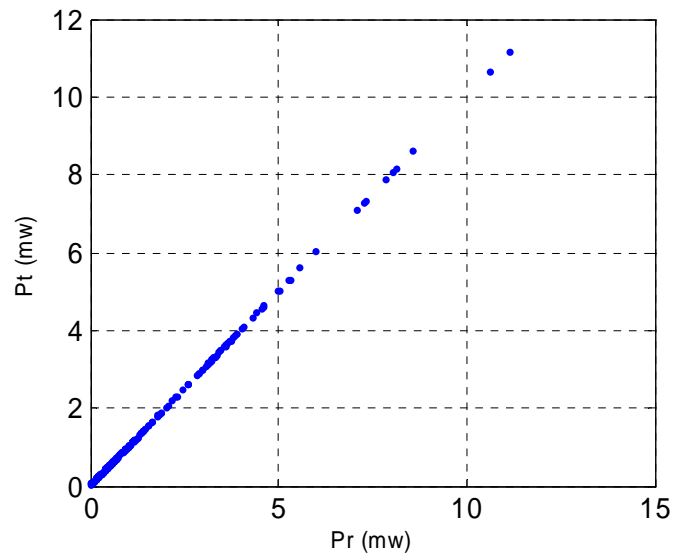


Fig. 4.40 Steps used for encoding and decoding the message.

The synchronization of the system in the presence of modulation is the same as that in the absence of modulation as shown in Fig. 4.41. This means that the receiver has received the right message.



(a)



(b)

Fig. 4.41 System synchronization in the presence (a) and absence (b) of modulation.

Chapter Five

Conclusions and Suggestions for Future Work

5.1 Conclusions

The performance of optical feedback chaotic optical communication (COC) system incorporating semiconductor lasers has been investigated theoretically. The laser rate equations have been used to address the synchronization state between the transmitter laser and the receiver laser and the results are used as a guideline to present a secure communication system. The effect of various system parameters on synchronization has been evaluated. The main conclusions drawn from this study are

- (i) A rich variety of chaotic behavior can be obtained by varying external cavity length, optical injection efficiency η_{inj} , optical feedback coefficient k_f , and external mirror reflectivity. Further, the delayed optical feedback can offer periodic solutions, subharmonic solutions, and chaotic solutions.
- (ii) Full synchronization between the transmitter laser and the receiver laser requires that both lasers should have identical structure parameters and bias conditions.
- (iii) For the system structure parameters used in the simulation, the best values of optical feedback and optical injection that make the system generates chaotic signals are $k_f = k_{inj} = 0.3$ when the lasers are biased at 1.4 of the threshold current.
- (iv) Full synchronization between the transmitter laser and receiver laser requires identical lasing frequency at the bias conditions. A frequency detuning as low as 10 GHz affects the state of synchronization.

- (v) To achieve an efficient operation for the COC systems, the transmitter and receiver laser sources must operate in synchronization in the absence of modulation.

5.2 Suggestions for Future Work

The analysis and simulation reported in this work can be extended in the future to address the following issues

- (i) Using the state of polarization of the optical feedback signal in order to control the chaotic dynamics of the semiconductor laser. This will give an additional degree of freedom to achieve chaos in this type of lasers.
- (ii) Investigating the performance of COC systems operating under wavelength division multiplexing (WDM) scheme. The synchronization between the multi laser sources implemented in the transmitter and the corresponding receiver laser sources should be addressed carefully here.
- (iii) Applying different cryptography schemes in order to implement secure communications in COC systems.

Republic of Iraq
Ministry of Higher Education
and Scientific Research
University of Technology
Laser and Optoelectronics Engineering Department



Performance Analysis of Semiconductor Laser- Based Chaotic Optical Communication Systems

A Thesis
Submitted to Laser and Optoelectronics Engineering Department
University of Technology
In partial fulfillment of the requirements
for the degree of Doctor of Philosophy
in
Laser Engineering

By
Shatha Mizhir Hasan
(M.Sc. 2005)

Supervised by

Prof. Dr. Mohammed S. Mehde

Prof. Dr. Raad S. Fyath

Safar 1431

Jan. 2010

References

References